The Self-Maintaining Nature of Ventricular Fibrillation

Contribution of L-type Ca^{2+} channels and Na^{+}/Ca^{2+} Exchange to Cardiomyocyte Ca^{2+} Overload in Ventricular Fibrillation. Surface Fluorescence Study in Isolated Perfused Rat Hearts.

Inauguraldissertation

zur

Erlangung der Würde eines Doktors der Philosophie
vorgelegt der Philosophisch-Naturwissenschaftlichen Fakultät
der Universität Basel

von

Sergey Driamov

aus Minsk, Belarus

Basel, Oktober 2004.

Genehmigt von der Philosophisch-Naturwissenschaftlichen Fakultät auf antrag von

Prof. Dr. Alex. N. Eberle,

Prof. Dr. Karl G. Hofbauer und

PD Dr. Christian E. Zaugg

Basel, den 19 Oktober 2004

Prof. Dr. Hans-Jakob Wirz

Dekanat der Philosophisch-
Naturwissenschaftlichen
Fakultät
Der Universität Basel

Acknowledgements

The present dissertation work was performed in the Departement of Research at the University Hospital Basel within the Cardiology Research Group conducted by Prof. Dr. med. Peter Buser and PD Dr. Christian Zaugg.

First, I would like to express my gratitude to PD Dr. Christian Zaugg for guiding me through the studies and for giving me a profound knowledge of heart physiology and pharmacology as well as introducing me into the techniques used in our laboratory. He provided his help whenever possible and encouraged me in developing my theoretical knowledge and practical skills.

I would like to express my gratitude to Prof. Dr. med Peter T. Buser for giving me the opportunity to perform my Ph.D. thesis in his laboratory.

I am deeply grateful to Prof. Dr. med. Alex N. Eberle for supervising my thesis. I am very much thankful to Prof. Dr. Karl G. Hofbauer for accepting being coreferent of my Ph.D. committee. I am also very much thankful to Prof. Dr. Phil. Ueli Aebi for being a chairman of my Ph.D. exam.

I am very grateful to Dr. André Ziegler for teaching me basics of MNR and in-vivo MRI.

I am very grateful to Dr. Mohamed Bellahcene for his thorough introduction into the Langendorff heart preparation technique.

Additional thanks to PD Dr. Christian E. Zaugg for teaching me basics of measuring indo-1 fluorescence in an isolated heart.

I would like to thank Dietlinde John for her help in solving many practical problems in the laboratory.

Furthermore, I would like to thank my colleagues, Dr. Silvia Butz, Dr. David Traub, Dr. Vania Barbosa, Dr. Dagmar Keller, Dr. Vivian Suarez, Dr. Thomas Grussenmeyer, Dr. Else Müller-Schweinitzer, Dr. David Reineke, Dr. Martin Grapow, Dr. Peter Matt and Laxman Iyer for creating a pleasant and creative atmosphere in the laboratory.

Special thanks to Ulrich Schneider and his team at the animal station for their professional care of the rats.

Thanks to the administration of our Research Departement, Prof. Radek Skoda, Heidi Hoyermann, Margrit Stähli, Monika Hermle, Armin Bieri, Reto Schaub and Thomas Gaida for organizing work in the Research Department in a best way and efficient help in many current problems.

Thanks to the Cardiology Department of Kantonsspital Basel for supporting my thesis financially.

I am deeply grateful to my mother and my sister for their love and support

I want to express especially cordial gratitude to my wife Julia. She provided an invaluable support of my scientific work with her love and gentle care. I am very much grateful to her for providing proper conditions in the day-to-day life. I am also extreemly grateful to her for making direct contribution to this thesis by constructing and tailoring elaborate black curtains that were necessary for the efficient fluorescence measurement experiments.

CONTENTS

SUMMARY

Approximately 40% of all deaths in Switzerland are due to cardiovascular diseases.[1] An important part of these deaths happen because of life-threatening cardiac arrhythmias. Ventricular fibrillation (VF) is the most dangerous cardiac arrhythmia usually caused by ischemic heart disease and infarction. It also happens in apparently healthy individuals representing the most common cause of sudden death. The problem of high mortality associated with sudden cardiac death due to VF is relevant to all industrialized countries. In the United States, VF accounts for approximately 300,000 deaths per year.[2] Currently the most important therapy is the implantable cardioverter-defibrillator (ICD). Recent clinical trials[3] have expanded the indications for device therapy to over 4 million patients in the US alone at a cost exceeding $50 billion if fully implemented.[2] This consideration provides a strong motive to develop alternative new therapies that are comparably effective but less expensive and invasive.[2] This requires a better understanding of VF pathogenesis at the molecular and cellular level. Therefore, our study was focused on elucidation of mechanisms of VF.

It has been proposed that detrimental effects of VF are partially due to rapidly developing overload of cytosol of cardiac cells with Ca^{2+}.[4] The Ca^{2+} overload is responsible for maintaining of VF as well as for reinduction of VF after defibrillation[5] and for the post-VF left ventricular (LV) disfunction.[6]

It is not clear, however, through which pathways Ca^{2+} enters cells during VF. Here we studied the role of different ion transport systems, particularly, of L-type Ca^{2+} channels and sodium-calcium (Na^+/Ca^{2+}) –exchange, in initiation and maintenance of Ca^{2+} overload during VF. We applied drugs specifically blocking each of these Ca^{2+} transport systems in an isolated perfused rat heart model. We used nifedipine, a blocker of L-type Ca^{2+} channels and KB-R7943, a specific blocker of the reverse mode of Na^+/Ca^{2+}-exchange. We induced VF in the hearts by rapid pacing and registered changes of intracellular Ca^{2+} concentration ($[Ca^{2+}]_i$) using surface fluorescence of the Ca^{2+} indicator indo-1. In order to get a better understanding of extend of Ca^{2+} overload during VF we calibrated fluorescence signal of indo-1 to $[Ca^{2+}]_i$. During the first two minutes of VF

$[Ca^{2+}]_i$ reached about double of the normal systolic concentration achieving ≈ 2000 - 2500 nM. With further VF duration $[Ca^{2+}]_i$ elevated less rapidly and achieved ≈ 3000 nM. We found that both L-type Ca^{2+} channels and Na^+/Ca^{2+}-exchange contribute to Ca^{2+} overload during VF. Specifically, when each of the drugs was perfused before VF induction, nifedipine reduced the extend and especially the rate while KB-R7943 mostly reduced the extend of Ca^{2+} accumulation in cardiomyocytes. Additionally, Na^+/Ca^{2+}-exchange also contributes to maintenance of Ca^{2+} overload during VF because perfusion of the hearts with KB-R7943 after VF has been induced also reduced $[Ca^{2+}]_i$. Finally, in all groups of hearts perfused with the drugs, spontaneous terminations of VF (defibrillations) were frequently observed. The spontaneous defibrillations did not happen in untreated control hearts. These results enabled us to conclude that both L-type Ca^{2+} channels and Na^+/Ca^{2+}-exchange are important ways of Ca^{2+} entry into the cardiomyocytes during VF. The L-type Ca^{2+} channels are more important for Ca^{2+} entry into cardiomyocytes at the initial stage of VF. The Na^+/Ca^{2+}-exchange is also important at the initial stage of VF but its contribution increases rapidly with progression of VF.

ABBREVIATIONS

AM	acetoxymethyl (esterified form of fluorescent dye indo-1)
AV	atrio-ventricular
$[Ca^{2+}]_i$	intracellular concentration of Ca^{2+}
$[Ca^{2+}]_m$	mitochondrial concentration of Ca^{2+}
CICR	Calcium-induced calcium release
ECG	electrocardiogram
i_{CaL}	inward calcium current through L-type Ca^{2+} channels
i_{Na+}	inward sodium current
LV	left ventricular
LVDP	left ventricular developed pressure
$[Na^+]_i$	intracellular concentration of Na^+
Na^+/Ca^{2+}-exchange	sodium-calcium exchange
RyR	ryanodine sensitive Ca^{2+} channels (ryanodine receptors)
SA	sino-atrial
SERCA	sarcoendoplasmic reticulum calcium ATP-ase
SR	sarcoplasmic reticulum
T-tubules	Transverse tubules
VF	ventricular fibrillation

1. INTRODUCTION

Cardiovascular diseases are the major cause of mortality in Switzerland today. They account for approximately 40% of all deaths.[1] An important part of these deaths happen because of cardiac arrhythmias. Among the cardiac arrhythmias, VF is most dangerous and usually is a direct cause of sudden cardiac death because of fast ischemic brain damage due to interrupted blood flow. VF is associated with ischemic heart disease and infarction. The underlying pathology, however, may be unknown and sudden death due to VF may be a first manifestation of disease in an apparently healthy individual.[7] Research of the last decades has provided a better understanding of the pathophysiology of VF.

There are several theories explaining mechanisms of initiation and maintenance of VF, such as the depressed conduction and unidirectional block generating reentry,[8] the wavebreack mechanism,[8] electrical cell-to-cell uncoupling induced by ischemia,[9] heterogeneous repolarization and prolonged refractoriness in hypertrophied and failing hearts,[10-12] delayed afterdepolarizations followed by triggered activity.[13-15] These events can lead to initiation of VF. On the other hand, initiation of potentially lethal ventricular tachyarrhythmias including VF in many pathological conditions such as digitalis toxicity, myocardial ischemia or heart failure has generally been accepted to be due to Ca^{2+} overload.[8,16-19]

Still, some important mechanisms of Ca^{2+} overload, like the ways of Ca^{2+} entry, are not clear. The present thesis is aimed at investigation of the ways of Ca^{2+} entry into the cardiomyocytes at different stages of VF.

1.1 Excitation-contraction coupling

1.1.1 Electromechanical activity of the heart

The heart is a muscular pump that propels blood throughout the circulation, delivering nutrients to and removing wastes from each of the organs and transporting hormones and other messengers between various regions of the body.[8] Cardiac muscle is very complex, highly regulated tissue. An elaborate and heterogeneous electrical system allows the heart to be excited in an orderly manner and to beat synchronously.[8] Electrical impulse generated in sinoatrial (SA) node causes atria to contract (Fig.1A). The signal then passes through the atrioventricular (AV) node to the AV bundle. Further division of the AV bundle into smaller and smaller branches of the Purkinje fibers system brings the signal to the working ventricular myocardium (Fig.1B) which finally leads to excitation of single cardiomyocytes (Fig.1C), eventually followed by their coordinated, nearly synchronous contraction and, therefore, by contraction of the whole ventricles. The process of coupling excitation to contraction at cellular level is very important and will be considered in detail.

1.1.2 Excitation-contraction coupling in cardiomyocytes

The cardiac cell membrane has specific foldings called Transverse tubules (T-tubules). The system of T-tubules in cardiac myocytes provides close spatial position between the sarcolemmal L-type Ca^{2+} channels and the ryanodine sensitive Ca^{2+} channels (ryanodin receptors or RyR) in the sarcoplasmic reticulum (SR)[8] (Fig. 2).

Electrical excitation of the surface membrane of the working cells of the atria and ventricles begins when opening of sodium channels. The resulting inward depolarizing sodium current (i_{Na+}) generates the initial upstroke of the cardiac action potential.[8] The action potential propagates as a wave of depolarization along the surface and along the T-tubules. Depolarization of the T-tubule opens L-type Ca^{2+} channels in the sarcolemma. Due to the close positioning of L-type Ca^{2+} channels and RyR the Ca^{2+} flux through L-type Ca^{2+} channels leads first of all to an increase of $[Ca^{2+}]_i$ locally in the close proximity of RyR.

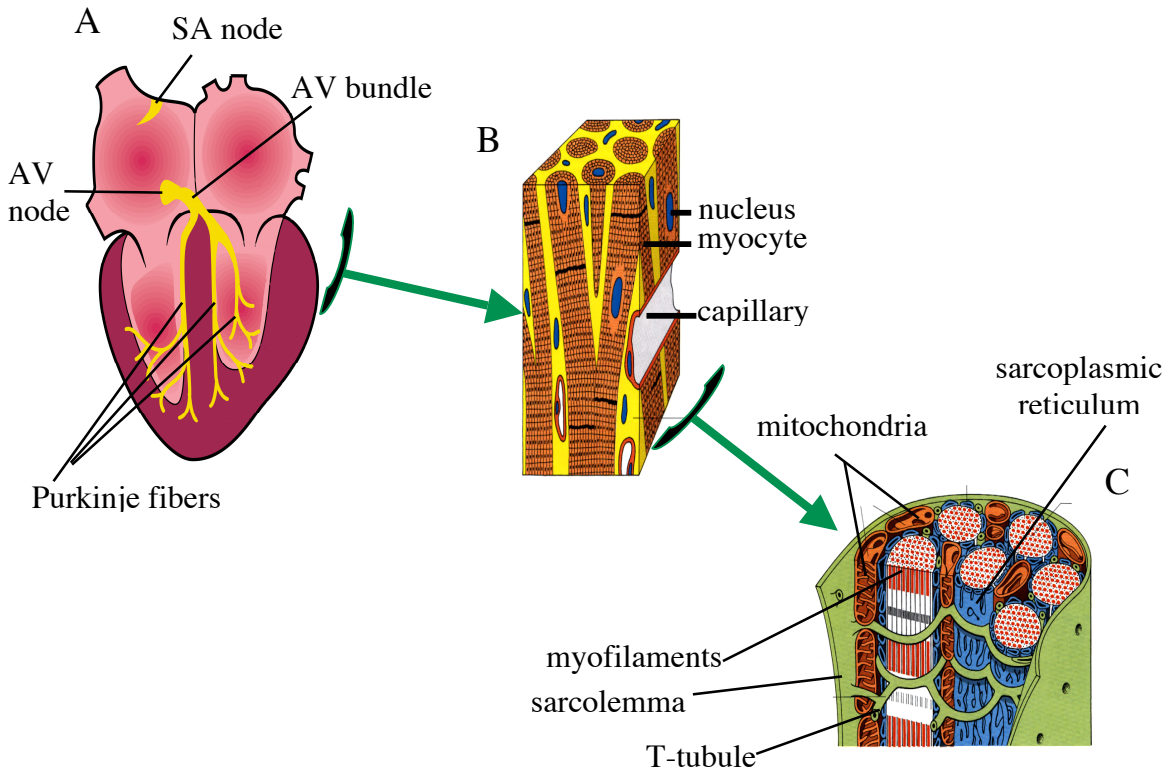

Figure 1. System of electrical conduction in the heart. Abbreviations: SA sino-atrial, AV atrio-ventricular, T-tubule transverse tubule. (A) from *R.F. Schmidt, 2000*, (B) and (C) from *C. Thomas et al., 1989*; modified by C.E. Zaugg.

This triggers opening of RyR channels and release of Ca^{2+} ions from the SR, the process known as calcium-induced calcium release (CICR).[20-22] In addition to the entry through L-type Ca^{2+} channels, Ca^{2+} enters from outside via reverse mode of Na^{+}/Ca^{2+}-exchange, which also contributes to CICR although to a smaller extent.[23] The operation of Na^{+}/Ca^{2+}-exchange in a reverse mode, favoring Ca^{2+} entry, is provided by membrane depolarization and increase of intracellular sodium concentration ($[Na^{+}]_i$). CICR and Ca^{2+} influx from outside lead to a quick rise of $[Ca^{2+}]_i$ from ≈100 nM during diastole to ≈1 μM during systole[24] followed by a quick decline, a process called Ca^{2+} transient. High systolic $[Ca^{2+}]_i$ promotes binding of Ca^{2+} ions to myofilament protein troponin C that triggers interaction between actin and myosin resulting in contraction.[8]

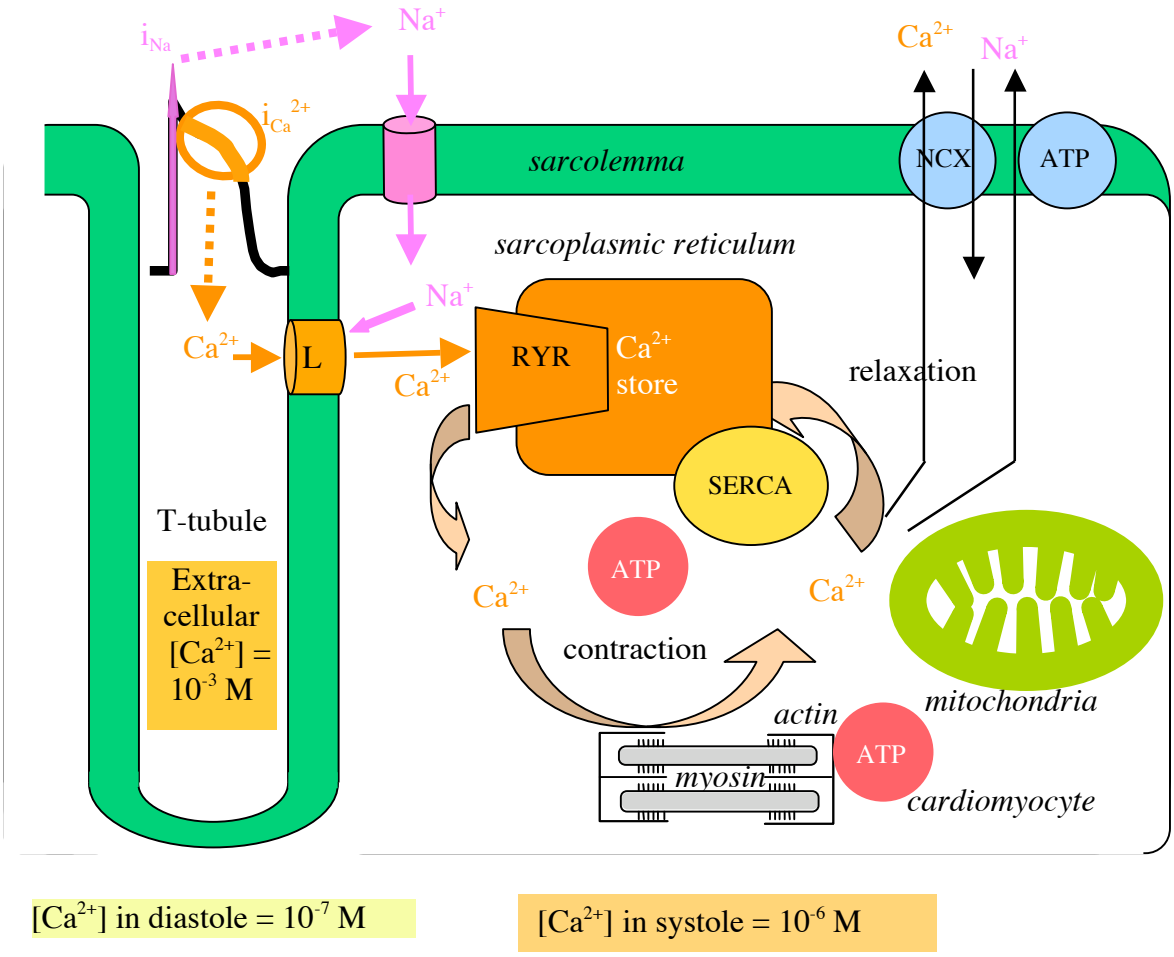

Figure 2. Excitation-contraction coupling in cardiomyocyte. Abbreviations: L L-type Ca^{2+} channels, RyR ryanodine receptor, T-tubule transverse tubule, NCX Na^+/Ca^{2+}-exchange, SERCA sarcoendoplasmic reticulum Ca^{2+} ATP-ase, ATP adenosintriphosphate. From *Bers D., Cardiac excitation-contraction coupling, 2002*;[25] modified by C. E. Zaugg.

So, Ca^{2+} is an agent that eventually passes the electric signal generated in the SA node to the contractile machinery of the heart. After contraction the heart has to relax in order to refill its chambers with blood. Relaxation, which is loosely synchronized with repolarization,[26] is provided by decline of Ca^{2+}, resulting from the following processes. First, further entry of Ca^{2+} into the cytosol is terminated. CICR inactivates Ca^{2+} current through L-type Ca^{2+} channels (i_{CaL}), the very process, which has triggered CICR itself.[27,28] RyRs also get inactivated, although the mechanism of this inactivation is unresolved.[26] There are theories explaining its inactivation to be Ca^{2+} -independent and due only to the

previous activation[29] or to be dependent on increase of $[Ca^{2+}]_i$ during CICR.[30] Second, there are mechanisms of Ca^{2+} removal from cytosol. Most of Ca^{2+} is pumped back into SR by the sarcoplasmic reticulum calcium ATP-ase (SERCA). Activation of SERCA takes place first of all due to the high level of its substrate, the cytosolic Ca^{2+}, during action potential.[8,26] Some amount is extruded out of the cell by the working in a forward mode Na^+/Ca^{2+}-exchange. The forward mode of Na^+/Ca^{2+}-exchange, favoring Ca^{2+} extrusion, is switched on by repolarization of sarcolemma. Least amount is removed by the sarcolemmal Ca^{2+} pump, which also extrudes the Ca^{2+} ions out into the extracellular space. Eventually $[Ca^{2+}]_i$ declines, which leads to dissociation of Ca^{2+} ions from troponin C and relaxation.[8]

It should be noted that excitation by fast depolarizing i_{Na+} takes place in all the heart except for the SA and AV nodes. The cells of the nodal tissue lack functional Na^+ channels. Excitation in the nodal tissue is provided by slow depolarizing Ca^{2+} currents, which are responsible for pacemaker activity of SA and for impulse propagation in AV.[8] Additionally, it should be noted, that although the SA node is the main, it is not the only source of excitation (pacemaker) in the heart. The SA node in the human heart normally fires 60 to 100 times per minute. There are also lower pacemakers. The most rapid is in AV node; it has an intrinsic rate of 40 to 55 beats/min. Cells of AV bundle and of His-Purkinje system also possess pacemaker activity. They can fire at rates of 25 to 40 beats/min. In pathological conditions, when the SA node is slowed or when conduction is impaired, the activity of the lower pacemakers becomes apparent.[8]

1.2 Arrhythmias - a brief classification

(Based on *Physiology of the Heart, A. Katz, 2001* [8])

There are two general types of arrhythmia: *bradycardia*, when the heart rate is too slow, and *tachycardia*, when the heart rate is too high. Each includes many specific arrhythmias that are generally described in terms of the structure where the arrhythmia originates and the type of abnormality responsible for the arrhythmia. Bradycardias (bradyarrhythmias) are readily diagnosed by palpation of the peripheral pulse. Tachycardias (tachyarrhythmias) are more complex because not all premature depolarizations alter the pulse. Supraventricular tachycardias arise above the ventricles, and tachyarrythmias originating in the His-Purkinje system and ventricles are called ventricular tachycardias.

Mechanisms responsible for bradyarrhythmias

The most common causes for an abnormally slow pulse are slowed pacemaker activity (chronotropy) and depressed conduction (dromotropy). The former is caused by changes in the ionic currents responsible for pacemaker activity in the SA node, and the latter, often called block, occurs when conduction of this impulse to the ventricles is impaired.

Slowed pacemaker activity

Slowing of the sinus pacemaker (*sinus bradycardia*) is commonly caused by excessive parasympathetic (vagal) tone. Sinus bradycardia is commonly seen in normal individuals in whom vagal tone is increased by training. Severe sinus bradycardia can cause vasovagal syncope (the “swoon”). Sinus pacemaker activity can be slowed by hypothyroidism as well as by many prescribed drugs, including b-adrenergic blockers and some L-type Ca^{2+} channels blockers. Slowing of lower pacemakers in the AV node or His-Purkinje system cannot cause bradycardia as long as ventricular beating is controlled by a normally functioning sinus pacemaker.

Depressed conduction (block)

The other cause of bradycardia is called block. It occurs when impulse conduction into the ventricles is impaired. It can produce "dropped" (absent) beats or depress conduction that can cause abnormal delay in impulse propagation. The later does not affect the pulse but causes abnormalities that are seen on the electrocardiogram (ECG). Three areas in the heart are especially vulnerable to the block. The first two, the SA and AV nodes, are regions where conduction is normally slow and the safety factor low. The third, the AV bundle, is anatomically precarious because this is the only strand of conducting tissue between atria and ventricles. SA and AV blocks are often caused by functional abnormalities produced by excessive parasympathetic tone or by drugs inhibiting Ca^{2+} channels. Block of AV bundle usually occurs when it is damaged or destroyed by disease.

Decremental conduction

Decremental conduction is seen when an action potential enters a region with progressively slowing conduction velocity. It is abnormal in all regions of the heart except for the nodal tissue. Conduction is slowed in energy-starving cells because of inhibition of sodium pump and increased extracellular potassium. Abnormal refractoriness also slows conduction by inactivating sodium and calcium channels, which decreases action potential amplitude and slows depolarization. If the ability to generate a propagated action potential in a region of decremental conduction is severely depressed, it can completely block impulse transmission.

Decremental conduction is a normal property of SA and AV nodes providing a normal conduction delay in these structures. Once the impulse reaches the AV bundle, conduction velocity again becomes rapid.

Block in the AV bundle, like block in the AV node, can cause AV conduction to fail. However, unlike block in the AV node, which is often functional and readily reversed, block in the AV bundle is usually dangerous. Block in AV bundle reflects anatomical damage and is frequently irreversible.

Conduction can also be blocked in the bundle branches and fascicles of the left bundle branch (bundle branch blocks and fascicular blocks). These localized blocks do not

themselves cause “dropped beats”, but like block in the AV bundle, they imply anatomic disease of the His-Purkinje system. Block in the distal His-Purkinje system called arborization block is evidence for diffuse myocardial disease, which occurs in end-stage heart failure.

Unidirectional block

Unidirectional block is a selective block of conduction in one direction. It is observed in the normal heart, like in the AV node, where antegrade (forward) conduction from atria to ventricles is more rapid than retrograde (backward). In diseased hearts it occurs in the areas that are inhomogeneously ischemic or scarred. Unidirectional block often leads to arrhythmias. Nonuniform abnormalities in diseased hearts may lead to an asymmetric reduction of action potential amplitude or rate of depolarization. Asymmetrically distributed resting potential or refractoriness, asymmetric fibrosis, which slows conduction by increasing longitudinal resistance, an uneven reduction of the number of open gap junction channels, asymmetric increase of depolarization threshold, these are conditions that often produce unidirectional block. Unidirectional block is a common cause of premature systoles and tachyarrhythmias because, in addition to causing conduction to fail, it can disorganize impulse propagation and cause reentry.

Mechanisms responsible for premature systoles and tachyarrhythmias

Most of tachyarrhythmias are described in terms of their clinical features because defining pathophysiology of a given arrhythmia is difficult and often impossible. A single early beat is called a *premature systole* (premature beat) and a series of premature beats a *tachycardia*. Very rapid regular depolarization of the atria or ventricles is called flutter, and complete disorganization of depolarization, where there is no effective beating, is called *fibrillation*. There are three mechanisms accounting for most of tachyarrhythmias. These are accelerated pacemaker activity, triggered depolarizations and reentry. All can be manifestations of more than one underlying mechanism, all can appear in many regions of the heart, and most can occur either as a single event (a premature systole) or as a sustained tachycardia.

Accelerated pacemaker activity

This mechanism represents an accelerated firing of pacemaker cells. When it occurs in the SA node, it causes *sinus tachycardia*. In lower pacemakers it can cause junctional and accelerated idioventricular rhythm.

Afterdepolarizations and triggered responses

Afterdepolarizations appear spontaneously during and after repolarization after an action potential. They are both seen in Ca^{2+} -overloaded hearts.[8] Large afterdepolarizations can generate propagated action potentials called *triggered responses*, which are important causes of lethal arrhythmias. There are two general types of aferdepolarization: early and delayed. The former appear before the end of the action potential, when the membrane potential is in the range between –10 and –30 mV; the latter appear after the membrane potential has returned to its resting level.

Early afterdepolarizations

Early afterdepolarizations appear at the end of the plateau of the cardiac action potential (Fig. 3 A), they are caused by inward currents, mostly by i_{CaL}. Early afterdepolarizations are provoked by diseases, by drugs that prolong the action potential, by □-adrenergic agonists and by phosphodiesterase inhibitors.

A

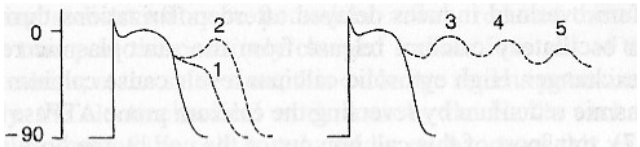

B

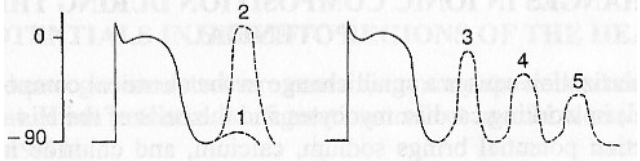

Figure 3. Afterdepolarizations: A early, B delayed. (from A.Katz, 2001[8]).

Delayed afterdepolarizations

Delayed afterdepolarizations occur after the cell has repolarized (Fig. 3 B). Like early afterdepolarizations, they are commonly seen in Ca^{2+} overloaded hearts and are provoked by inotropic drugs administered to patients with heart failure. Ca^{2+} overload induces delayed afterdepolarizations through interplay between oscillatory calcium release from SR and Na^{+}/Ca^{2+}-exchange. High systolic Ca^{2+} levels cause Ca^{2+} release from SR by reversing the SERCA reaction.[31] Transport of this Ca^{2+} out of the cell by Na^{+}/Ca^{2+}-exchange generates an inward current that can initiate triggered responses.[8]

Reentry

Disorganization of the spread of a wave of depolarization as it passes over the heart, especially the ventricles, not only reduces mechanical efficiency but is an important cause of arrhythmias. Premature systoles and tachycardias caused by decremental conduction can emerge as two or more impulses. This can occur at the junction between Purkinje fiber and the ventricular myocardium or within a bundle of myocardium (Fig. 4). In both, reentry is caused by an impulse entering an area of slow conduction and unidirectional block.[8]

A premature systole can arise in an area of slow conduction and unidirectional block when an approaching wave of depolarization reaches the end at which antegrade conduction is blocked (Fig. 4). Although the impulse cannot cross this region, propagation through other, normally conducting tissue can bring it to a point distant to the depressed area, which it can enter in a retrograde direction (Fig. 4). If the unidirectional block is only in the antegrade direction, the impulse can propagate through the area of decremental conduction, returning to the proximal end of the depressed area (A) after a delay. If the delay is sufficient to allow the proximal tissues to recover their excitability, the retrograde impulse can depolarize (reenter) the normal tissue proximal to the depressed area, generating a second impulse. The latter represents a premature systole. This process can become repetitive if, when the second impulse approaches point B in Fig. 4, the same mechanism initiates one or more additional reentrant beats generating in such way a run of premature systoles or a sustained tachycardia. In most cases, however, passage of the retrograde impulse increases the refractoriness of the depressed area, which causes conduction to be blocked in both directions. When this occurs, the unidirectional block becomes complete, retrograde conduction no longer occurs and the reentrant arrhythmia is terminated.[8] Unfortunately, in some cases reentry may initiate VF. Impaired Ca^{2+} handling by cardiomyocytes leading to abnormally increased concentration of Ca^{2+} in cytosole favors VF initiation.[16-19]

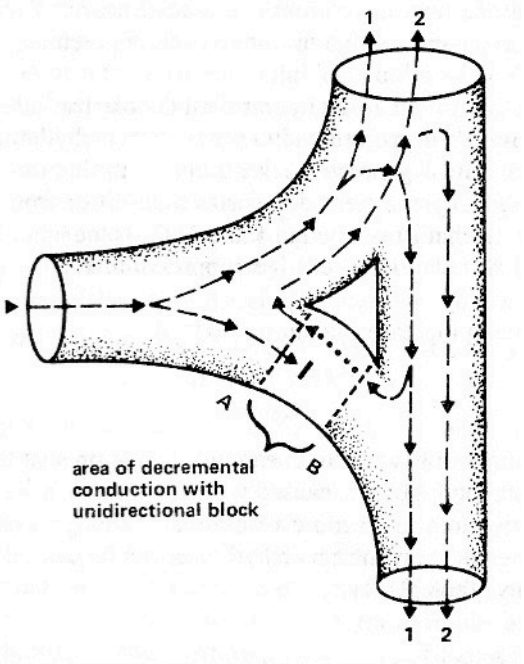

Figure 4. Reentry at the point of impingement of a Purkinje fiber on the ventricular myocardium. A region of decremental conduction and unidirectional block (from A to B) prevents antegrade conduction (1). If the impulse travels around the depressed area, it can be conducted slowly through the depressed region in the retrograde direction (dotted line from B to A). After a delay a retrograde impulse can reenter the myocardium proximal to the region of decremental conduction. If this occurs after the tissue proximal to the depressed area has recovered from the first impulse, the retrograde impulse can initiate a premature systole (2).[8]

Ventricular fibrillation (VF)

Ventricular fibrillation is a lethal arrhythmia disorganizing contraction of ventricles to such extend that the heart cannot sustain either blood pressure or cardiac output.[8] Chaotic oscillations replace QRS complexes of the ECG. Premature systole may provoke VF formation (Fig. 5).

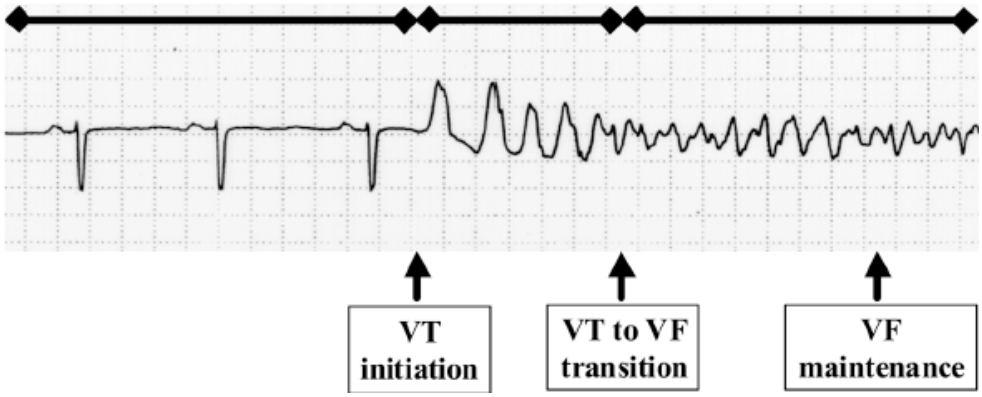

Figure 5. A progression leading to development of VF. A premature ventricular extrasystole initiates reentrant ventricular tachyarrhythmia (VT), which degenerates to VF. [2]

However, not only premature ectopic beats, such as the one shown at Fig. 5, are capable to initiate reentry. Localized wavebreak of the cardiac electrical wave can initiate and maintain reentry developing into VF.[32,33] Wavefront of depolarization moving through the heart begins to slow at its edges, which causes the front to become curved (Fig. 6). This slows conduction at the edges of the front because the electrical vectors in a curved region are not parallel to the direction of propagation. As a result, the curvature of the wavefront tends to increase and eventually causes spirals to appear at the edges. These spirals slow conduction further and bring the edges of the wavefront behind tissue that has already been depolarized. The result is a growing area of decremental conduction and block that causes the edges of the spiral to break down into multiple disordered wavelets.

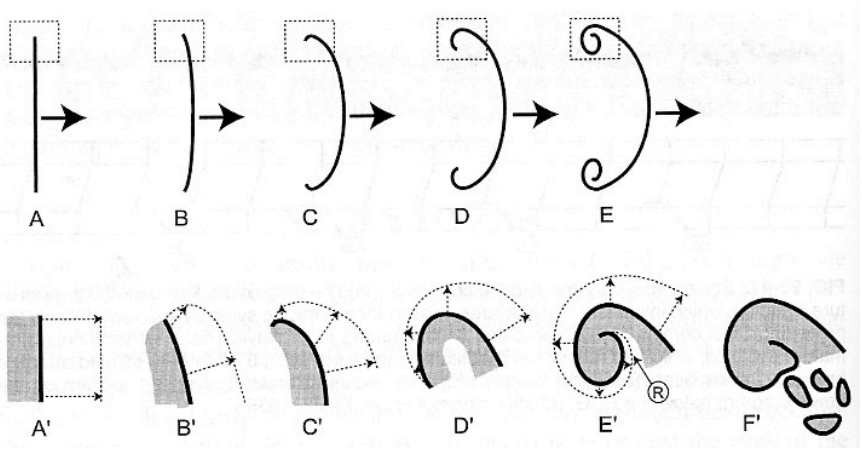

Figure 6. Wavebreak mechanism of VF formation.[8]

The ongoing wavebreaks in VF have been attributed to preexisting anatomical and electrophysiological heterogeneities (e.g. dispersion of refractoriness). Theories based on computer simulations, however, say about dynamic factors, which may combine with preexisting tissue heterogeneities, amplify instability synergetically and promote both initiation and maintenance of VF.[2] Abnormal $[Ca^{2+}]_i$ cycling is among these factors.[2] There is, however, enough of experimentally obtained evidence of the important, even crucial role of $[Ca^{2+}]_i$ in VF.[4]

1.3 Role of Ca^{2+} in VF

Based on the vicious circle theory originally developed by C. E. Zaugg.[4]

1.3.1 Myocyte Ca^{2+} overload initiates ventricular fibrillation

Elevated myocyte $[Ca^{2+}]_i$ (Ca^{2+} overload) is known to be responsible for the initiation of potentially lethal ventricular tachyarrhythmias including VF in various pathological conditions such as digitalis toxicity, myocardial ischemia, or heart failure.[16-19] Specifically, the accumulation of Ca^{2+} in cardiomyocytes has long been suggested to cause delayed afterdepolarizations, triggered activity, and consequently life-threatening ventricular tachyarrhythmias.[19] Accordingly, myocyte Ca^{2+} overload has been shown to be related to the initiation of tachyarrhythmic activity in isolated hearts or in cardiomyocytes of rats or ferrets using bioluminescence or fluorescence of intracellular Ca^{2+} indicators (e.g. aequorin or indo-1).[16,34] Further evidence of the importance of myocyte Ca^{2+} for the vulnerability to VF arises from a close correlation between myocyte Ca^{2+} levels and VF thresholds.[17]

In general, when Ca^{2+} loading of cardiomyocytes becomes sufficiently high, the sarcoplasmic reticulum can generate spontaneous Ca^{2+} oscillations that are not triggered by sarcolemmal depolarizations.[16,18,34] If sufficiently synchronized, these Ca^{2+} oscillations may cause delayed afterdepolarizations and initiate VF or modulate the initiation of VF.[18] Additionally, myocyte Ca^{2+} overload may facilitate the initiation of VF by Ca^{2+}-induced cell-to-cell uncoupling,[19] thereby slowing conduction and amplifying the tendency for reentrant arrhythmias. This tendency is particularly amplified in the hypertrophied heart where repolarization is heterogeneous and refractoriness prolonged.[10] Similarly, mutations in Ca^{2+} handling proteins have been suggested to contribute to hereditary arrhythmias. For example, defective ryanodine type 2 receptors or reduced levels of calsequestrin (a high-capacity Ca^{2+} binding protein expressed inside the sarcoplasmic reticulum), may cause increased Ca^{2+} discharge from the sarcoplasmic reticulum, and consequently ventricular tachyarrhythmias and sudden cardiac death induced by exercise, stress, or heart failure.[35-37]

1.3.2 VF causes myocyte Ca^{2+} overload

Furthermore, myocyte Ca^{2+} and VF are mutually related. Myocyte Ca^{2+} overload can induce VF and conversely, VF itself causes myocyte Ca^{2+} overload.[5,17,38-40] Studies using the Ca^{2+} sensitive fluorescent dye indo-1 in isolated rat hearts suggest that myocyte Ca^{2+} rises biphasically during VF (Fig. 7). In the first 2 min of VF, mean myocyte Ca^{2+} (expressed as fluorescence ratio) rises steeply and rapidly reaches about double of normal levels. Thereafter, myocyte Ca^{2+} continues to rise but at a slower rate.[38-41] Additionally, successful defibrillation (electrical or pharmacological) led to a sudden reduction of VF-induced myocyte Ca^{2+} overload (Fig. 7).[5] In contrast, failed defibrillation shocks did not alter Ca^{2+} [5]. This demonstrates that VF directly and (dependent on VF duration) reversibly causes myocyte Ca^{2+} overload. The Ca^{2+} channel blocker diltiazem (1 μM) largely prevented VF-induced myocyte Ca^{2+} overload in the initial phase of VF [6]; therefore, most of the Ca^{2+} contributing to myocyte Ca^{2+} overload presumably enters the cells through L-type Ca^{2+} channels. This is likely due to the rapid activation rate in VF as the pacing cycle length was inversely related to both the rate and the degree of myocyte Ca^{2+} overload induced by rapid pacing.[17] As VF persists, the contribution of Ca^{2+} entry through L-type Ca^{2+} channels to myocyte Ca^{2+} overload appears to decrease because diltiazem perfusion after 5 min of VF could not prevent myocyte Ca^{2+} to increase further in perfused rat hearts.[5] At this stage, further myocyte Ca^{2+} overload may arise from SR Ca^{2+} release, from reverse Na^{+}/Ca^{2+}-exchange and/or from other sources whereas individual contributions may vary species-dependently.

1.3.3 VF-induced myocyte Ca^{2+} overload maintains VF

As proposed by C. E. Zaugg,[4] independent of the Ca^{2+} source, VF-induced myocyte Ca^{2+} overload contributes to VF maintaining, leading to a self-maintaining vicious circle in which termination of VF becomes increasingly difficult (Fig. 8). Consequently, myocyte Ca^{2+} overload can cause electrical defibrillation to fail and postshock re-induction of VF.[5] It was shown that energy levels for successful electrical defibrillation (defibrillation thresholds) increase as both VF and Ca^{2+} overload progress.[5]

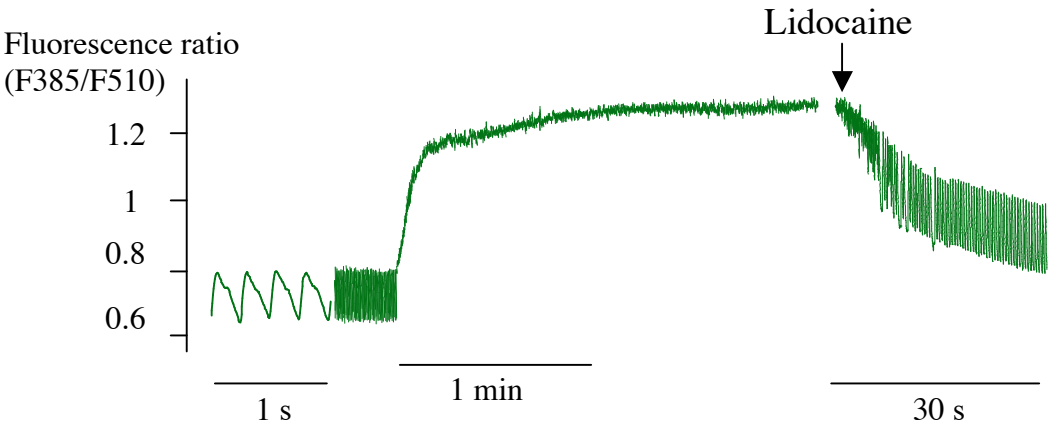

Fig. 7: Original tracings of indo-1 fluorescence ratio transients (F385/F510), an index of myocyte Ca^{2+}, in intact perfused rat hearts after the initiation of sustained VF (induced by 1-min rapid pacing at 20 Hz) and after defibrillation by lidocaine infusion. Note that myocyte Ca^{2+} rises rapidly and steeply upon VF to decrease again upon defibrillation.

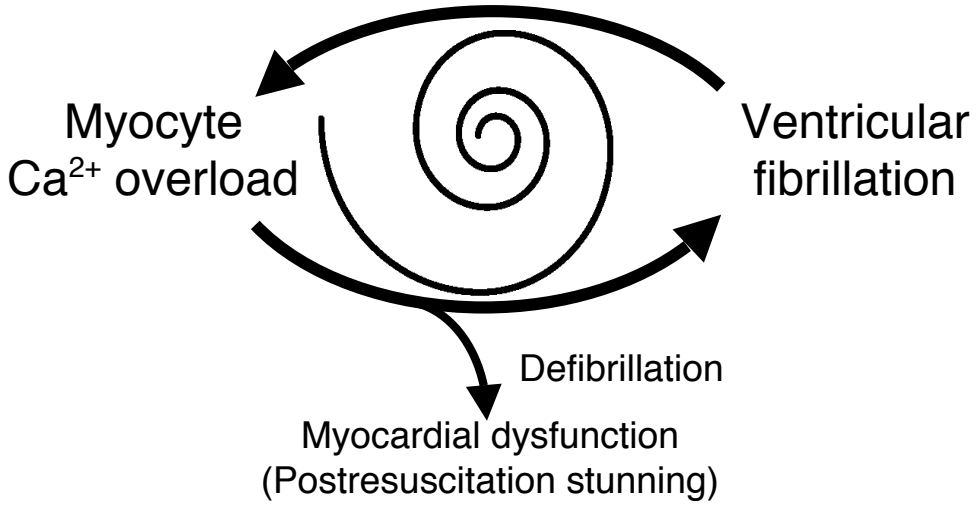

Figure 8: Myocyte Ca^{2+} overload and VF form a vicious circle in which elevated Ca^{2+} can induce VF and conversely, VF promotes Ca^{2+} overload maintaining the arrhythmia. As both VF and Ca^{2+} overload progress, energy levels for successful electrical defibrillation increase (symbolized by spiral). If defibrillation succeeds, VF-induced Ca^{2+} overload may cause postfibrillatory myocardial dysfunction (postresuscitation stunning). From C. E. Zaugg. [4]

So, by manipulating myocyte $[Ca^{2+}]_i$ before defibrillation (increasing extracellular Ca^{2+} during VF in perfused rat hearts) in the above mentioned study a following causal relationship was demonstrated: the longer VF lasts, the higher both myocyte Ca^{2+} concentration and defibrillation threshold rise. This relationship was not due to prolonged myocardial ischemia because the hearts were continuously perfused during VF (normal levels of coronary flow, of coronary effluent pH, and of myocardial O_2 consumption).[6] Moreover, with increasing duration of VF, modulation of intracellular Ca^{2+} gets more difficult. Neither the Ca^{2+} channel blocker diltiazem (in a negative inotropic concentration of 1 μM)[42] nor low extracellular Ca^{2+} (reduction from 3.0 mM to 0.6 mM) could significantly decrease myocyte Ca^{2+} in fibrillating rat hearts.[5] Accordingly, diltiazem or low extracellular Ca^{2+} could not decrease defibrillation thresholds.[5] as previously had been found for verapamil, another Ca^{2+} channel blocker, in pigs.[43] or human beings in vivo.[44] The mechanism by which VF-induced myocyte Ca^{2+} overload increases defibrillation thresholds is probably related to a Ca^{2+}-induced increase in the likelihood of defibrillation shocks to re-induce VF. It has been shown that Ca^{2+} modulates the induction of VF by an electrical stimulus applied during the vulnerable period of repolarization. [17,45] As some portion of the fibrillating myocardium is always repolarizing,[46] myocyte Ca^{2+} overload could increase the likelihood of a shock to reinduce VF. Thus, a shock applied to Ca^{2+} overloaded myocardium may terminate VF but simultaneously re-induce it by stimulating myocardium that is in the vulnerable period of repolarization. Furthermore, the chances for re-induction of VF increase as VF persists because normalization of myocyte Ca^{2+} becomes increasingly difficult. Incomplete reduction of myocyte Ca^{2+} overload after initially successful defibrillation can be followed by synchronized spontaneous Ca^{2+} oscillations from the sarcoplasmic reticulum and subsequent reinduction of VF.[5] Because VF inevitably causes myocyte Ca^{2+} overload, this vicious circle between myocyte Ca^{2+} and VF might be a critical mechanism of failed defibrillation and postshock reinduction of VF. Moreover, this vicious circle concept suggests that the probability of these events is best reduced by early detection and rapid termination of VF to prevent or limit Ca^{2+} overload, and of course to prevent cerebral ischemia.

1.3.4 Myocyte Ca^{2+} overload causes myocardial stunning after defibrillation

Even if the self-maintaining vicious circle of Ca^{2+} and VF is interrupted and defibrillation succeeds, myocyte Ca^{2+} overload continues to cause problems because transitory Ca^{2+} overload that occurs during VF can lead to reduced myofilament Ca^{2+} responsiveness[6] and consequently to postfibrillatory myocardial dysfunction,[6,38] a condition termed postresuscitation stunning.[6] It has been found that the degree of Ca^{2+} overload during VF was inversely associated with the reduction of myofilament Ca^{2+} responsiveness after pacing-induced VF in experiments in isolated rat hearts.[6,38] Accordingly, as Ca^{2+} overload progressed during VF, longer episodes of VF led to a more pronounced myocardial dysfunction than short episodes of VF. Moreover, increasing or decreasing Ca^{2+} overload during VF led to parallel changes in myofilament Ca^{2+} responsiveness (estimated as ratio of left ventricular developed pressure over myocyte Ca^{2+} transient amplitudes). The molecular mechanisms whereby transitory Ca^{2+} overload undermines contractile protein function seem to be related to proteolysis that is mediated at least partly by Ca^{2+}-activated proteases (calpains).[47] The substrates of calpains with respect to cardiac myofibrillar proteins include troponin I, troponin T, and others.[47]

1.4 Sodium-Calcium exchange and its physiological function

Na^+/Ca^{2+}-exchange promotes electrogenic exchange of Na^+ and Ca^{2+} across the plasma membrane in either the Ca^{2+}-efflux or Ca^{2+}-influx mode, depending on the electrochemical gradients of the substrate ions. Thus, Na^+/Ca^{2+}-exchange is modulated by electrical activity of cardiac myocytes. The electrogenic properties of Na^+/Ca^{2+}-exchange are due to stochiometry of exchange: 3 Na^+ for 1 Ca^{2+};[48-50] therefore, net positive charge moves in the direction of Na^+. The Na^+/Ca^{2+}-exchange operation mode when Na^+ is moved inside and Ca^{2+} outside the cell is called forward while the opposite mode is called reverse.[51] The primary function of Na^+/Ca^{2+}-exchange in the heart is extrusion of Ca^{2+} from myocytes during relaxation and diastole, which balances Ca^{2+} entry via L-type Ca^{2+} channels during cardiac excitation.[52] Na^+/Ca^{2+}-exchange extrudes ≈30% of the Ca^{2+} required to activate the myofilaments in rabbit, guinea pig, and human ventricles but a much smaller portion (≈7%) in rat and mouse ventricles.[25] SERCA removes most of the remaining Ca^{2+}. In failing rabbit or human heart, Na^+/Ca^{2+}-exchange and SERCA contribute nearly equally to Ca^{2+} removal from the cytoplasm.[24] The SR Ca^{2+} load, a predominant determinant of cardiac contractility, is determined by the competition between SERCA and Na^+/Ca^{2+}-exchange for the cytosolic Ca^{2+}.[24] Therefore, modulation of Na^+/Ca^{2+}-exchange activity by physiological regulatory factors as well as by alterations in cytosolic ion concentrations and the action potential duration exerts profound influence on the overall contractile function of the heart.[53] Thermodynamic basis for direction of the ion transport by Na^+/Ca^{2+}-exchange is the following. For electrochemical gradient favoring extrusion of one Ca^{2+} ion in exchange for 3 Na^+ ions is, it can be written:

$$n(E_{Na+} - E_m) > 2(E_{Ca2+} - E_m);$$

here n is the coupling ratio, E_m is the membrane potential and E_{Na+} and E_{Ca2+} are the equilibrium potentials for Ca^{2+} and Na^+.[54] For n=3 the potential at which the gradients are equal ($E_{Na+/Ca2+}$) is the E_m at which the total current ($I_{Na+/Ca2+}$) is zero. Therefore,

$$E_{Na+/Ca2+} = 3E_{Na+} - 2E_{Ca2+}$$

Thus, whenever E_m is more positive than $E_{Na+/Ca2+}$ Ca^{2+} entry via the Na^+/Ca^{2+}-exchange is favored and vise versa, when E_m is more negative Ca^{2+} extrusion is favored. For typical diastolic values of $[Na^+]_o$ = 140, $[Na^+]_i$ = 8.9 mM and $[Ca^{2+}]_i$ = 150 nM, $[Ca^{2+}]_o$ = 2 mM estimated $E_{Na+/Ca2+}$ would be –32.6 mV. Fig. 9 illustrates the changes happening during cardiac action potential in rabbit ventricle. A very brief period when Ca^{2+} influx via Na^+/Ca^{2+}-exchange is favored ($E_m > E_{Na+/Ca2+}$) is shaded (Fig 9 A). The length of this period is sensitive to changes of peak $[Ca^{2+}]_i$, the time course of the Ca^{2+} transient, $[Na^+]_i$, and the shape of the action potential.[26] Increasing intracellular $[Na^+]_i$ from 8.9 to 12.7 mM (Fig. 9 B) prolongs the time when Ca^{2+} influx is favored, even though peak $[Ca^{2+}]_i$ is much higher. The lower panels show changes of the thermodynamic driving force. (E_m – $E_{Na+/Ca2+}$).[26]

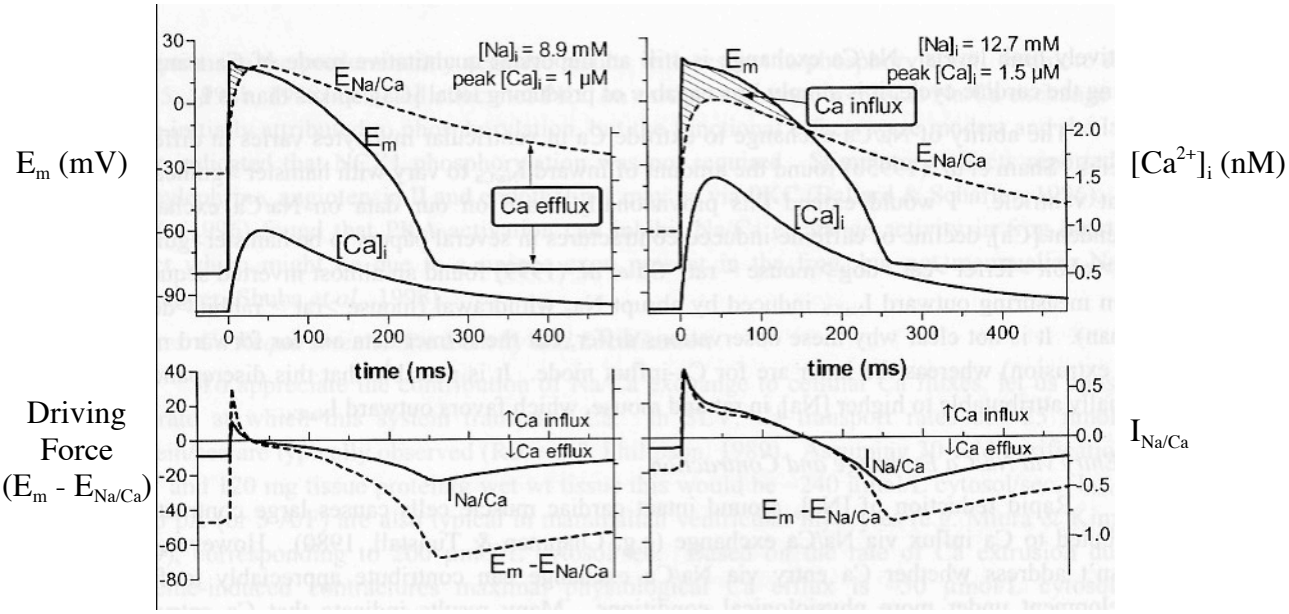

Figure 9. Changes of direction of ion transport by Na^+/Ca^{2+}-exchange caused by changes of electrochemical gradients during an action potential in rabbit ventricle.[26] Abbreviations: E_m membrane potential $E_{Na/Ca}$ elquilibrium potential for Na^+/Ca^{2+}-exchange, $I_{Na/Ca}$ current through Na^+/Ca^{2+}-exchange. From D. Bers, 2002.[26]

Na^+/Ca^{2+}-exchange is capable to trigger the release of Ca^{2+} from the SR during membrane depolarization, although much less efficient than the L-type Ca^{2+} channels.[23,48,55] Eventually, Na^+/Ca^{2+}-exchange acts synergistically providing additional Ca^{2+} entry and

amplifying the triggering effect of L-type Ca^{2+} channels on SR Ca^{2+} release.[56] In heart failure enhanced Ca^{2+} entry due to increased Na^{+}/Ca^{2+}-exchange expression may provide inotropic support for failing myocytes, in which the SR function is often defective.[51,57] Under other pathological conditions, such as cardiac ischemia/reperfusion[58] or digitalis intoxication,[59] the Na^{+}/Ca^{2+}-exchange -mediated increase in Ca^{2+} entry or decrease in Ca^{2+} exit due to a rise in $[Na^{+}]_i$ results in Ca^{2+} overload of the SR, leading to mechanical and electrical dysfunction of myocytes. As was mentioned in the previous section, Na^{+}/Ca^{2+}-exchange may be an important source of Ca^{2+} in persisting VF, supervening L-type Ca^{2+} channels, which are considered to be important for VF initiation. Therefore, the goals of the present study were the following.

2. GOALS OF THE STUDY

1. To determine, to what extend $[Ca^{2+}]_i$ can rise during VF. To do this, we calibrated fluorescence of the intracellular Ca^{2+} indicator indo-1 to $[Ca^{2+}]_i$ in cardiomyocytes.

2. To determine the ways of Ca^{2+} entry into cardiac myocytes during VF. A former study has shown that at the initial stage of VF Ca^{2+} enters cardiomyocytes to a large extend via L-type Ca^{2+} channels.[6] We decided to check whether Na^+/Ca^{2+}-exchange also contributes to Ca overload during initial phase of VF and to compare its role with the role of L-type Ca^{2+} channels.

3. Additionally, we decided to check whether Na^+/Ca^{2+}-exchange is important as a Ca^{2+}-source for maintaining VF.

To this end, we performed experiments measuring intracellular Ca^{2+} concentration by surface fluorometry of dye indo-1 in isolated perfused rat hearts. The role of L-type Ca^{2+} channels in VF was tested using nifedipine, a specific blocker of these channels. The role of Na^+/Ca^{2+}-exchange was tested using KB-R7943, a specific blocker of the reverse mode of Na^+/Ca^{2+}-exchange.

3. METHODS

3.1 The Langendorff perfusion system according to Schuler

In our experiments we used the Langendorff perfusion system according to Schuler (Hugo Sachs Elektronik–Harvard Apparatus, March-Hugstetten, Germany). This system allows perfusion of the heart under stable and reproducible conditions at constant perfusion pressure or constant flow and has been proved by more than 100 years of use in various types of experiments on isolated heart. The general idea of this method is, that an isolated heart can be kept alive outside the body if it receives oxygen and nutrients through the coronary circulation. The aorta of the heart is tied to the canula filled with blood at a hydrostatic pressure corresponding to a diastolic pressure of the mammalian circulation system (≈ 80 mm Hg). Perfusion is done retrogradely. After passing the aorta, the blood through the orifices of the coronary arteries gets into the coronary circulation and supplies the heart with the necessary nutrients and oxygen. After flowing through the coronary vascular system, the blood passes the coronary sinus and flows into the right atrium. Then the blood leaves the heart via the openings of caval veins or the pulmonary artery. Initially isolated hearts have been perfused with blood but very soon it was found that it can be substituted with an oxygenated glucose-containing saline medium.

The Langendorff system according to Schuler is shown at Fig. 10. The perfusate is transferred from a stock bottle by a peristaltic pump into a temperated (37.0°C) oxygenator. A sling disk spreading the perfusate out over the entire inner surface of the oxygenator provides efficient oxygenation and heating. Additionally we bubbled the perfusate with a gas mixture containing 95% O_2 and 5% CO_2, which resulted in a partial oxygen pressure 600-650 mm Hg. The surplus of the gas goes into a water filled column (Gottlieb valve) where by adjusting the immersing depth a constant perfusion pressure of the Schuler system is provided. The in vivo perfusion pressure of warm-blooded rat hearts corresponds to a large extent to their diastolic aortic pressure, normally between 70 and 90 mm Hg. Thus, the recommended perfusion pressure for the isolated rat heart is around 80 mm Hg.[60] A constant perfusate level is maintained with the help of two contact

electrodes placed inside the temperated oxygenator controlling a connected circulating pump.

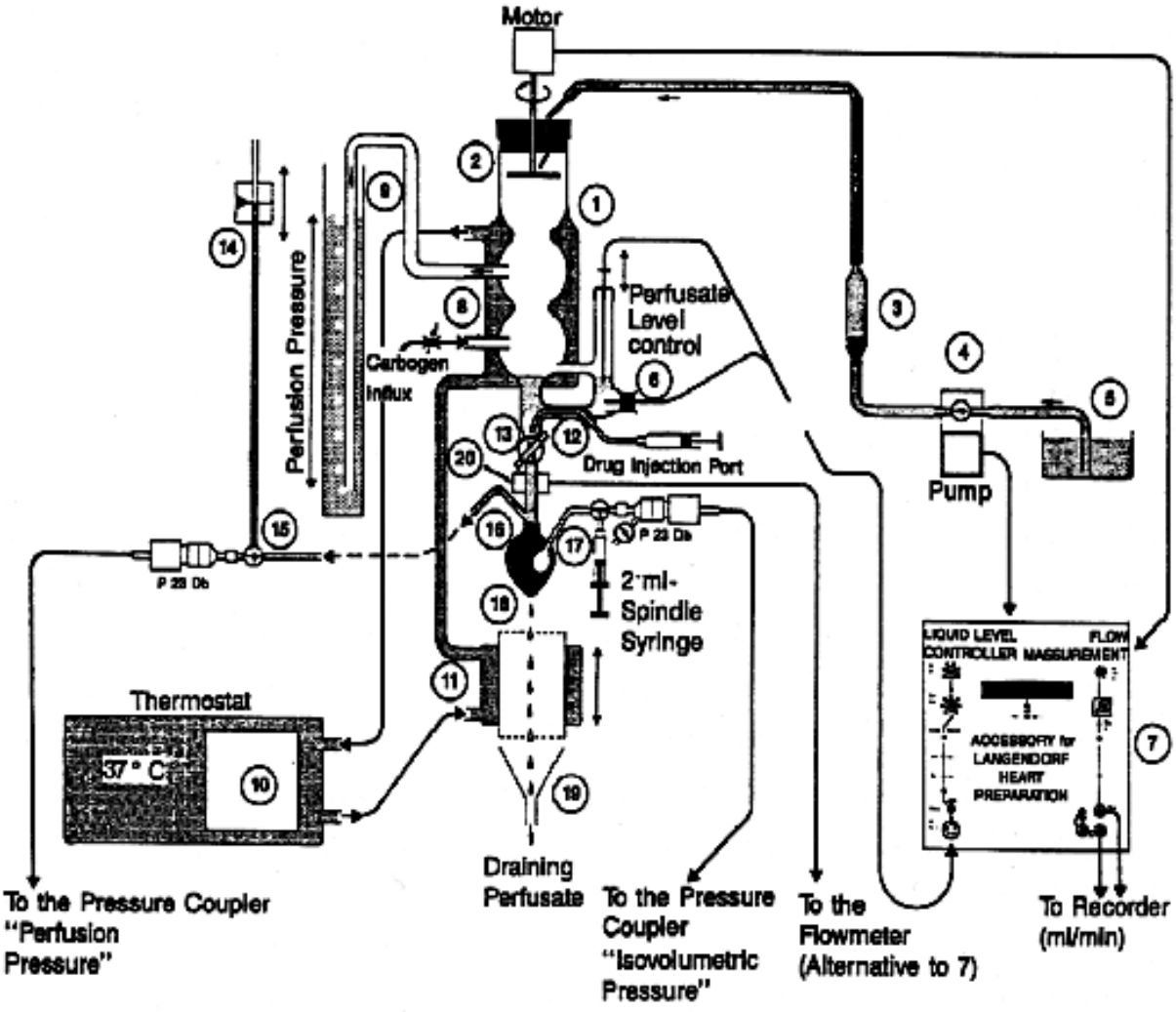

Figure 10. A Langendorff perfusion system according to Schuler.[61]
Figures indicate: 1. Oxygenator; 2. Sling disc; 3. Non-return valve; 4. Gear pump for perfusion solution (perfusate); 5. Supply vessel for perfusate; 6. Contact electrode for perfusate level control; 7. Electronic control for measurement of flow; 8. Inlet and outlet for gas; 9. Gotlieb valve for perfusion pressure adjustment; 10. Thermostat; 11. Heart recipient; 12. Tube catheter for drug addition by way of injection syringe; 13. Stopcock; 14. Water manometer or mechanoelectric pressure transducer for perfusion pressure; 15. Three-way cock; 16. Aortic canula with side nozzle; 17. Balloon catheter with pressure transducer for isovolumetric measurement of ventricular pressure; 18. Heart; 19. Collective funnel for perfusate dripping off the heart; 20. Flowprobe.

3.2 Measurement of physiological variables

Coronary flow was measured within the aortic canula using an inline flowprobe (Transonic 2N) connected to a transit time flowmeter (Transonic TTFM-SA type 700, Hugo Sachs Elektronik-Harvard Apparatus, March-Hugstetten, Germany).
Left ventricular (LV) pressure was measured by a fluid-filled polyethylene catheter inserted into the LV cavity through the left atrial appendage. The catheter was connected to a pressure transducer (MLT1050 Pressure transducer, AD Instruments, Castle Hill, Australia). Left ventricular (LV) developed pressure (LVDP) was defined as the difference between systolic and diastolic values of LV pressure. Simultaneously, a bipolar electrocardiogram (ECG) was recorded using electrodes implanted superficially in the outflow tract of the right ventricle and in the apex of the heart. Ventricular pacing was carried out using a pair of platinum wire electrodes connected to a pulse generator (Grass S9, Grass Instruments, Quincy, MA, USA). The pacing electrodes were implanted in the right ventricular free wall below the circular cut for $[Ca^{2+}]_i$ measurement (see 5.4.4.5). A digitized readout of the LV pressure and the ECG was recorded at 200 Hz sampling rate throughout the experiment using PowerLab 8e (AD Instruments, Castle Hill, Australia) connected to a Macintosh computer (Apple, Cupertino, CA, USA) running Chart software (AD Instruments, Castle Hill, Australia). Cardiac rate was computed from the digitized ECG using Chart software.

3.3 Animals and perfused heart preparation

3.3.1 Choice of the animal model

We carried out experiments on isolated perfused rat hearts. In these hearts changes of $[Ca^{2+}]_i$ can be measured accurately using indo-1 at high time resolution even during VF.[17,39,42] Because isolated rat hearts easily return to sinus rhythm after electrically induced VF, repeated estimation of Ca^{2+} accumulation during VF in the same heart preparation is possible.[Lubbe WF, 1975 #1] The central role of Ca^{2+} in excitation-contraction coupling in cardiac muscle[25] suggests that VF leads to Ca^{2+} overload in most

mammalians including human beings.[4] However, relative contribution of the sarcoplasmic reticulum, of L-type Ca^{2+} channels and of Na^{+}/Ca^{2+}-exchange to $[Ca^{2+}]_i$ varies depending on species.[25] Nevertheless, although different sources of Ca^{2+} overload during VF may contribute not to the same extend, the fundamental difference between adult human and rat ventricles is not expected.[4] Based on these considerations we have chosen isolated rat heart as the model for our experiments.

3.3.2 Preparation of isolated hearts

Treatment of animals conformed to the rules of the Swiss Federal Act on Animal Protection (1998), and was approved by the veterinary department of Basel (Switzerland). Male Sprague-Dawley rats (Charles River Laboratories, France) weighing 390-510 g were anesthetized by intraperitoneal injection of 30 mg/kg pentobarbital (Nembutal, Abbot Laboratories, Chicago, IL, USA). After midline sternotomy, the ascending aorta was clamped at the aortic arch and the heart was cut out together with the lungs within a few seconds and immersed immediately into an ice-cold modified Krebs-Henseleit buffer solution (composition is given in Table 1) in order to provide cardioplegia. The aorta was quickly prepared and fixed with a clamp to the canula of the Langendorff perfusion system with a partly open inline cock. After cannulation the inline cock was immediately open completely and the aorta was tied around the canula with a string. The whole procedure lasted in general less than 60 sec. Thereafter the right ventricular outflow tract was cut open, the pulmonary vessels were ligated at the hilus and the lung tissue was removed. A small incision was made in the left atrium and a pressure catheter was inserted through the mitral valve into the left ventricle and tied with the surgery string at the appendix (Zaugg et al., 1996b). Perfusion was performed retrograde via the aorta at a constant pressure of 80 mm Hg using the same nonrecirculating solution at 37°C, pH 7.4, saturated with gas mixture of 95% O_2 and 5% CO_2.

Compound	Concentration
NaCl	117.0 mmol/L
KCl	4.3 mmol/L
$MgCl_2$	1.2 mmol/L
$CaCl_2$	2.0 mmol/L
$NaHCO_3$	25.0 mmol/L
EDTA	0.5 mmol/L
Glucose	15.0 mmol/L
Albumin	10.0 mg/L

Table 1. Composition of the modified Krebs-Henseleit perfusion solution.
At a certain stage of experiments 4.5 mM instead of 2 mM $CaCl_2$, was used providing 4 mM instead of 1.5 mM effective concentration of Ca^{2+} in the perfusate (see experimental protocols).

3.4 Measuring intracellular Ca^{2+}

3.4.1 General information

The importance of measuring concentrations of intracellular Ca^{2+} ($[Ca^{2+}]_i$) is determined by the key role played by this ion in nearly all types of cells extending far beyond coupling of excitation to contraction in cardiac and skeletal muscles.[62] Therefore, especial tools such as fluorescent dyes have been developed over decades of research. Chemical substances of such type are also used for assessment of intracellular concentrations of other important ions (e.g. Na^+, K^+, Mg^{2+}). When loaded into the cytosol of investigated cells they change fluorescence parameters upon changing of the ion concentration. For example, a rise of $[Ca^{2+}]_i$ leads to binding of Ca^{2+} ions to the molecules of fluorescent dye fluo-3 resulting in prominent (≈100 times) increase of its fluorescence intensity. Dyes of

another type shift the wavelengths of fluorescence excitation or emission upon binding of an ion. For example, fluorescent indicator fura-2 shifts the wavelength of maximally efficient excitation when it binds Ca^{2+} while the wavelength of emission stays nearly the same. In our study we used fluorescent indicator indo-1. This dye shifts the wavelength of maximal emission upon binding of Ca^{2+} while shift of the excitation wavelength is negligible (Fig. 11); changes of $[Ca^{2+}]_i$ are evaluated by comparing ratio of fluorescence intensities at the two wavelengths, so the indicators of such type are called ratiometric.

Fura-2 and indo-1 were synthesized by *Grynkiewicz G. et al., 1985* [63] in the University of California. Since then indo-1 became the tool of choice for quantitative measurement of fast $[Ca^{2+}]_i$ transients in contractile cells and tissues such as heart and skeletal muscles while fura-2 is mostly used for imaging slow changes of $[Ca^{2+}]_i$. Shift of wavelength upon binding Ca^{2+} ions is the main advantage of ratiometric dyes because the ratio of fluorescence intensities F_1 and F_2 at two wavelengths λ_1 and λ_2 is in principle sufficient to calculate $[Ca^{2+}]_i$ (Fig. 12); this ratio is independent of total dye concentration, optical path length, or absolute sensitivity of the instrument.[63]

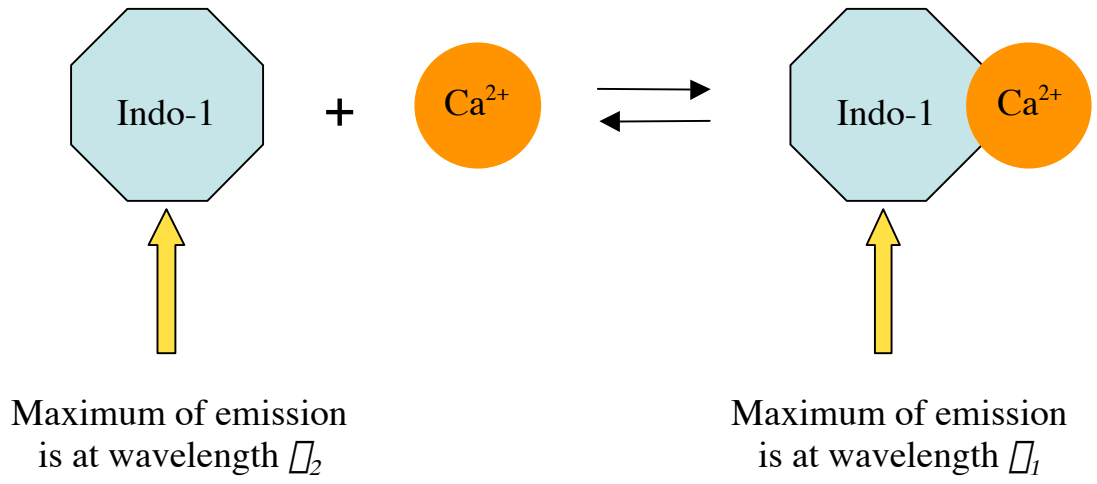

Figure 11. Interaction of fluorescent indicator indo-1 with Ca^{2+} leads to the shift of the emission wavelength (ratiometric indicator).

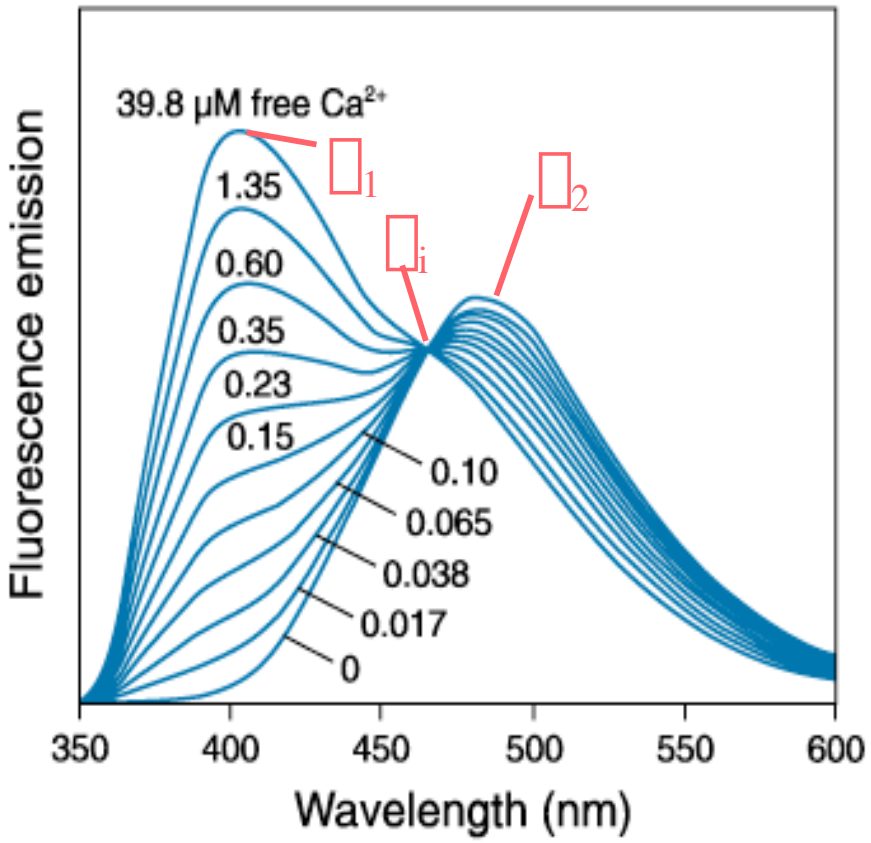

Figure 12. Emission spectra of indo-1 in solutions with different concentrations of free Ca^{2+} (0 - 39.8 μM); λ_1 and λ_2 designate maximal emission wavelengths of Ca^{2+} -bound and Ca^{2+} -free indo-1, respectively; λ_i is a so called isofluorescent point, a wavelength at which emission does not depend on $[Ca^{2+}]_i$.[64]

3.4.2 Principles of $[Ca^{2+}]_i$ calculation using fluorescence ratio

The group, which has synthesized the ratiometric dyes,[63] has also developed the theory for calculating $[Ca^{2+}]_i$ using fluorescence ratio. Fluorescence intensity F at a given wavelength can be expressed as:

$$F = S*c \qquad (1)$$

Here c is a concentration of a fluorescent dye in a solution and S is a proportionality coefficient of fluorescence specific for this fluorescent dye at this wavelength. All molecules of indo-1 in cytosol can be considered as two chemical species: Ca^{2+} - bound and Ca^{2+} - free (Fig. 11) with concentrations cb and cf and fluorescence proportionality coefficients, Sb and Sf, correspondingly. So, indo-1 fluorescence at any wavelength λ can be expressed as:

$$F_{\lambda} = Sb_{\lambda}*cb + Sf_{\lambda}*cf \qquad (2)$$

Designating wavelengths of peak fluorescence intensity for Ca^{2+} -bound and Ca^{2+} -free indo-1 as λ_1 and λ_2, (Fig. 12), four *S* coefficients can be written:

Sf_1 and Sf_2 - for Ca^{2+} -free dye measured at wavelengths λ_1 and λ_2;
Sb_1 and Sb_2 - for Ca^{2+} -bound dye at λ_1 and λ_2, correspondingly.

Therefore, the fluorescence intensities F_1 and F_2 at the wavelengths λ_1 and λ_2 can be expressed as:

$$F_1 = Sf_1*cf + Sb_1*cb \qquad (3a);$$

$$F_2 = Sf_2*cf + Sb_2*cb \qquad (3b).$$

Correspondingly, the ratio of fluorescence at two wavelengths can be expressed as:

$$R = \frac{F_1}{F_2} = \frac{Sf_1*cf + Sb_1*cb}{Sf_2*cf + Sb_2*cb} \quad (4).$$

Indo-1 forms complex with Ca^{2+} 1:1 (Fig. 11). Therefore, *cf* and *cb* are related to $[Ca^{2+}]_i$ according to equation:

$$cb = \frac{cf * [Ca^{2+}]_i}{K_d} \qquad (5)$$

Where K_d is the effective dissociation constant. We can substitute *cb* in the equation (4) for the expression at the right side of the equation (5), cancel *cf* out and transform the resulting equation in order to express $[Ca^{2+}]_i$:

$$R = \frac{F_1}{F_2} = \frac{Sf_1*\cancel{cf} + Sb_1*\cancel{cf} * [Ca^{2+}]_i / K_d}{Sf_2*\cancel{cf} + Sb_2*\cancel{cf} * [Ca^{2+}]_i / K_d}$$

$$R = \frac{Sf_1 + Sb_1 * [Ca^{2+}]_i / K_d}{Sf_2 + Sb_2 * [Ca^{2+}]_i / K_d} \quad (7)$$

$$\Downarrow$$

$$R*Sf_2 + R*Sb_2*[Ca^{2+}]_i / K_d = Sf_1 + Sb_1*[Ca^{2+}]_i / K_d$$

$$\Downarrow$$

$$R*Sb_2*[Ca^{2+}]_i / K_d - Sb_1*[Ca^{2+}]_i / K_d = Sf_1 - R*Sf_2$$

$$\Downarrow$$

$$[Ca^{2+}]_i * (R*Sb_2 - Sb_1) = K_d * (Sf_1 - R*Sf_2)$$

$$\Downarrow$$

$$[Ca^{2+}]_i = K_d * \frac{Sf_1 - R*Sf_2}{R*Sb_2 - Sb_1} \quad (8)$$

The expression (8) for $[Ca^{2+}]_i$ is modified further by introducing further constants representing combinations of the already known fluorescence constants *S* from equations (3):

$$\frac{F_1^{min}}{F_2^{min}} = \frac{Sf_1}{Sf_2} = R^{min} \quad (9); \qquad \frac{F_1^{max}}{F_2^{max}} = \frac{Sb_1}{Sb_2} = R^{max} \quad (10);$$

$$\frac{F_1^{min}}{F_1^{max}} = \frac{Sf_1}{Sb_1} = S_1 \quad (11); \qquad \frac{F_2^{min}}{F_2^{max}} = \frac{Sf_2}{Sb_2} = S_2 \quad (12);$$

Here R^{min} and R^{max} correspond to the limiting values of *R* at zero and saturating $[Ca^{2+}]_i$, respectively; S_2 is a ratio of the longer and S_1 of the shorter wavelength fluorescence intensities at zero and saturating $[Ca^{2+}]_i$, respectively. The equation (8) can be modified now in the following way:

$$[Ca^{2+}]_i = K_d * \frac{(Sf_1 - R * Sf_2) / Sf_2}{(R*Sb_2 - Sb_1) / Sb_2} * \frac{Sf_2}{Sb_2} \quad .$$

$$\Downarrow$$

$$[Ca^{2+}]_i = K_d * \left(\frac{R^{min} - R}{R - R^{max}}\right) * S_2 ; \quad .$$

rewritten in another way:

$$[Ca^{2+}]_i = K_d * S_2 * \left(\frac{R - R^{min}}{R^{max} - R}\right) \qquad (12)$$

This basic equation for measuring $[Ca^{2+}]_i$ using a ratiometric dye resembles an expression for a fluorescent dye with a peak fluorescence at a single wavelength:[63]

$$[Ca^{2+}]_i = K_d \left(\frac{F - F^{min}}{F^{max} - F}\right) \qquad (13)$$

Equation (13) in contrast to (12) requires that F, F_{min}, and F_{max} all be determined at the same effective total concentration of fluorescent dye.[63] This is not satisfied in an isolated perfused heart model because of constant dye leaking from the cytosol of cardiomyocytes followed by removal with a nonrecirculating perfusate.

3.4.3 Measuring $[Ca^{2+}]_i$ using fluorescence ratio in isolated rat heart

3.4.3.1 Difficulties of fluorescence measurement in isolated heart

Estimating $[Ca^{2+}]_i$ in isolated hearts using fluorescent indicators is difficult. Experiments of such type performed in isolated cells/tissue or in cell/tissue culture are known as a routine established over the decades the fluorescent indicators have been in use. Application of the same technique to an isolated heart, however, is far less practicable. A simple test shows the following. Entering a combination of words "*indo-1, isolated*

cardiac myocytes" in sum with "*indo-1, cultured cardiac myocytes*" in a Medline (http://www.ncbi.nlm.nih.gov/entrez/query.fcgi) gives 97 search results (this search does not include another combinations, like "*isolated cardiomyocytes*" or "*cultured cardiomyocytes*"; it also does not take into account isolated/cultured heart tissue). Entering a combination "*indo-1, isolated perfused heart*" gives 33 search results. This is considering numerous reviews citing both types of the technique application and in spite of the fact that many important questions to intracellular $[Ca^{2+}]_i$ handling could be only answered if tested in isolated heart or are more correct to be tested in isolated heart. The reason for such disparity is the difficulty of fluorescence measurement experiments in isolated heart. It is more difficult to provide proper and sufficient loading of fluorescent dye into the cells of the whole heart compare to isolated cells/tissue. Accordingly, it is more difficult to provide stable conditions from one experiment to another in order to obtain comparable results. Finally, it is more difficult to obtain a reliable fluorescence signal from the contracting hearts.

3.4.3.2 Importance of calibrating fluorescence signal to $[Ca^{2+}]_i$

Many authors perform fluorescence measurements and present their data without relating them to any $[Ca^{2+}]_i$. They show only raw fluorescence ratio and its relative changes. Although acceptable, it is still not the best way for the following reasons.

Accumulation of Ca^{2+} in cytosol of cardiomyocytes during VF is a crucial destructive factor. Progressively increasing $[Ca^{2+}]_i$ contributes to maintain VF, leading to a self-maintaining vicious circle[4] and reducing chances for resuscitation[5]. Ca^{2+}-activated proteases (calpain)[47] can damage contractile elements, such as tropoinin I, tropoinin T and others[47] that results in stunning during reperfusion after defibrillation.[6,38] Therefore, it is important to know $[Ca^{2+}]_i$ in order to be able to judge about extend of Ca^{2+} accumulation.

According to equation (12) relation between fluorescence ratio R and $[Ca^{2+}]_i$ is not linear. Fig. 13 shows graphic dependence of $[Ca^{2+}]_i$ on R with R^{max} obtained in our calibration experiments, R^{min} and S_2 calculated and K_d obtained by [65] in a protein mixture solution simulating intracellular conditions of rat cardiomyocytes. With bigger R $[Ca^{2+}]_i$ increases

faster (Fig. 13); at high fluorescence ratio (R>2), with any given increment of R, $[Ca^{2+}]_i$ increases ≈ 10 and more times more rapidly, compared to increase with the same increments of R at smaller R (≈1). In order to estimate how much $[Ca^{2+}]_i$ exceeds physiological range during VF, one should determine, which part of this curve is covered by $[Ca^{2+}]_i$ changes at physiological and pathological conditions. Therefore, calibration of $[Ca^{2+}]_i$ to fluorescence ratio R is important.

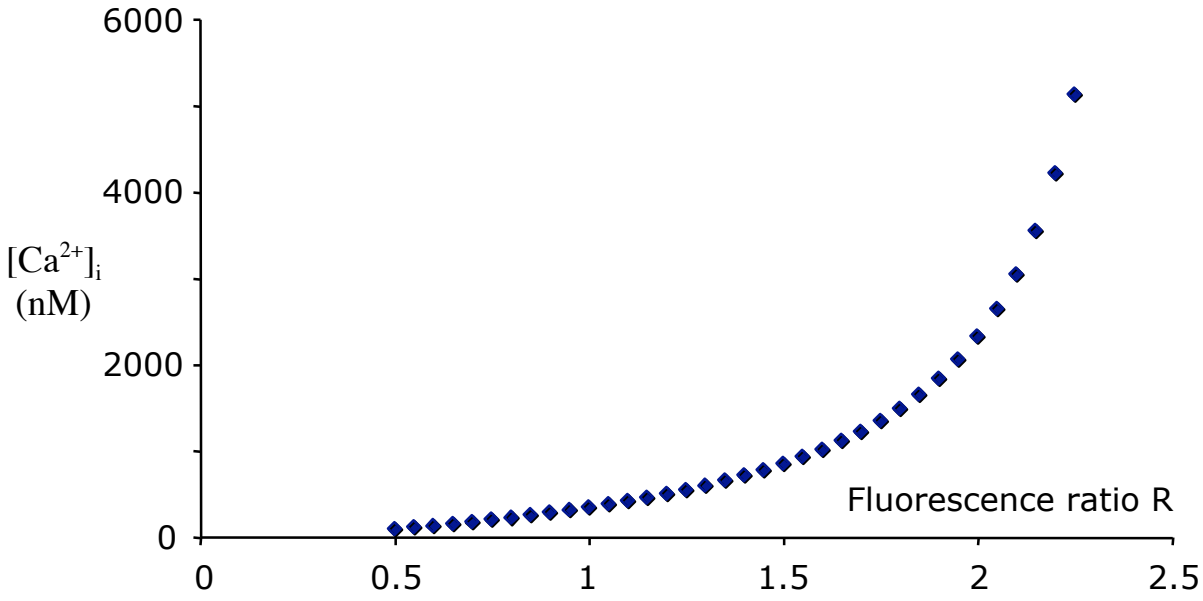

Figure 13. Graphical dependence of $[Ca^{2+}]_i$ on fluorescence ratio R based on equation (12) with constants R^{max} obtained in our calibration experiments, R^{min} and S_2 calculated (see below) and K_d obtained by Baker et al., 1994.[65]

3.4.3.3 Problems of calibration

The authors presenting their data as raw fluorescence ratio do so because calibration of fluorescence to $[Ca^{2+}]_i$ is complicated by some specific problems. Calibration in a solution it straightforward: by measuring parameters of fluorescence of a solution containing known fixed concentrations of Ca^{2+} the corresponding values of fluorescence ratio, including R^{max} and R^{min}, are obtained and S_1 , S_2 and K_d are calculated. However, parameters of fluorescence *in vitro* and *in vivo* are not the same and differ as much as an intracellular environment differs from any buffered solution. So, in order to get proper quantitation of $[Ca^{2+}]_i$, calibration has to be done *in vivo*. It is difficult, however, to fix an intermediate $[Ca^{2+}]_i$ in living cells/tissues and impossible to do it in an isolated heart. So, usually in cells K_d and S_2 are not determined and calibration is only performed with limiting concentrations of $[Ca^{2+}]_i$. High $[Ca^{2+}]_i$ concentration for saturating the fluorescent indicator in order to determine R^{max}, which is relatively easy. "Zero" $[Ca^{2+}]_i$ in order to determine R^{min}, which is difficult because fluorescence signal at such conditions is unstable: some amount of $[Ca^{2+}]_i$ has tendency to remain in cytosol [66,67]. Determination of S_2 and K_d in contractile cells requires control over many conditions and has been performed not often.[68] Calibration with determination of only R^{max} and R^{min} is done by many research groups on a regular base; usually the absolute values of $[Ca^{2+}]_i$ obtained in such experiments are to a large extend arbitrary and only relative changes of $[Ca^{2+}]_i$ are important.[62]

Possibilities to determine fluorescence constants and calibrate $[Ca^{2+}]_i$ in isolated heart are even more limited. First calibration of $[Ca^{2+}]_i$ in isolated rat heart with R^{max} measured in the whole heart was performed by *Brandes R. et al., 1993* [69,70]. Based on obtained R^{max} and using S_1 and S_2 obtained in a protein solution they calculated R^{min}; K_d = 250 nM obtained in a buffered saline solution was chosen arbitrary. Later on this group calibrated K_d in a protein solution mimicking intracellular environment of rat cardiomyocytes.[65] Interestingly, the results of this calibration were rarely applied afterwards to an isolated heart even by the authors who made it. In one of the later experiments performed on isolated perfused rat heart [71] co-authors of this group (not including R. Brandes who made the practical part of the calibration experiment) normalized $[Ca^{2+}]_i$ and expressed changes

as % of baseline. In further experiments,[72-74] they abandoned the isolated perfused rat heart model in favor of isolated rat heart trabeculae. However, this group has found an important relation between fluorescence intensities at two detection wavelengths, which they applied for the calibration of $[Ca^{2+}]_i$ using indo-1 fluorescence in isolated rat hearts.[70]

3.4.3.4 Theory of calibration of fluorescence ratio to $[Ca^{2+}]_i$ in isolated heart

We used mathematical formulas developed by *Brandes R. et al., 1993* [70] for $[Ca^{2+}]_i$ calibration in isolated perfused rat heart. Their calculation was based on the following considerations. According to equation (13) $[Ca^{2+}]_i$ can be estimated, in principle, by measuring fluorescence at each of wavelengths used for ratiometric measurements. So, from measurement at λ_1 $[Ca^{2+}]_i$ equals:

$$[Ca^{2+}]_i = K_d \left(\frac{F_1^{min} - F_1}{F_1 - F_1^{max}} \right) \qquad (14);$$

Correspondingly, from measurement at λ_2 :

$$[Ca^{2+}]_i = K_d \left(\frac{F_2^{min} - F_2}{F_2 - F_2^{max}} \right) \qquad (15).$$

Since $[Ca^{2+}]_i$ is independent on the wavelength of fluorescence measurement:

$$\cancel{K_d} \left(\frac{F_1^{min} - F_1}{F_1 - F_1^{max}} \right) = \cancel{K_d} \left(\frac{F_2^{min} - F_2}{F_2 - F_2^{max}} \right)$$

$$\Downarrow$$

$$(F_1 - F_1^{min}) * (F_2^{max} - F_2) = (F_2 - F_2^{min}) * (F_1^{max} - F_1)$$

$$\Downarrow$$

$$F_2^{max}F_1 - F_1F_2 - F_1^{min}F_2^{max} + F_1^{min}F_2 = F_1^{max}F_2 - F_1F_2 - F_2^{min}F_1^{max} + F_2^{min}F_1$$

$$\Downarrow$$

$$F_1^{min}F_2 - F_1^{max}F_2 = F_2^{min}F_1 - F_2^{max}F_1 + F_1^{min}F_2^{max} - F_2^{min}F_1^{max}$$

$$\Downarrow$$

$$F_2(F_1^{min} - F_1^{max}) = F_1(F_2^{min} - F_2^{max}) + F_1^{min}F_2^{max} - F_2^{min}F_1^{max}$$

$$\Downarrow$$

$$F_2 = F_1 * \frac{(F_2^{min} - F_2^{max})}{(F_1^{min} - F_1^{max})} + \frac{F_1^{min}F_2^{max} - F_2^{min}F_1^{max}}{(F_1^{min} - F_1^{max})} \qquad (16)$$

After denoting $\frac{(F_2^{min} - F_2^{max})}{(F_1^{min} - F_1^{max})} = b$ (17a) and $\frac{F_1^{min}F_2^{max} - F_2^{min}F_1^{max}}{(F_1^{min} - F_1^{max})} = a$ (17b)

equation (16) can be rewritten as: $F_2 = F_1 * b + a$ (18).

So, the fluorescence intensities F_1 and F_2 are related linearly. Since they change constantly with each heart cycle due to change of $[Ca^{2+}]_i$, by plotting them against each other parameters b and a can be calculated. Multiplying (17a) by (10) we obtain:

$$b*R^{max} = \frac{F_2^{min} - F_2^{max}}{F_1^{min} - F_1^{max}} * \frac{F_1^{max}}{F_2^{max}} \quad .$$

$$\Downarrow$$

$$b*R^{max} = \frac{S_2 - 1}{S_1 - 1} = S_R \qquad (19)$$

So, the multiplication of b and R^{max} results in an important parameter S_R. Being a combination of intrinsic parameters of indo-1 fluorescence at given conditions, in our case an isolated rat heart, it does not depend on measurement setup and stays constant.

By measuring b in each experiment and knowing constants S_R and S_1 or S_2 (another is calculated from (19)) R^{max} can be obtained from (19) and R^{min} is calculated from ratio obtained by combination of (9), (10), (11) and (12):

$$\frac{R^{min}}{R^{max}} = \frac{S_1}{S_2} \qquad (20).$$

Calibration of $[Ca^{2+}]_i$ was done in the following steps. By plotting the changes of fluorescence at λ_1 and λ_2 corresponding to the $[Ca^{2+}]_i$ transients against each other (x-y plot) we measured b; R^{max} was calibrated at the end of experiments and eventually S_R was calculated. Knowing S_1 for λ_1 = 386 nm obtained in a protein solution[65] we calculated S_2 for λ_2 = 510 nm in our experiments.

3.4.4 Practical aspects of measuring fluorescence in isolated rat heart

3.4.4.1 Background correction

Calculation of $[Ca^{2+}]_i$ using fluorescence ratio requires subtraction of tissue autofluorescence (arising from NADH and NADPH) before estimating constants and R. The background fluorescence intensities at each wavelength were determined prior to indo-1 loading and subsequently subtracted from the fluorescence intensities after loading in order to obtain corrected Indo-1 fluorescence intensities and ratio.

3.4.4.2. Loading intracellular indicator indo-1 into the heart

After preparation of the heart and equilibration by perfusion with standard perfusate background fluorescence was measured; thereafter the heart was loaded with the acetoxymethyl (AM) ester form of indo-1 (Calbiochem, Calbiochem-Novabiochem Corporation, La Jolla, CA 92039). The AM ester of indo-1 can passively diffuse across cell membranes (Fig. 14); once inside the cell, it is cleaved by intracellular esterases to yield cell-impermeant fluorescent indicator.[75] 4 mg (≈ 4 μM) of indo-1 AM ester was initially dissolved in 1 ml of DMS containing, 5% calf serum (Kojima et al, 1993); afterwards it was added to 150 ml of modified Krebs-Henseleit perfusate

adjusted to pH 7.4 (Table 1) containing 4 mM $CaCl_2$ and 10 mM pyruvate instead of glucose and loaded for 20-30 min in a recirculating mode (in order to conserve indo-1). Thereafter extracellular indo-1 was washed out by perfusion with standard perfusate for another 20 min before fluorescence measurements. After pilot experiments resulting in an unacceptably low fluorescence signal and, therefore, high noise (Fig. 15), the loading solution was complemented by 20% w/v Pluronic F-127 initially dissolved in DMS and by 0.1 mM probenecid added to the loading solution.[70] Pluronic F-127 was necessary in order to facilitate solubilization of indo-1 AM. Probenecid is an inhibitor of outward transport of anions; its presence in a loading solution helps obtaining sufficiently high concentrations of Indo-1 in cardiomyocytes.

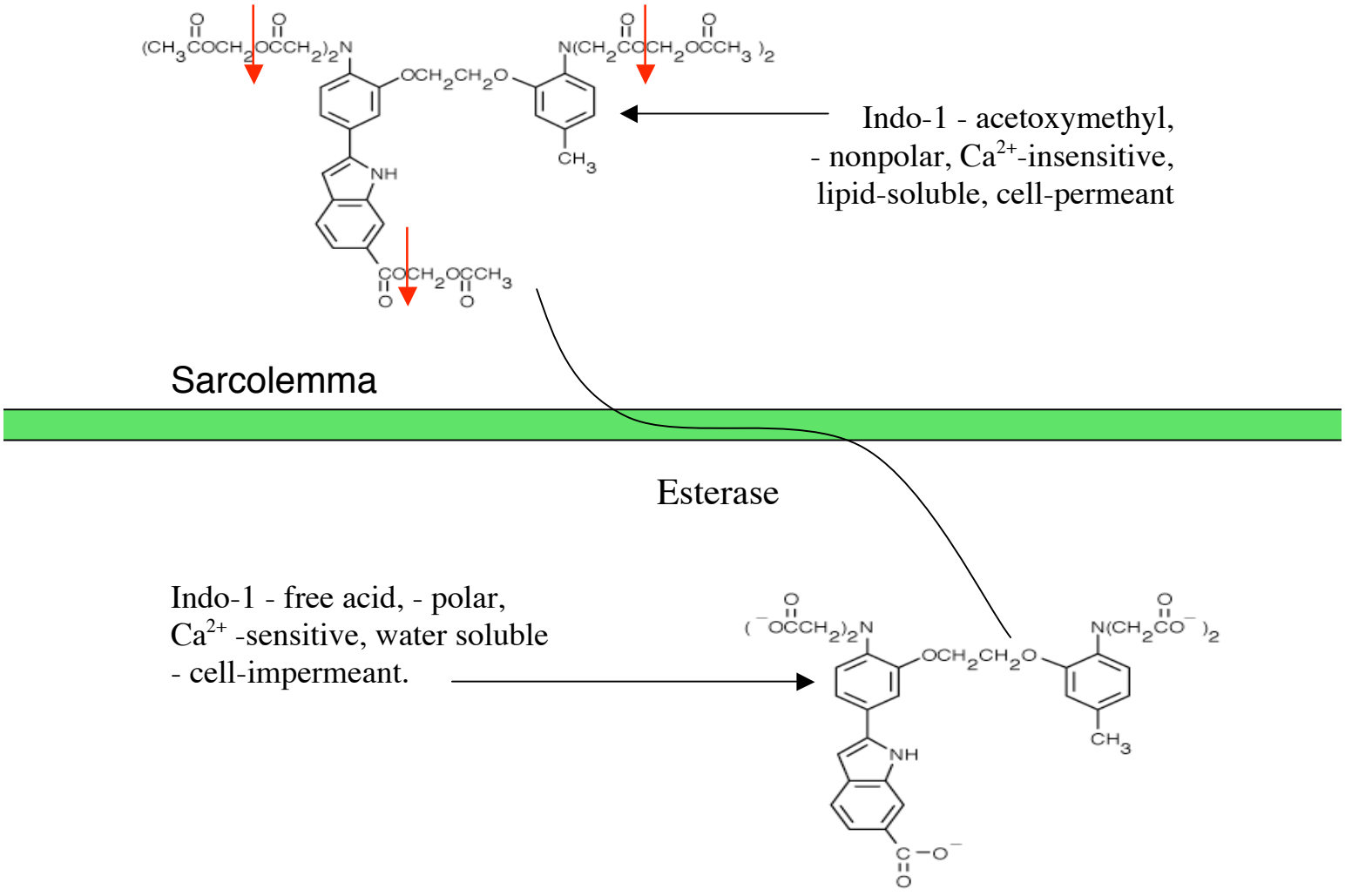

Figure 14. Loading indo-1 AM into the cardiomyocyte (*from Molecular Probes Handbook*[75]) modified.

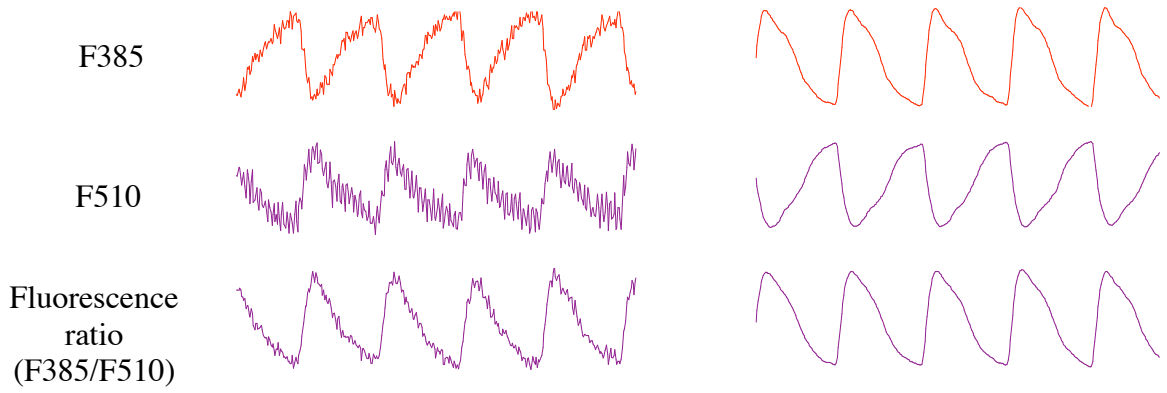

Figure 15. Original recordings of indo-1 fluorescence at wavelengths 385 and 510 nm and fluorescence ratio in a pilot experiment. Due to poor loading of indo-1 into cardiac myocytes the fluorescence signal-to noise ratio is low (left). The high noise in fluorescence channels, especially at 510 nm (middle curve), results in high noise in the fluorescence ratio channel (lower curve). Addition of Pluronic F-127 and probenecid to the loading solution has improved loading of indo-1, which enabled to get much higher fluorescence signal and signal-to noise ratio (right).

3.4.4.3 Determination of slope b and R^{max} in the whole heart

We determined slope b by plotting fluorescence intensities at two wavelengths against each other (Fig. 16 A and B) and finding the corresponding correlation coefficient by linear regression. Because of motion artifacts the correlation of the fluorescence intensities deviates from linearity. In order to overcome this problem we cropped only the initial part of the curve cycle (Fig. 16 A and C) when fluorescence at λ_1 = 385 nm starts increasing and at λ_2 = 510 starts decreasing. At this period motion artifacts are close to zero due to the lag between Ca^{2+} transient and contraction.[70]

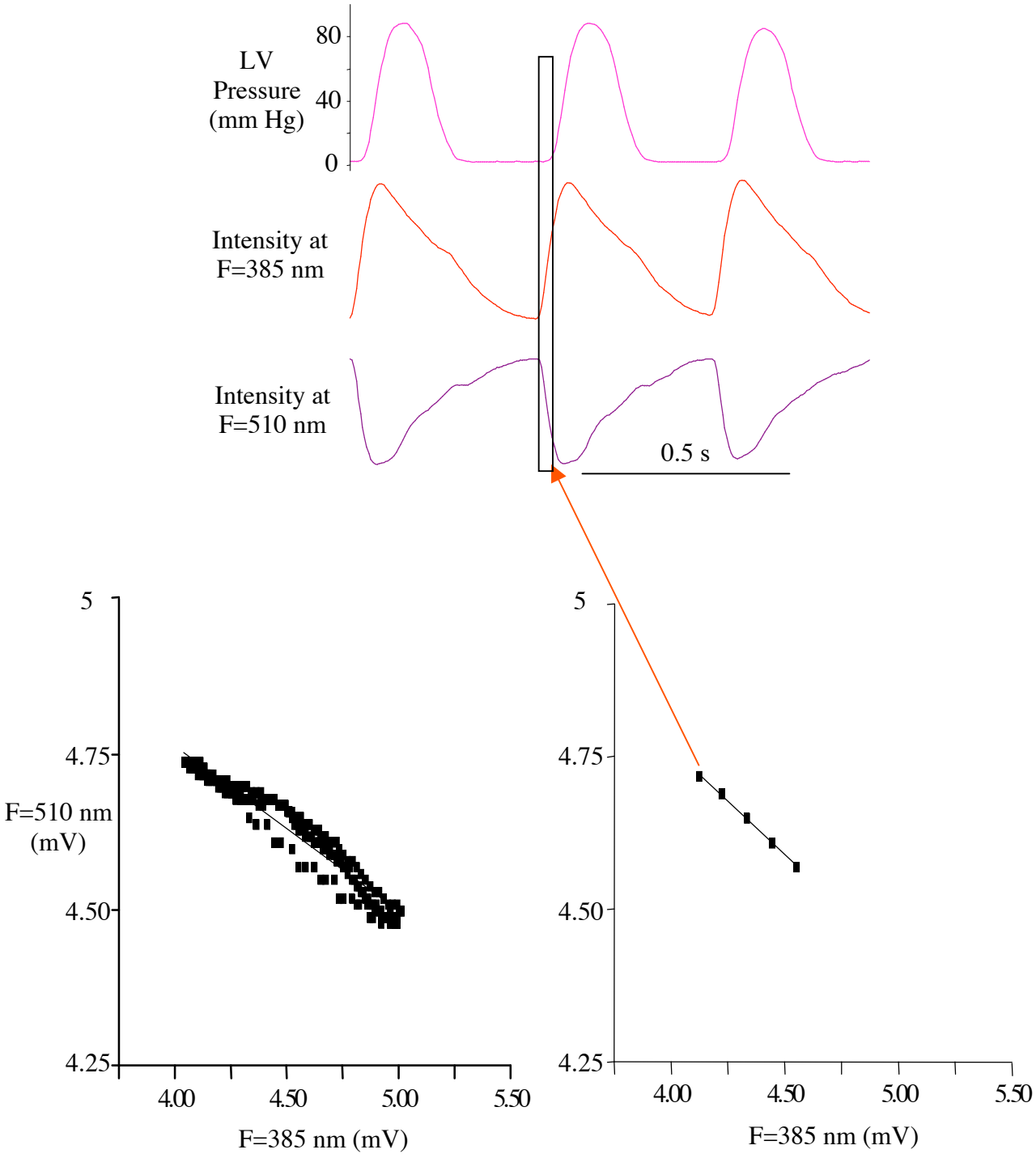

Figure 16. Determination of slope *b* by plotting fluorescence at two wavelengths.
Two fluorescence curves followed by pressure curve (upper) corresponding to 3 cardiac cycles recorded with Chart software and cropped for plotting fluorescence intensities at F=385 and F=510 against each other (B). Deviation from linearity due to motion artifacts can be observed. (C) A narrow extract shown at (A) with a rectangle was cropped for determination of slope b. Relation between F=385 and F=510 is linear.

R^{max} was determined by perfusing the heart with solution providing saturation of loaded into the cytosol of cariomyocytes indo-1 with Ca^{2+} (Table 2).

Table 2

R_{max} determination solution,[70]
pH adjusted to 7.4.

Compound/component	Concentration
HEPES	5 mM
$CaCl_2$	80 mM
KCl	6 mM
$MgCl_2$	1.2 mM
Na_2EDTA	0.5 mM
Fetal calf serum	6%

3.4.4.4 Fluorescence setup

Fluorescence excitation of hearts loaded with intracellular indo-1 was provided by ultraviolet light at 365±10 nm generated by a 100 W mercury vapor lamp and directed through a custom-made tripod silica fiberoptic cable (Volpi AG, CH-8952 Schlieren, Switzerland), designed to provide excitation and assess emission simultaneously (Fig. 17). The emitted fluorescence was filtered at 385±6 and 510±12.5 nm before reaching the photomultiplier tubes. Photomultiplier output at 385 nm (indo-1 bound to Ca^{2+}) and at 510 nm (free indo-1) were recorded at a compensated fluorometer (University of Pennsylvania, Johnson Foundation). The fluorescence ratio F385/F510, an index of $[Ca^{2+}]_i$, was recorded simultaneously with the left ventricular pressure and the ECG at a sampling rate of 200 Hz on MacLab 8e (AD-Instruments, Milford, MA, USA). Various authors use slightly different wavelengths for registering fluorescence of indo-1. Our choice was based on previous studies performed on isolated rat hearts[69,70] and in protein

extract from rat heart.[65] We used constant S_R obtained according to [70] in our experiments in isolated rat heart and K_d, S_1 and S_2 [65] obtained in a protein extract from rat heart. The constants S_1 and S_2 were obtained by measuring fluorescence at wavelengths 385 and 456 nm.[65] It has been also found that at 385, 456 and 510 nm fluorescence intensity does not depend on tissue oxygenation.[76] Additionally, in our pilot experiments we have found that setting λ_2 at 510 nm is preferable over 456 nm because of brighter fluorescence and therefore better signal-to-noise ratio.

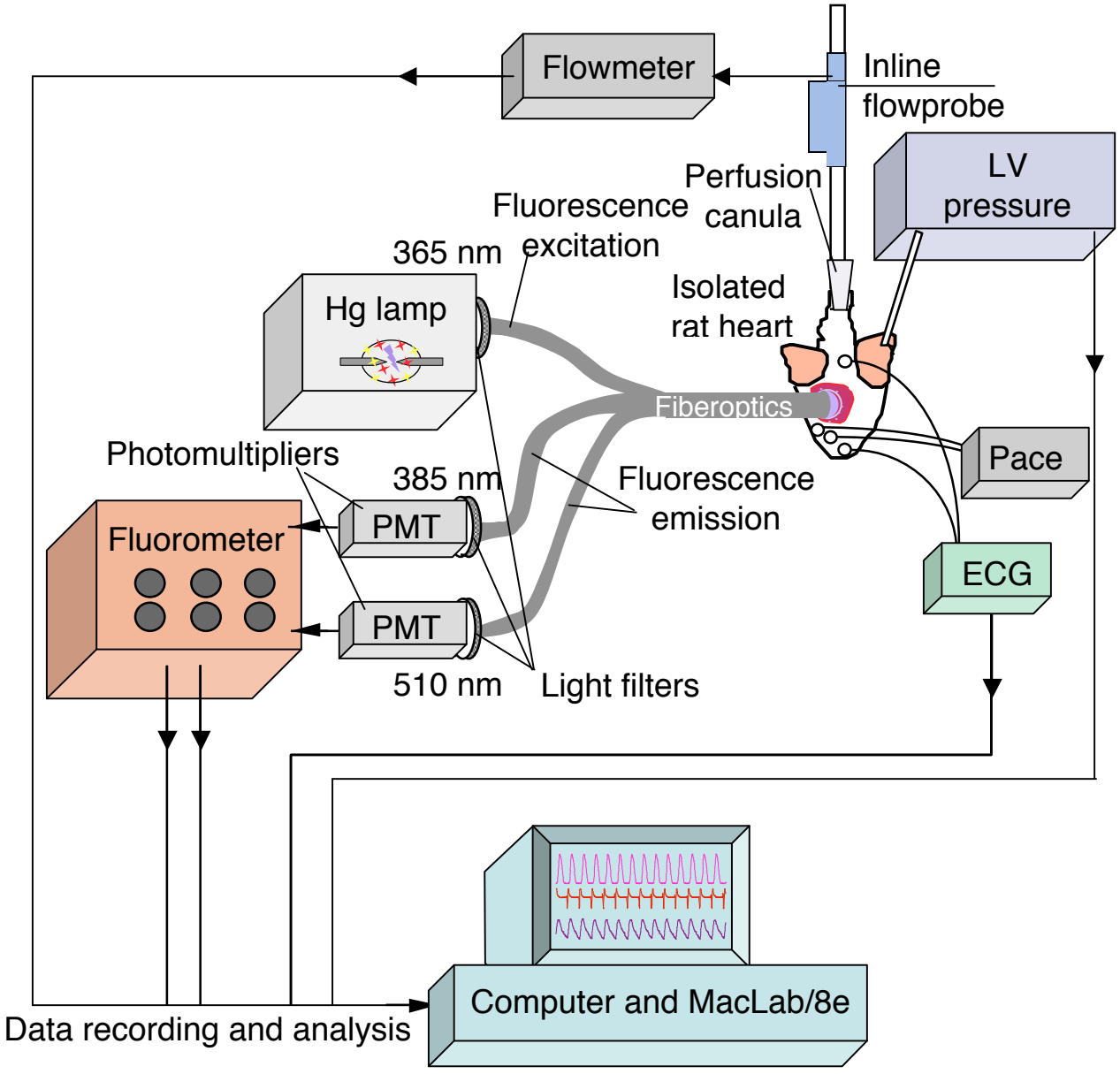

Figure 17. Setup for measuring fluorescence in isolated heart. *(Artwork by C. E. Zaugg)*

3.4.4.5 Fluorescence measuring procedure

Measurement of $[Ca^{2+}]_i$ was performed by surface fluorometry at the interventricular septum containing the fluorescent dye indo-1 according to [17,39,40,42,77,78] The tip of the fiberoptic cable was inserted through a circular cut in the inferior apical portion of the right ventricular free wall and fixed firmly on the right ventricular side of the interventricular septum (Fig. 18). The interventricular septum, functionally part of the left ventricle, was preferred to epicardial sites in order to avoid motion artifacts and contribution of endothelial cells or vasculature. The approach of the fiberoptic through a hole in the right ventricular wall does not interfere with left ventricular or septal perfusion because the right ventricular coronary artery does not supply the left ventricular wall or the interventricular septum in rat hearts.[79] Firm contact between the fiberoptic and cardiac surface was required in order to obtain a reliable signal.[42] Because forceful compression by the fiberoptic could cause changes in the shape of the left ventricle and alterations in myocardial perfusion, the placement of the fiberoptic was confirmed not to change developed pressure more than 5% of the control value. During the measurements the perfused heart and the optical system were covered completely by a light-proof black curtain in order to avoid contamination by external light. Reliability of the protection from the external light was checked by registering signal from photomultipliers at bright versus dark conditions in the laboratory.

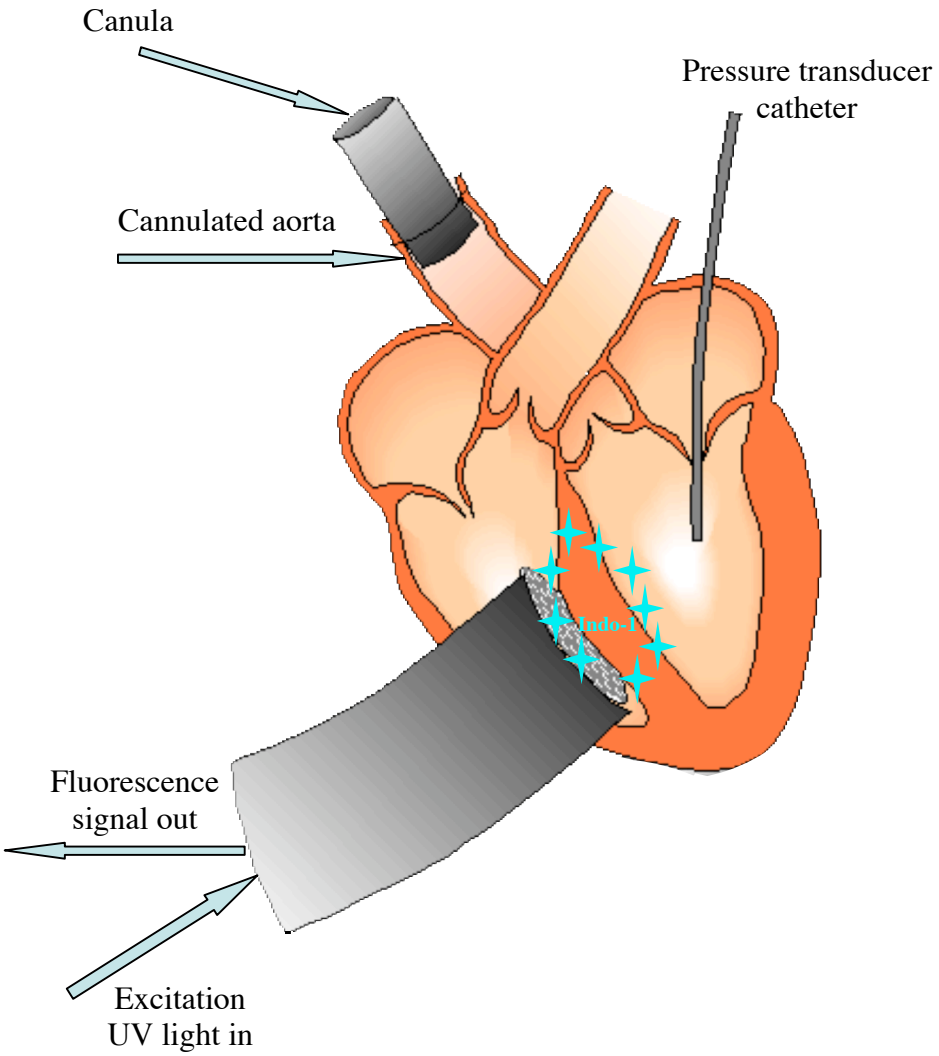

Figure 18. Measuring fluorescence in the rat heart by surface fluorometry at interventricular septum. (*Artwork by C. E. Zaugg, modified)*

3.4.4.6 Limitations of the method

The following known limitations of the indo-l surface fluorometry technique should be considered.[42,80] Sequestration of indo-l in mitochondria potentially leads to interferences of mitochondrial fluorescence with cytosolic. It was demonstrated, however, that mitochondrial Ca^{2+} shows no transient.[81] So, the fluorescence ratio changes are considered to reflect cytosolic phenomena. Yet, sequestration of indo-l in mitochondria potentially provokes a spatial heterogeneity of fluorescence[81,82] and therefore makes estimation of the cytosolic Ca^{2+} levels from fluorescence ratio less accurate. Another possible limitation is reduction of fluorescence by time-dependent ultraviolet bleaching and indo-l leakage during the experiment. However, reduced fluorescence does not influence the fluorescence ratio and, therefore, the estimation of $[Ca^{2+}]_i$.[83] Yet, reduced fluorescence could be of importance because of variation of autofluorescence between hearts or because of changes of autofluorescence over the experimental period. Such changes could possibly alter the ratio of indo-l fluorescence to autofluorescence.[84] The ultraviolet bleaching can be neglected in many types of experiments in which only short exposure of the heart to the excitation ultraviolet light (several seconds) is sufficient for fluorescence measurements or when instead of calibration to $[Ca^{2+}]_i$ the fluorescence ratio is normalized (diastolic value is considered to be zero and systolic 100%) or the data are analyzed simply as a raw fluorescence ratio.[42] In our experiments involving calibration of the fluorescence ratio to $[Ca^{2+}]_i$ the ultraviolet bleaching represents a problem which has to be considered; it is discussed further in the "Results" section. Another limitation could be caused by fluorescence from the endothelium or the vasculature. However, the contribution of the endothelium and vasculature to indo-l fluorescence was shown to be almost negligible in such type of preparation, as evaluated by bradykinin administration.[69,85]

3.5 Experimental protocols

3.5.1 Choice of drugs and concentrations

Contribution of L-type Ca^{2+} channels and Na^+/Ca^{2+}-exchange to Ca^{2+} overload during VF was tested in the following way. VF was induced in hearts treated with drugs specifically blocking L-type Ca^{2+} channels and Na^+/Ca^{2+}-exchange and the obtained results were compared with control.

To block the reverse mode of Na^+/Ca^{2+}-exchange we used KB-R7943 at concentrations 10 and 5 μM; KB-R7943 specifically blocks the reverse mode of Na^+/Ca^{2+}-exchange with little or no effect on the forward mode or on another ion transport systems. In concentrations up to 30 μM KB-R7943 is known to have little effect on Na^+-Ca^{2+}-K^+ exchanger,[86] the Na^+ -H^+ exchanger, sarcolemmal Ca^{2+}-ATPase, SR Ca^{2+}-ATPase, or Na^+-K^+-ATP-ase.[87] However, using voltage-clamp technique and ramp pulse protocol, it has been shown that KB-R7943 inhibits voltage-sensitive Na^+ currents, L-type Ca^{2+} currents and inward rectifier K^+ currents with IC_{50} 14, 8 and 7 μM, respectively.[88] This study has been reasonably criticized for overestimating the effects of KB-R7943 because the ramp pulse protocol is too severe and has little relevance to physiological conditions.[53] Other studies showed that in rat ventricular myocytes KB-R7943 at 5 μM did not alter steady-state twitches, Ca^{2+} transients, Ca^{2+} load in the SR, or rest potentiation.[89] In guinea pig papillary muscle, however, KB-R7943 at up to 10 μM did not significantly affect the resting membrane potential or various action potential parameters.[87,90] Similarly, 10 or 30 μM KB-R7943 did not alter spontaneous beating rate and developed tension in isolated guinea pig atria.[91] Based on these data, we have chosen 5 and 10 μM KB-R7943 for our experiments, the concentrations known to inhibit the reverse mode of Na^+/Ca^{2+}-exchange by 90[89] and by 100%,[92] correspondingly.

To block L-type Ca^{2+} channels we used nifedipine at concentrations 0.2 and 0.05 μM. Nifedipine belongs to the group of dihydropyridine calcium antagonists. In contrast to nondihydropyridines, it only slightly slows SA node pacemaker activity and inhibits conduction in the AV node.[8] Due to this difference, we preferred nifedipine over

nondihydropyridines in our experiments, including the rapid pacing protocol. The choice of the concentrations was based on the following reasoning. First, the steady-state IC50 for nifedipine was found to be 0.3 μM at a holding potential of -80 mV and 50 nM at a holding potential of -40 mV;[93,94] depolarization is known to promote i_{CaL} blocking by nifedipine because affinity of dihydropyridines for receptor is greatest as L-type channels shift toward the inactivated state.[95] Second, recordings of membrane potentials during VF showed oscillations about –60 mV.[96] Therefore, we have chosen concentrations presumably close to IC50 at this voltage (-60 mV), one presumably higher (0.2 μM) and one known to be lower (0.05 μM). Administration of both 0.2 μM and 0.05 μM of nifedipine in the first experiments produced no effect on cardiac rhythm; however, an effect on Ca^{2+} transient amplitude was present.

3.5.2 Experimental protocols and groups

Effects of the drugs were compared to vehicle in the following way. After equilibration, loading of indo-1 and washing the heart from the loading solution VF was induced twice in the same heart, the first time without drug and the second time with a drug (or second vehicle in case of control). The experimental protocol is shown in Fig. 19. Perfusion of a drug started 5 min before induction of VF. One min before VF induction pacing at 4 Hz was started in order to provide reproducible baseline conditions. VF was induced by 1 min rapid pacing at 20 Hz with 5 V rectangle pulses and duration 1 ms. After the rapid pacing was stopped, VF terminated spontaneously in some hearts; when it was sustained for 1 min, termination was performed by infusion of a 0.25 mg bolus of lidocaine hydrochloride (Sintetica, Switzerland) followed by a 10 min washout. Lidocaine has been shown to effectively terminate VF and reduce $[Ca^{2+}]_i$ during VF in this model;[97] already 5 min after administration of a lidocaine bolus reproducibility of VF in experiments studying VF thresholds was not affected.[17]

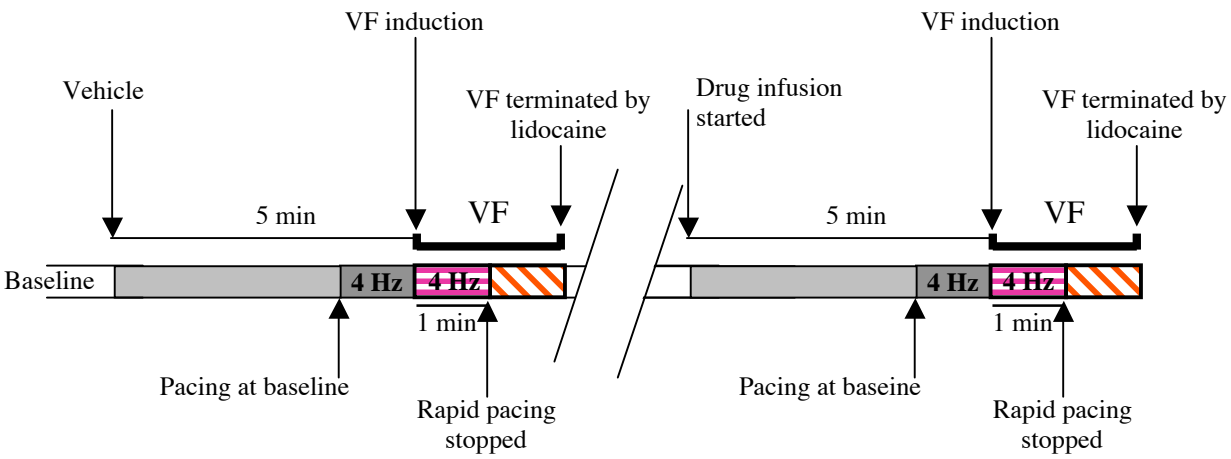

Figure 19. Experimental protocol for testing the roles of L-type Ca^{2+} channels and Na^{+}/Ca^{2+}-exchange in VF.

A slightly different protocol was used for testing the role of Na^{+}/Ca^{2+}-exchange in maintaining VF. After induction of VF the hearts were allowed to fibrillate for 5 min, then infusion of 10 μM KB-R7943 was started. In a control group the hearts were allowed to fibrillate further without any drug being infused (Fig. 19).

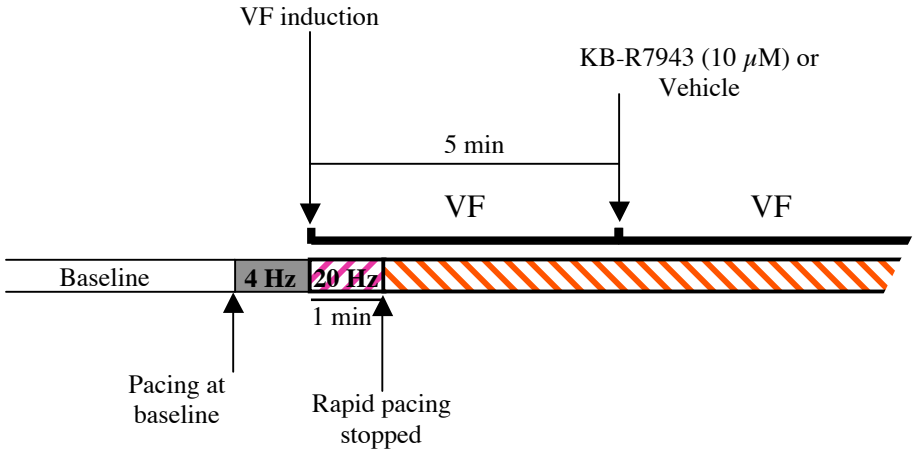

Figure 20. Experimental protocol for testing the role of Na^+/Ca^{2+}-exchange in VF maintaining.

All together we had 7 experimental groups. Below is the summary of experimental protocols in different groups with regard to the number of hearts in each group:

Group 1. 1st VF → 0.05 μM nifedipine → 2nd VF	4 hearts
Group 2. 1st VF → 0.2 μM nifedipine → 2nd VF	5 hearts
Group 3. 1st VF → 5 μM KB-R7943 → 2nd VF	6 hearts
Group 4. 1st VF → 10 μM KB-R7943 → 2nd VF	6 hearts
Group 5. 1st VF → vehicle → 2nd VF	8 hearts
Group 6. VF sustained for 5 min → 10 μM KB-R7943	7 hearts
Group 7. VF sustained for 5 min → vehicle	7 hearts

In Fig. 21 on the next page the representative recordings of LV pressure, ECG and fluorescence ratio during VF induction in our experiments are shown.

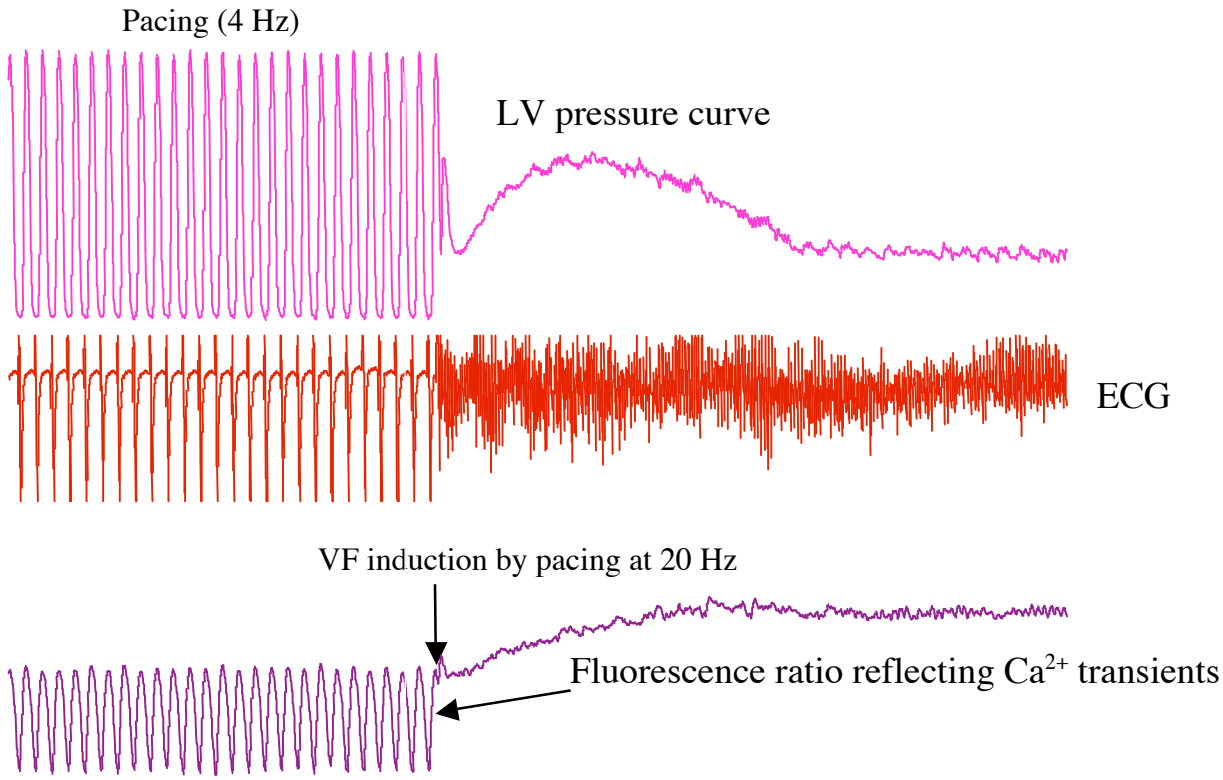

Figure 21. Original tracings of LV pressure, ECG and fluorescence ratio curves at the time around induction of VF.

3.6 Chemicals

KB-R7943 mesylate

Chemical structure:

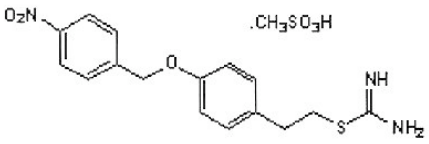

Molecular weight: 427.49
Chemical formula: $C_{16}H_{17}N_3O_3S.CH_3SO_3H$
Solubility: DMSO to 100 mM
Water to 100 mM
Stability: Solid is stable at room temperature
Manufacturer: Tocris Cookson Inc., USA
Application: blocker of reverse mode of sodium-calcium exchange

Nifedipine

Chemical structure:

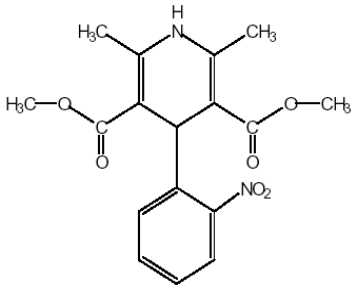

Molecular weight: 346.3
Chemical formula: $C_{17}H_{18}N_2O_6$
Solubility: Ethanol to 17 g/L
Stability: Solid is stable at 4ºC in dark.
Aqueous solution is extremely light-sensitive and unstable, at 25ºC concentration degrades to ≈90% of the initial value within 6 hours of preparation.
Manufacturer: Sigma
Application: blocker of L-type Ca^{2+} channels

Lidocaine

Chemical structure:

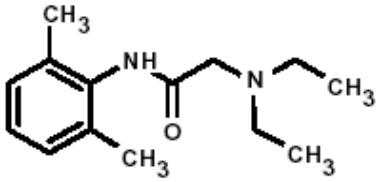

Molecular weight:	234
Chemical formula:	$C_{14}H_{22}N_20$
Solubility:	soluble in water
Stability:	stable under normal conditions
Manufacturer:	Sintetica, Switzerland (Rapidocain® 1%)
Application:	Sodium channel blocker

Pluronic F-127

Nonionic surfactant polyol
Chemical structure:

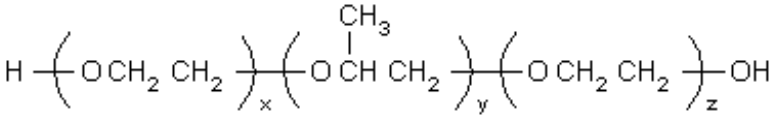

Molecular weight: approximately 12,500 daltons

Chemical formula: see chemical structure
Manufacturer: Sigma
Application: Facilitates solubilization of indo-1

Probenecid

Chemical structure:

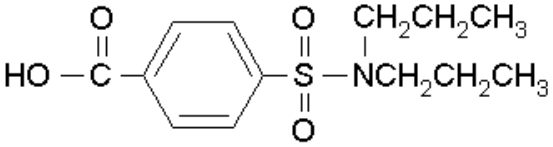

Molecular weight: 285.4
Chemical formula: $C_{13}H_{19}NO_4S$

Manufacturer: Sigma
Application: inhibits outward transport of anions from cytoplasm of cardiomyocytes improving loading of indo-1

Indo-1 acetoxymethyl ester

Chemical structure:

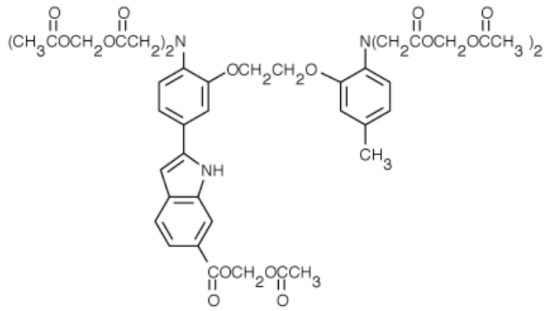

Molecular weight:	1009.93
Chemical formula:	$C_{47}H_{51}N_3O_{22}$
Solubility:	DMSO, 4 mg/ml, Pluronic F-127 facilitates solubilization
Stability:	aqueous solution is unstable, light-sensitive. Storage of solid: desiccated and protected from light at room temperature, 2-6°C or ≤-20°C without compromising stability.
Manufacturer:	Calbiochem-Novabiochem Corporation, La Jolla, CA 92039
Application:	Ratiometric fluorescent indicator of $[Ca^{2+}]_i$ changes in cytosole of cardiomyocytes.

3.7 Evaluation of results and statistical analysis

The rats used in the experiment were characterized by body weight and by wet and dry heart weight. The data on coronary flow and LVDP together with the ECG, cardiac rate and indo-1 fluorescence were recorded using Chart software (version 4.2 for Macintosh). The variables were compared among groups by t-test, unpaired or paired, if appropriate, using Prism software (version 3.0, Ocx, June 2002) and expressed as mean±SD. The null hypothesis was rejected at the 95% level, considering $p < 0.05$ significant. The incidence of spontaneous defibrillation was evaluated on digitized ECG and pressure readouts, listed in a table and analyzed using Chi-square statistics for hearts treated with the drugs prior to VF and using Fisher exact test for hearts treated with KB-R7943 after VF induction.

$[Ca^{2+}]_i$ was calculated from the fluorescence ratio R according to the results obtained at calibration; thereafter in all analyses absolute values of $[Ca^{2+}]_i$ have been used.

$[Ca^{2+}]_i$ was evaluated as an increase over baseline and measured at three time points.

1) 10 seconds after beginning of VF induction by rapid pacing; 2) at the end of the 1 minute-long VF induction by rapid pacing; 3) at the end of the following 1 min if VF was sustained. The $[Ca^{2+}]_i$ data obtained with a drug perfused were compared with corresponding data obtained at previous VF induction in the same heart without a drug (or with the previous vehicle in a control group) using paired t-test. Additionally, we analyzed difference of the effects of the drugs on Ca^{2+} overload 10 seconds after rapid pacing and at the end of rapid pacing, also using paired t-test. Finally, in the hearts perfused with drugs before VF, we analyzed the rate of $[Ca^{2+}]_i$ accumulation during the initial phase of VF by monoexponential curve fitting (time constant □) using paired t-test.

At an intermediate stage after experiments on 3 hearts in 2 groups we used preliminary data on variability of VF-induced $[Ca^{2+}]_i$ elevation for a sample size determination. It has shown that groups of 6 hearts have 90% power to detect a 20% difference in $[Ca^{2+}]_i$.

In hearts perfused with KB-R7943 after VF has been induced we estimated the difference (delta) between the mean $[Ca^{2+}]_i$ of a 1 min period measured 15 min after start of KB-R7943 perfusion and the mean $[Ca^{2+}]_i$ of the last 1 min before start of KB-R7943 perfusion. The mean delta±SD of the whole group was compared using unpaired t-test

with the mean delta±SD of the control group in which measurements of $[Ca^{2+}]_i$ were performed at corresponding periods after VF induction.

4 RESULTS

4.1 Results of calibration

S_R was found to be -1.027±0.358 (mean±SD, n=32 hearts). The value of S_1 = 0.174 for λ_1 = 385 as well as *Kd* = 594 nM were taken from the literature [65] as obtained in a solution of soluble proteins from rat cardiomyocytes. Based on known S_1 and S_R and on equation (19) we calculated S_2 = 1.848 for λ_2 = 510. Thereafter R^{max} for each heart was calculated using equation (19), *b* measured in this heart and mean S_R calculated previously; R^{min} was calculated from equation (20). These obtained constants were used for calculating $[Ca^{2+}]_i$ using Chart software and recordings of *R* obtained in experiments. Calculated in such way mean diastolic and mean systolic $[Ca^{2+}]_i$ were found to be 389±169 and 791±191, correspondingly. While the diastolic value corresponds, the systolic is smaller than the one obtained using the same constants by [70,69,65,] 391 and 1015 nM, correspondingly. The difference can be explained by the fact that we did not account for mitochondrial $[Ca^{2+}]$ ($[Ca^{2+}]_m$) and for the fraction of indo-1 loaded into mitochondria.[69,81,98] In order to do it, we should have applied quenching of fluorescence of the cytosolic fraction of indo-1 by manganese. [81,98-100] Estimated in such way mitochondrial fluorescence is subtracted from the total fluorescence (at each of the wavelengths of measurement) for obtaining corrected $[Ca^{2+}]_i$. Increase of $[Ca^{2+}]_i$ during VF, however, is also expected to lead to an increase of $[Ca^{2+}]_m$.[39] Therefore, in order to be consistent, we should have applied the quenching by manganese during VF induction and the following sustained VF, too. Our experiments include two consecutive VF inductions in the same heart with measuring $[Ca^{2+}]_i$ both at baseline and during VF each time and with 10 min recovery between the VFs. Therefore, the Mn^{2+} ions (100 μM $MnCl_2$,[81,98-100]) should have been present in cytosol for relatively long time (≈20-30 min), the entire period of measurements, or loaded and washed out twice. This condition is far from physiological. Therefore, we have chosen not to measure $[Ca^{2+}]_m$. So, the estimated $[Ca^{2+}]_i$ in our experiments can be considered to reflect an average of $[Ca^{2+}]$ in mitochondria and in cytosol. The mitochondrial $[Ca^{2+}]_i$ is considered to show no transient.[81,101,102] Although some authors have demonstrated the opposite,[103,104] the mitochondrial $[Ca^{2+}]_i$ transients in rat cardiomyocytes in their studies are still 4-5 times smaller compared to cytosol. Therefore,

the estimate of the $[Ca^{2+}]_i$ transient amplitude without accounting for mitochondrial indo-1 fluorescence is smaller in principle. Another bias could arise from photobleaching of indo-1 by ultraviolet light. Control experiments with repeated vehicle, however, have shown that it is not high at least in this type of experimental protocol (see results below). Still, in experiments with KB-R7943 infused after VF induction photobleaching of indo-1 should have been more prominent due to longer exposure to ultraviolet light both in the control and in the KB-R7943 –treated hearts. Eventually, calibration of R^{max} at the end of experiments should have also been biased by photobleaching during previous fluorescence measurements. This also could have influenced the estimation of $[Ca^{2+}]_i$.
During the first two minutes of VF $[Ca^{2+}]_i$ increased to ≈2 – 2.5 μM. Thereafter it was increasing slowly, approaching ≈3 μM. It should be noted, however, that at concentrations as high as 1 μM and more sensitivity of fluorescence ratio to $[Ca^{2+}]_i$ is decreased (Fig. 13).

4.2 Exclusions and the data on body and heart weight of rats

Fifty rats were used for the experiments of this thesis. In four hearts it was not possible to induce VF, so they were excluded from analysis. One heart was excluded because of no LVDP recovery after the first VF induction, another heart because of low coronary flow (< 15 ml/min at baseline) and one more heart because it showed spontaneous VF already before any pacing protocol has been applied. The data on these rats are summarized in Table 3.

Table 3. Body weight, wet heart weight and dry heart weight of the 43 rats used in the experiments expressed as mean ± SD.

Body weight, g	Wet heart weight, g	Dry heart weight, g
421.39 ± 23.25	1.37 ± 0.15	0.26 ± 0.02

4.3 Hemodynamic variables

In all hearts in which VF was induced twice, including control, there was a small but significant reduction of coronary flow (Fig. 22 A) obviously due to a gradual deterioration of the isolated heart preparation. In addition, both drugs at both

concentrations produced a significant, albeit small reduction of LVDP (Fig. 22 B). Extend of the reduction of LVDP in the control group (7.9%), although it did not reach statistical significance (p = 0.13), was comparable to other groups (Fig. 22 B). So, some part of the LVDP reduction was due to a deterioration of the preparation, while another part was presumably due to reduced Ca^{2+} entry into the cardiomyocytes during systole.

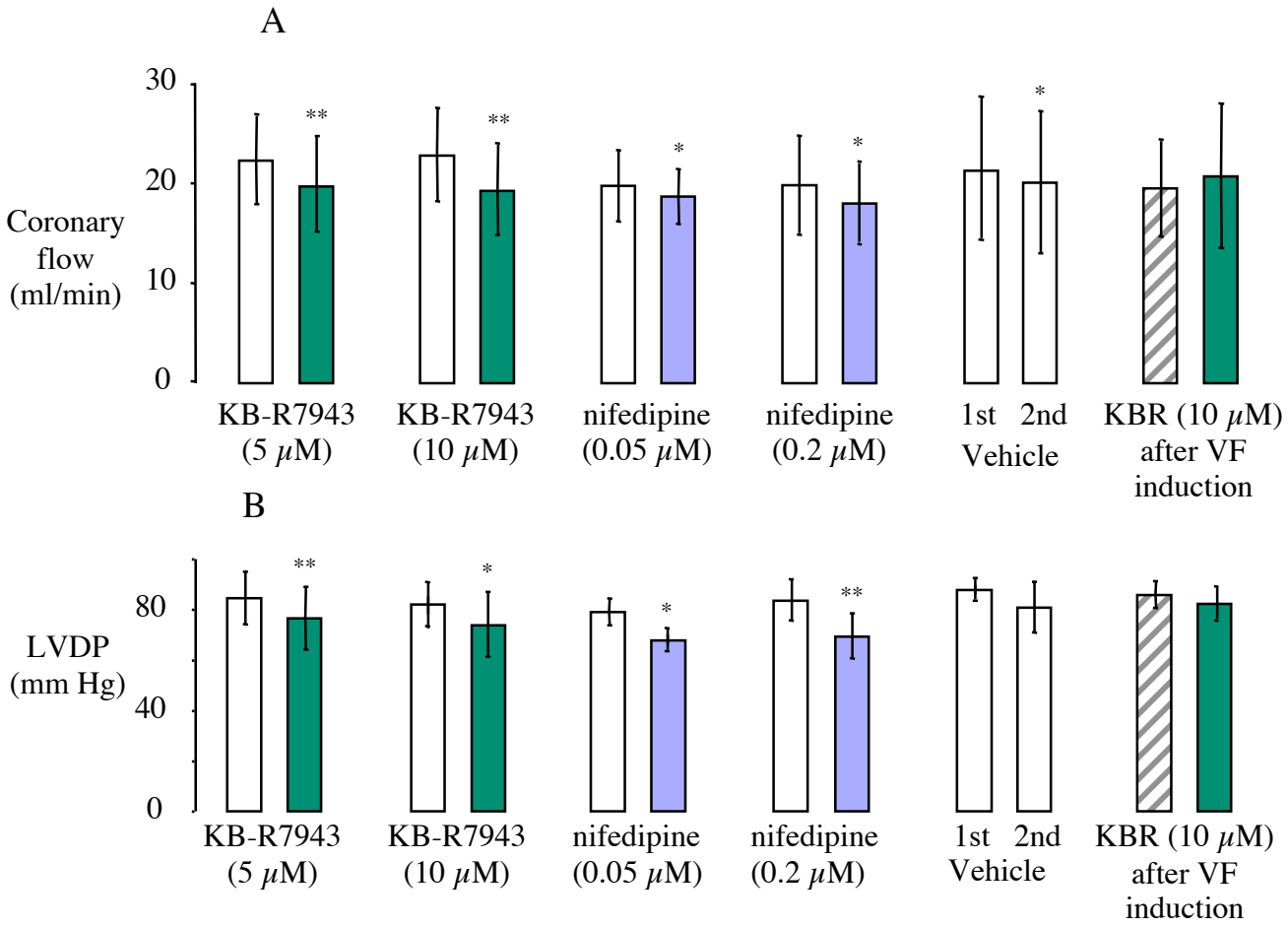

Figure 22. Mean coronary flow (**A**) and left ventricular developed pressure (LVDP) (**B**). Each pair of bars represents: open bars vehicle, filled bars drug treatments (see subscripts). The data are paired, i.e. measured consecutively in the same heart, exept for the last two bars (10 μM KB-R7943 after VF induction). To distinguish with paired data, the bar standing for vehicle in this pair is hatched. **p<0.01, *p<0.05.

4.4 Diastolic $[Ca^{2+}]_i$ at baseline

None of the drug treatments significantly changed diastolic level of $[Ca^{2+}]_i$ at baseline (Fig. 23). Except for the group treated with 0.05 μM nifedipine, in all groups including control diastolic $[Ca^{2+}]_i$ before second VF was slightly reduced. Treatment with 10 μM KB-R7943 showed a trend towards reduction of diastolic $[Ca^{2+}]_i$ (p=0.095). Large increase of diastolic $[Ca^{2+}]_i$ in the 0.05 μM nifedipine treated group (288 nM or 68%) was not significant (p=0.163, Fig. 23) due to high scatter of data. Other treatments produced following mean reduction of diastolic $[Ca^{2+}]_i$: 5 μM KB-R7943 34 nM or 8%, 10 μM KB-R7943 64 nM or 21%, 0.2 μM nifedipine 27 nM or 7%, repeated vehicle 25 nM or 6%. Comparison of diastolic $[Ca^{2+}]_i$ before the first VF among the all groups showed no significant difference (p=0.534, ANOVA).

4.5 Systolic $[Ca^{2+}]_i$ at baseline

Both 5 and 10 μM KB-R7943 infused before VF significantly ($p<0.01$) reduced systolic $[Ca^{2+}]_i$ at baseline (Fig. 23) by 147 and 164 nM (18 and 24%), respectively. Nifedipine at 0.05 μM elevated baseline systolic $[Ca^{2+}]_i$ by 168 nM (19%), which was statistically not significant (p=0.458, Fig. 23) due to high scatter of data. Nifedipine at 0.2 μM reduced baseline $[Ca^{2+}]_i$ by 273 nM (35%), which was not significant (p=0.111, Fig. 23), but on average larger than in the groups treated with KB-R7943. Repeated vehicle slightly reduced baseline systolic $[Ca^{2+}]_i$ by 58 nM (7%), which was not significant (p=0.475, Fig. 23). Comparison of systolic $[Ca^{2+}]_i$ before the first VF among the all groups showed no significant difference (p=0.539, ANOVA).

Elevation of both diastolic and systolic $[Ca^{2+}]_i$ produced by 0.05 μM nifedipine can be attributed to measurement artifact. This consideration is based on extensive knowledge of Ca^{2+} -antagonism of this drug, on the reducing effect on baseline systolic and diastolic $[Ca^{2+}]_i$ produced by nifedipine at 0.02 μM and on the consistent effects of both concentrations of nifedipine on Ca^{2+} overload during VF presented below. Elevation of the mean systolic $[Ca^{2+}]_i$ in the 0.05 μM nifedipine group (168 nm) is not as high as

elevation of the mean diastolic $[Ca^{2+}]_i$ (288 nM), which means overall reduction of $[Ca^{2+}]_i$ transient amplitude, an effect, also observed in the other drug-treated groups.

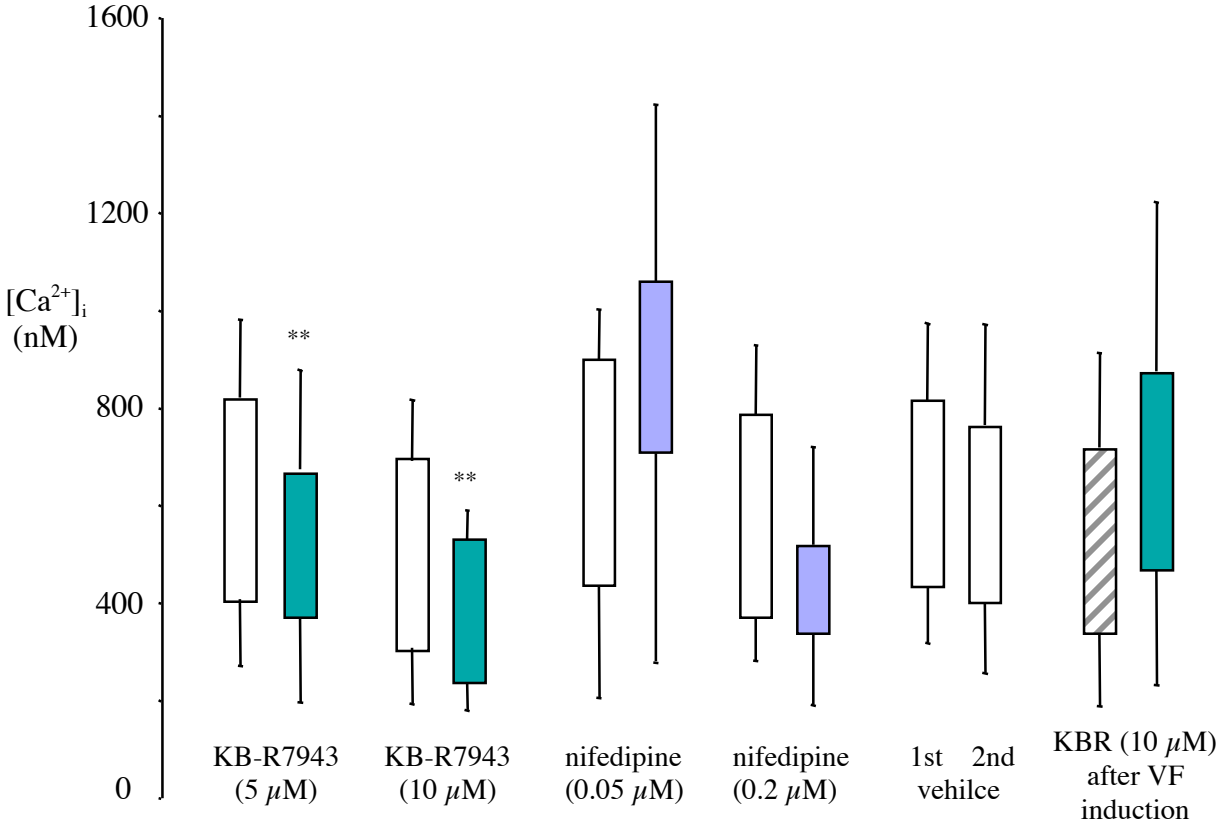

Figure 23. Upper end of bars shows mean diastolic $[Ca^{2+}]_i$ before VF induction; lover end of bars shows mean systolic $[Ca^{2+}]_i$ before VF induction. Open bars stand for vehicle, closed for drug treatment (see subscripts). The data are paired, i.e. measured sequentially in the same heart except for the last two bars (10 μM KB-R7943 after VF induction). To distinguish with paired data, the bar standing for vehicle in the last pair is hatched. **p<0.01, paired t-test. Additionally, baseline systolic and diastolic values of $[Ca^{2+}]_i$ with vehicle (1st VF induction) were compared among all groups using ANOVA and showed now significant difference.

4.6 Effects of KB-R7943 and nifedipine infusion before VF

4.6.1 Effects of KB-R7943

Both 5 and 10 μM KB-R7943 infused before VF significantly reduced $[Ca^{2+}]_i$ accumulation during entire period of VF ($p<0.01$) (Fig. 24 A and B, Fig 25 A and B, Fig. 30 A , B and C). On average, 5 μM KB-R7943 reduced $[Ca^{2+}]_i$ accumulation by 559 nM (51%) after 10 sec of VF induction and by 494 nM (40%) at the end of rapid pacing (Fig. 30 A and B). 10 μM KB-R7943 reduced $[Ca^{2+}]_i$ by 709 nM (59%) after 10 sec of VF induction and by 1148 nM (70%) at the end of rapid pacing (Fig. 30 A and B). Additionally, in both these groups spontaneous defibrillations occurred several seconds after the rapid pacing was stopped. Of six hearts treated with 5 μM KB-R7943 two defibrillated spontaneously. Therefore, $[Ca^{2+}]_i$ accumulation after 1 min sustained VF was analyzed only in the four hearts in which VF was sustained; 5 μM KB-R7943 reduced $[Ca^{2+}]_i$ by 643 nM (43%) after 1 min sustained VF (Fig. 30 C). Of six hearts treated with 10 μM KB-R7943 five defibrillated spontaneously. Therefore, $[Ca^{2+}]_i$ accumulation after 1 min sustained VF was not analyzed in this group. The incidence of spontaneous defibrillations in the group treated with 10 μM KB-R7943 was significantly ($p<0.05$, Chi-square test, Table 5) different from control. Both 5 and 10 μM KB-R7943, did not significantly change the $[Ca^{2+}]_i$ accumulation rate ($p=0.19$ and 0.26, correspondingly, paired t-test,) although on average in the both groups was increased (Fig. 31).

4.7.1 Effects of nifedipine

Both 0.05 and 0.2 μM nifedipine infused before VF significantly ($p<0.05$) reduced $[Ca^{2+}]_i$ elevation during VF (Fig. 26 A and B, Fig. 27 A and B, Fig. 30 A and B). On average, nifedipine at 0.05 μM reduced $[Ca^{2+}]_i$ accumulation by 535 nM (50%) after 10 sec of VF induction and by 496 nM (40%) at the end of rapid pacing (Fig. 30 A and B). Nifedipine at 0.2 μM reduced $[Ca^{2+}]_i$ accumulation by 886 nM (82%) after 10 sec of VF induction and by 656 nM (58%) at the end of rapid pacing (Fig. 30 A and B). The effect of 0.2 μM nifedipine on $[Ca^{2+}]_i$ overload at the end of rapid pacing was significantly ($p<0.02$) smaller than after 10 s of rapid pacing, on average it was smaller by 230 nM (26%) (Fig.

30 A and B). There was no significant difference of $[Ca^{2+}]_i$ overload reduction measured after 10 s and at the end of rapid pacing within other groups (Fig. 30 A and B). Additionally, in both groups spontaneous defibrillation occurred after the rapid pacing was stopped. Out of the four hearts treated with 0.05 μM nifedipine two defibrillated spontaneously. Out of the five hearts treated with 0.2 μM nifedipine three defibrillated spontaneously. Therefore $[Ca^{2+}]_i$ accumulation was not analyzed after 1 min sustained VF in both groups. The incidence of spontaneous defibrillation in both groups was not significantly different from control (Table 5). Both 0.05 and 0.2 μM nifedipine, however, increased and, therefore, reduced $[Ca^{2+}]_i$ accumulation rate ($p<0.01$ and $p<0.05$, correspondingly; Fig. 31).

In the control group (repeated vehicle) there was no statistically significant difference of extend of $[Ca^{2+}]_i$ overload between the first and the second VF (Fig. 28, 29, 30). The difference of $[Ca^{2+}]_i$ between two sequential VFs at baseline (diastolic: decreased by 25 nM or 6%, systolic: decreased by 58 nM or 7%, after 10 sec of VF (increased by 59 nM or 5%) and at the end of rapid pacing (decreased by 81 nM or 5%) was negligible; the maximal difference observed after 1 min sustained VF (decreased by 448 nM or 20%) was not statistically significant ($p=0.196$). Together with the results of no effect of repeated VF induction on Ca^{2+} transient amplitude at baseline this indicates that photobleacing and deterioration are not important in our experiments and that effects of the drugs on $[Ca^{2+}]_i$ during VF are valid. Additionally, no spontaneous defibrillations occurred in this group. Finally, there was no change of $[Ca^{2+}]_i$ accumulation rate between the first and the second VF with vehicle ($p=0.95$, Fig. 31).

4.8 Effects of KB-R7943 infusion during VF

Perfusion with KB-R7943 starting 5 min after VF induction significantly ($p<0.01$) reduced $[Ca^{2+}]_i$ accumulation (Fig. 32, 33, 34). On average, $[Ca^{2+}]_i$ during VF was reduced by 1288 nM (Fig. 34). Additionally, of seven hearts treated with KB-R7943 six defibrillated spontaneously after VF induction was stopped. The incidence of

spontaneous defibrillations was significantly different from the control group ($p<0.01$) in which no spontaneous defibrillations have been observed (Table 4).

Table 4. Occurrence of spontaneous defibrillations with regard to treatment groups. Incidence of spontaneous defibrillations in the groups treated with KB-R7943 or nifedipine before VF and in the group treated with 10 μM KB-R7943 after VF induction was analyzed by Chi-square and Fisher exact test, correspondingly. *$p<0.05$; **$p<0.01$.

Treatment groups	No of hearts	No of spontaneous defibrillations
5 μM KB-R7943 before VF	6	2
10 μM KB-R7943 before VF	6	5*
0.05 μM nifedipine before VF	5	2
0.2 μM nifedipine before VF	5	3
Repeated vehicle	8	0
10 μM KBR 5 min after VF induction	7	6**
Vehicle after VF induction	7	0

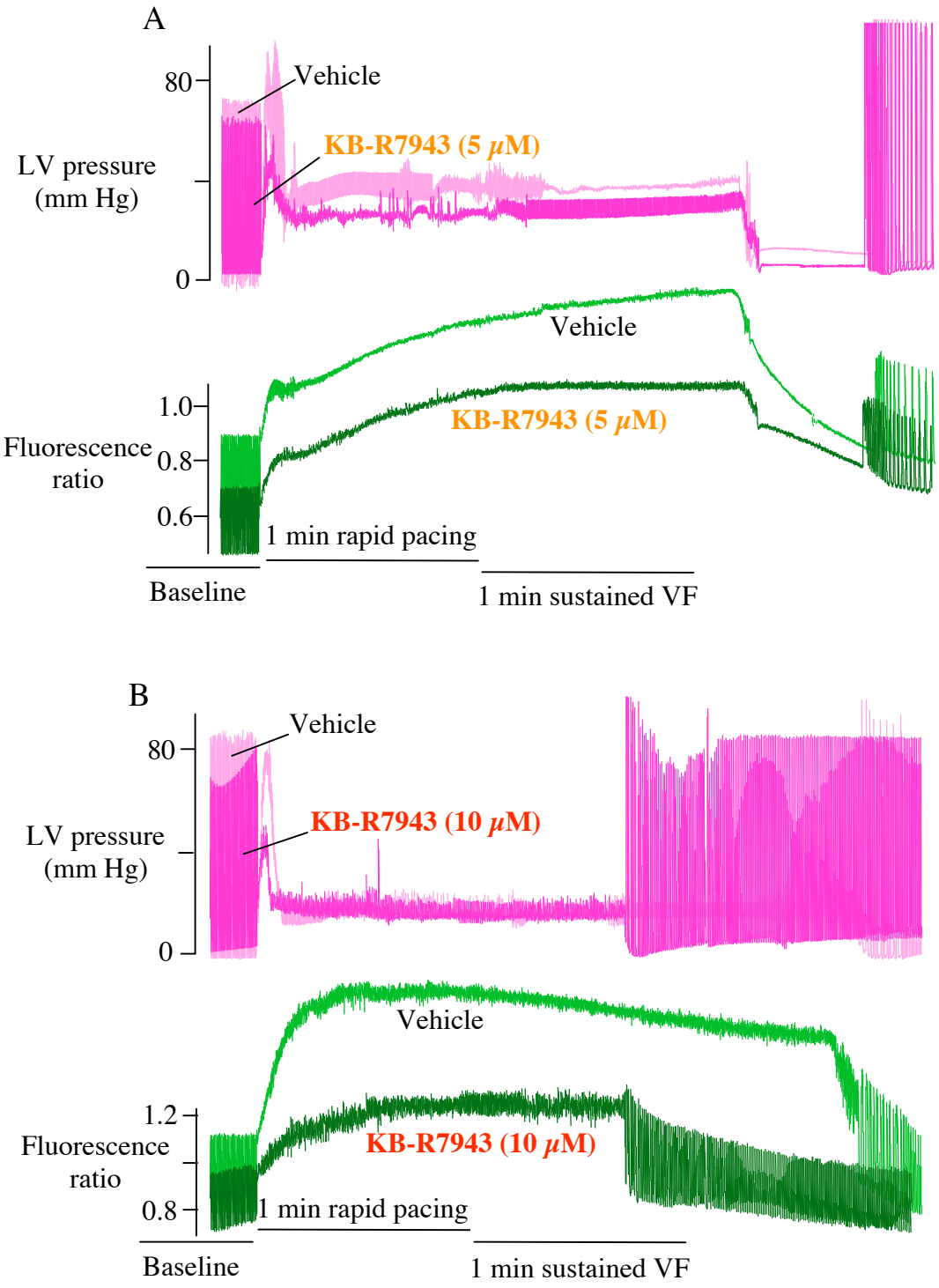

Figure 24. Original recordings of fluorescence ratio and LV pressure of hearts treated with KB-R7943: (A) 5 μM, (B) 10 μM. The tracings of two sequential VF inductions in the same heart with the vehicle and the drug perfusion are overlayed.

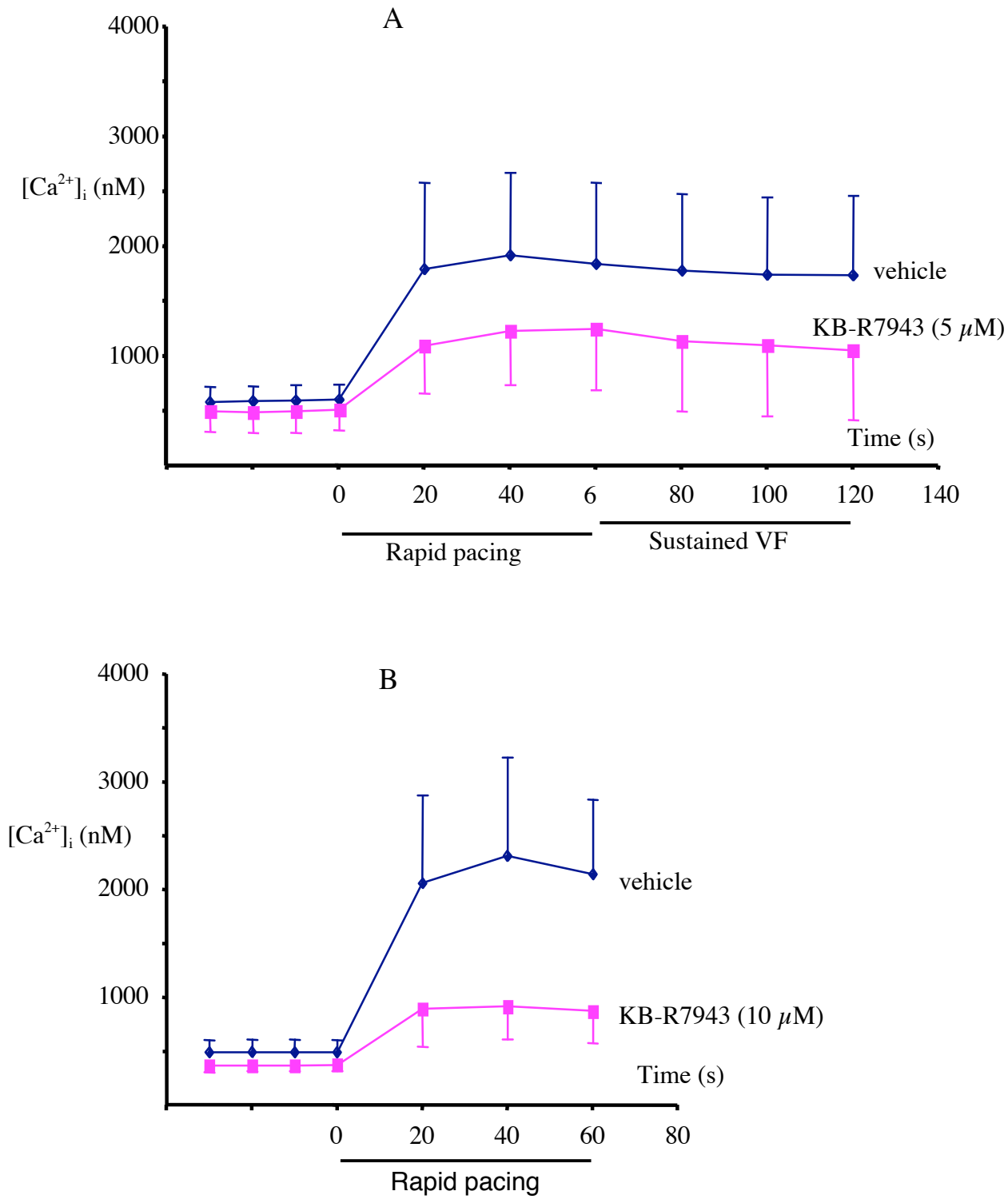

Figure 25. Mean±SD $[Ca^{2+}]_i$ accumulation during VF in hearts treated with KB-R7943: (A), 5 μM and (B), 10 μM. Sampling intervals were 10 s beginning 30 s before VF induction and 20 s after VF was induced.

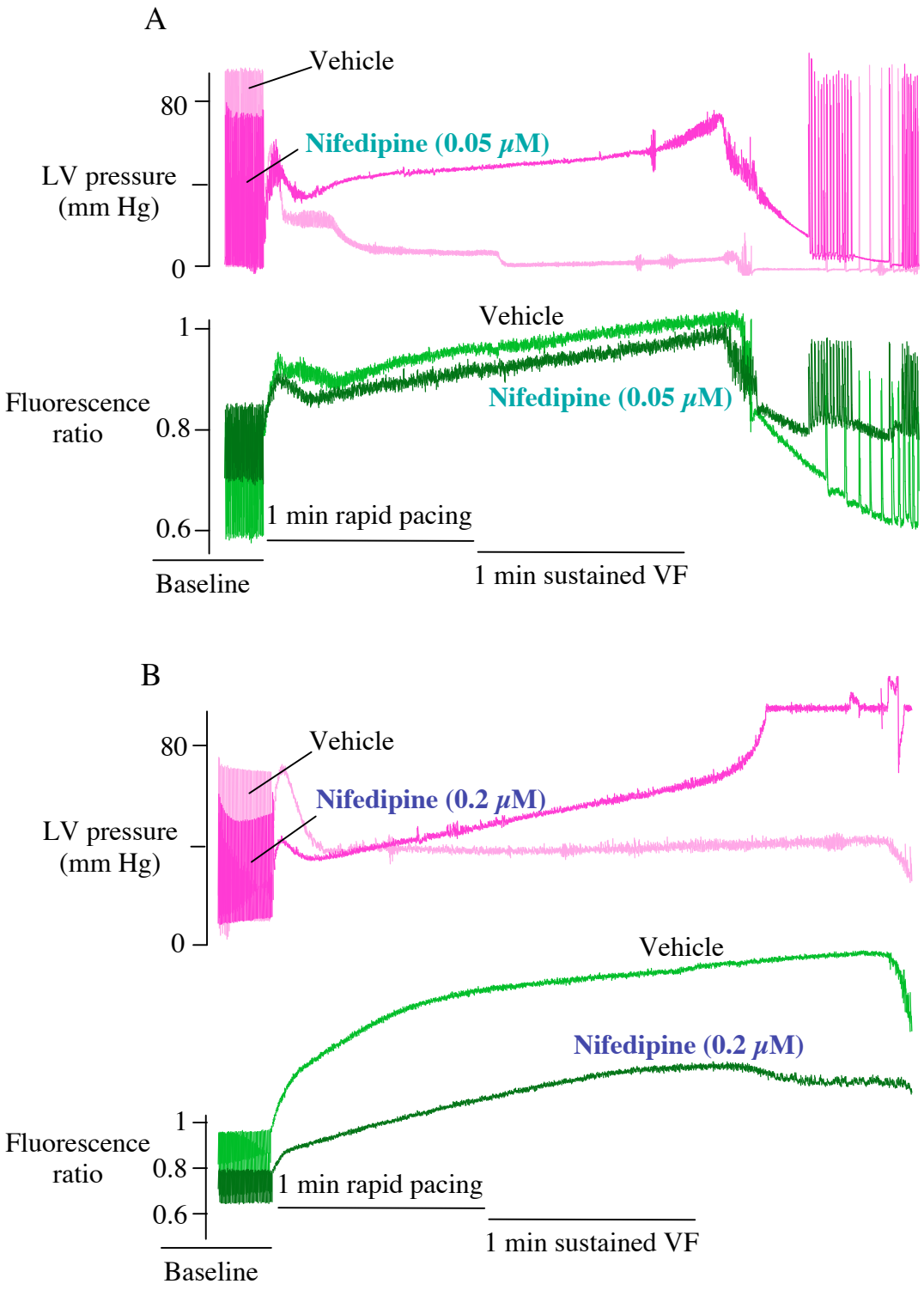

Figure 26. Original recordings of fluorescence ratio and LV pressure of hearts treated with nifedipine: (A) 0.05 μM, (B) 0.2 μM. The tracings of two sequential VF inductions in the same heart, the vehicle and the drug perfusion, are overlayed.

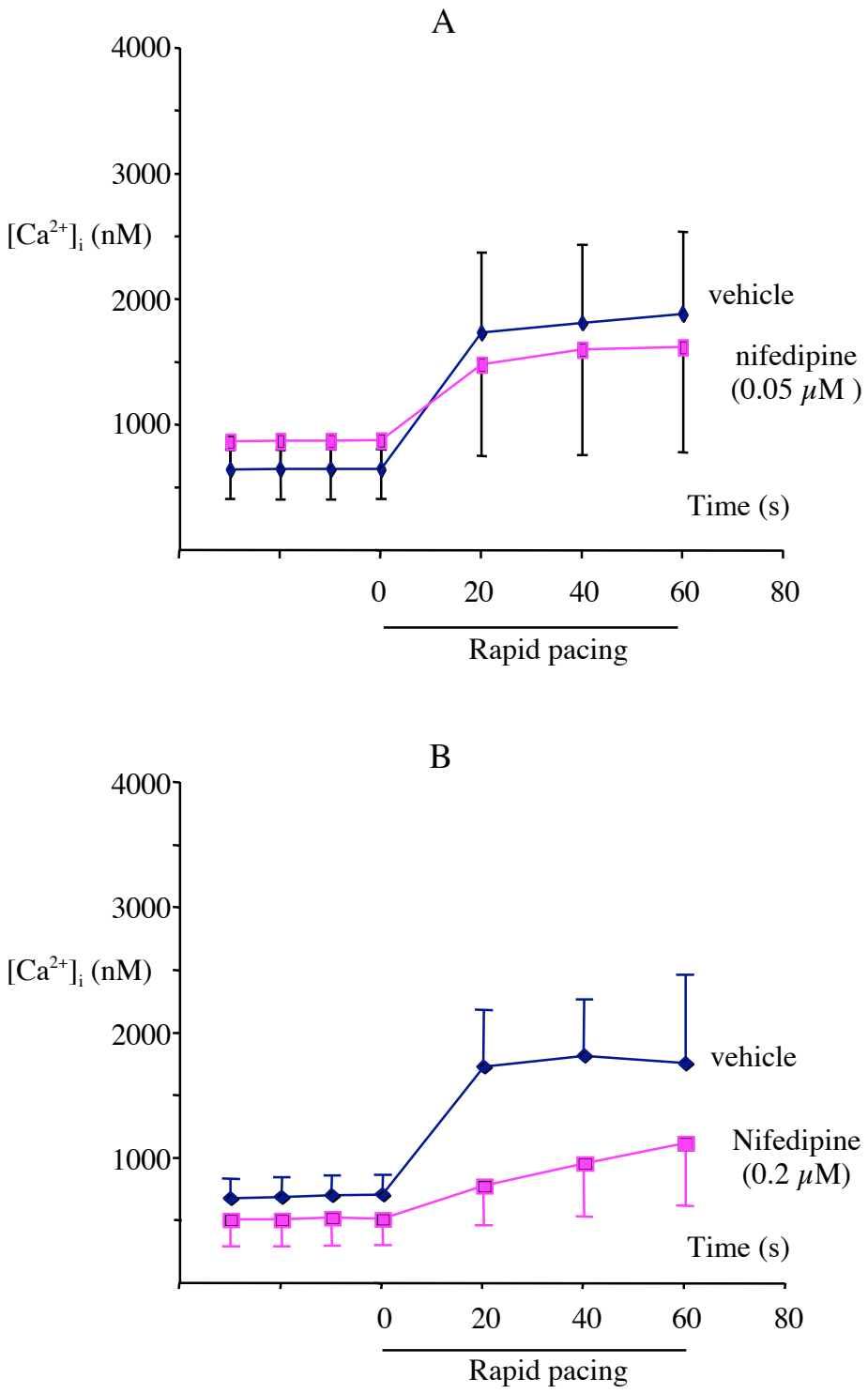

Figure 27. Mean±SD $[Ca^{2+}]_i$ accumulation during VF in hearts treated with nifedipine: (A) 0.05 μM, (B) 0.2 μM. Sampling intervals were 10 s before VF induction and 20 s after VF was induced.

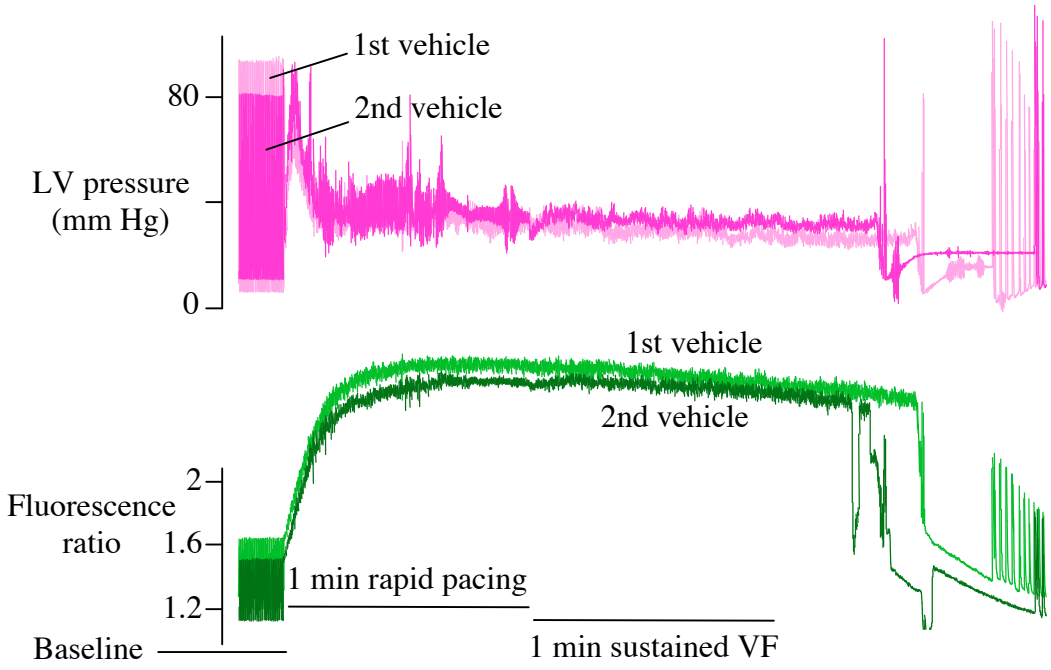

Figure 28. Original recordings of fluorescence ratio and LV pressure of a control heart (repeated vehicle). The tracings of two sequential VF inductions in the same heart are overlayed.

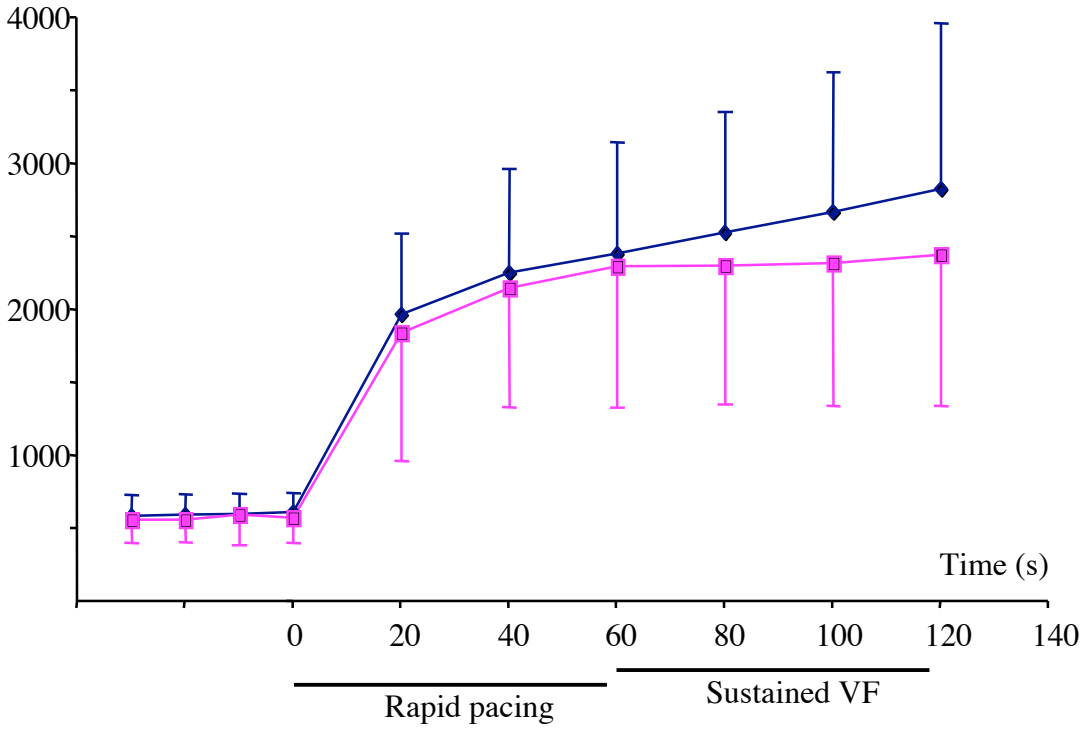

Figure 29. Mean±SD $[Ca^{2+}]_i$ accumulation during VF in hearts of the control group (repeated vehicle). Sampling intervals were 10 s before VF induction and 20 s after VF was induced.

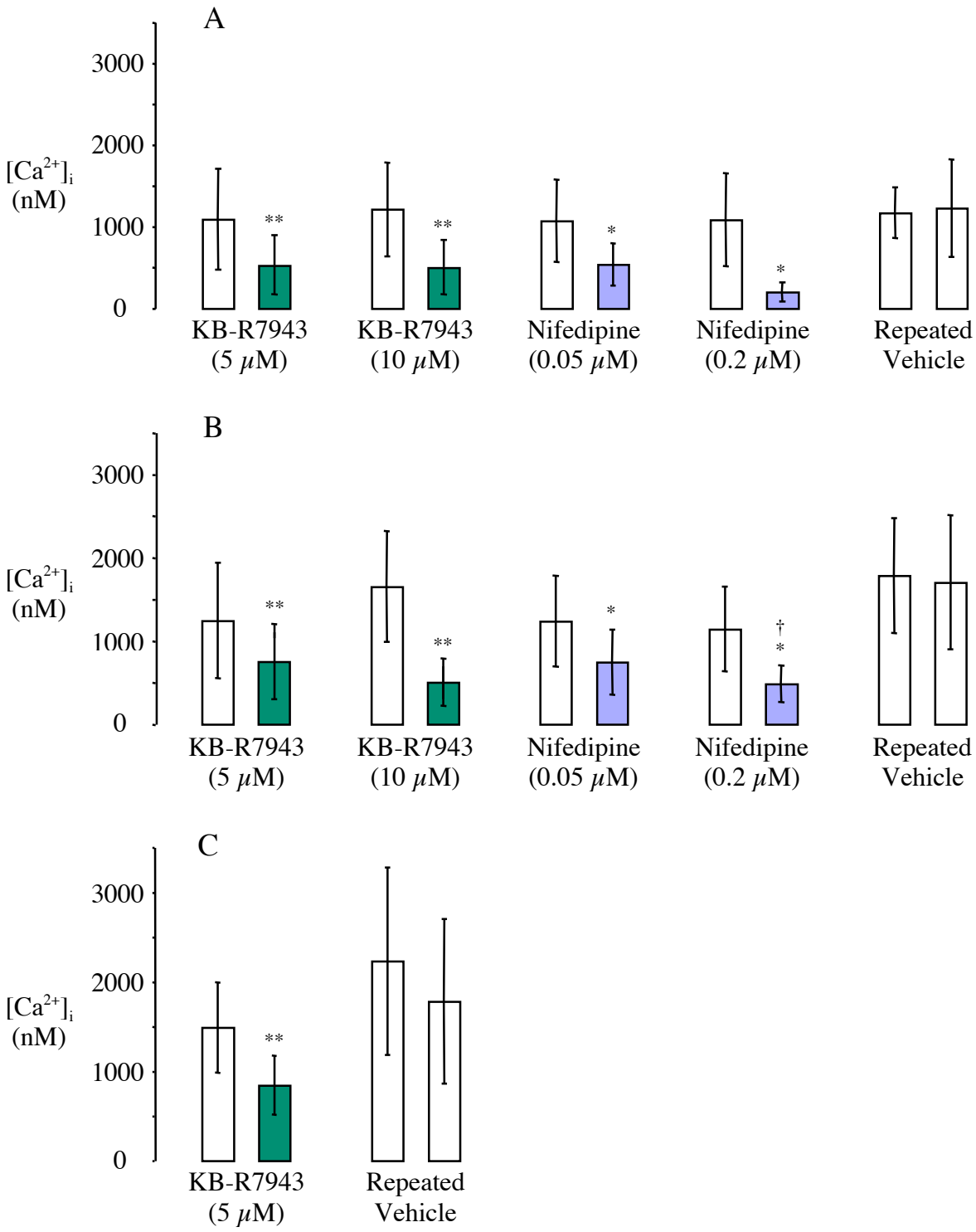

Figure 30. $[Ca^{2+}]_i$ accumulation extend (mean±SD) during VF in hearts treated with KB-R7943 and nifedipine before VF induction. Measurements performed (A) 10 sec after VF induction, (B) at the end of rapid pacing, (C) after 1 min sustained VF. Open bars stand for vehicle, closed for drug treatment (see subscripts). Statistical comparison was made using paired t-test. **p<0.01 vs. vehicle; *p<0.05 vs. vehicle; †p<0.02 at the end of rapid pacing vs. 10 s of after VF.

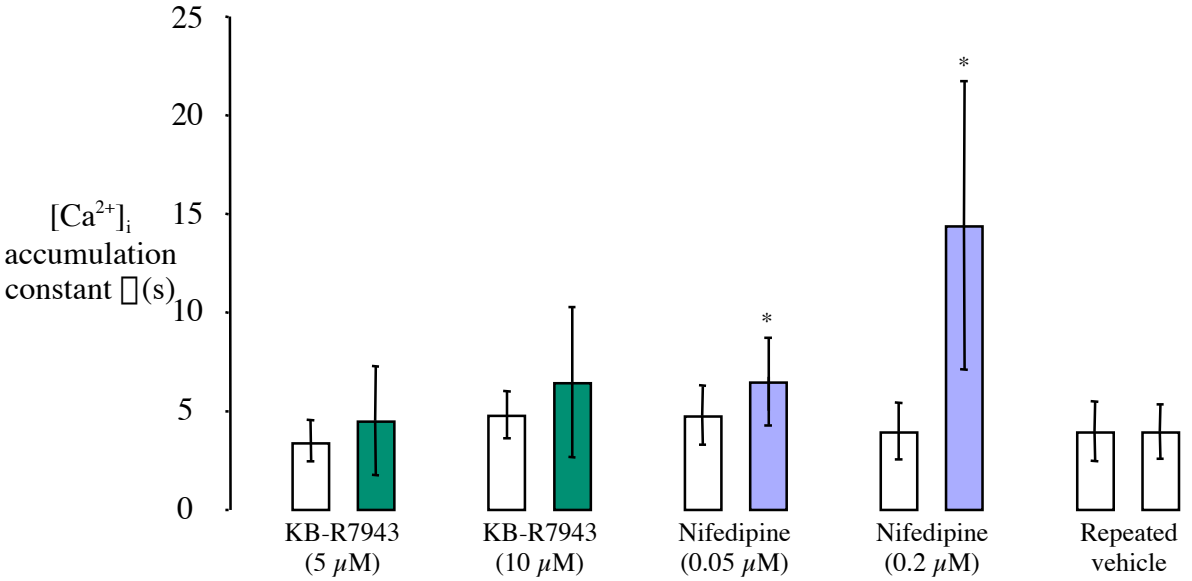

Figure 31. $[Ca^{2+}]_i$ accumulation rate (expressed as time constant τ) during VF in hearts treated with KB-R7943 and nifedipine before VF induction. Open bars stand for vehicle, closed for drug treatment (see subscripts). Statistical comparison was performed using paired t-test. *$p < 0.05$.

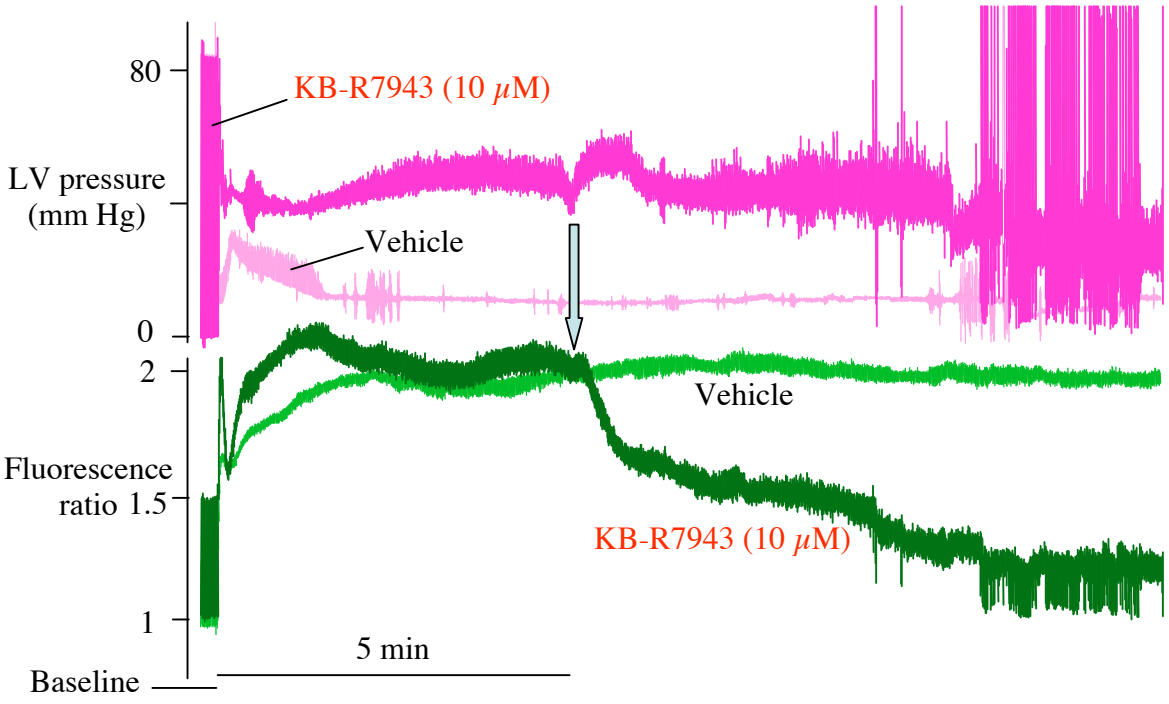

Figure 32. Original recordings of fluorescence ratio and LV pressure of a heart perfused with KB-R7943 beginning 5 min after VF induction overlayed with corresponding recordings of a control heart. Arrow indicates beginning of KB-R7943 infusion.

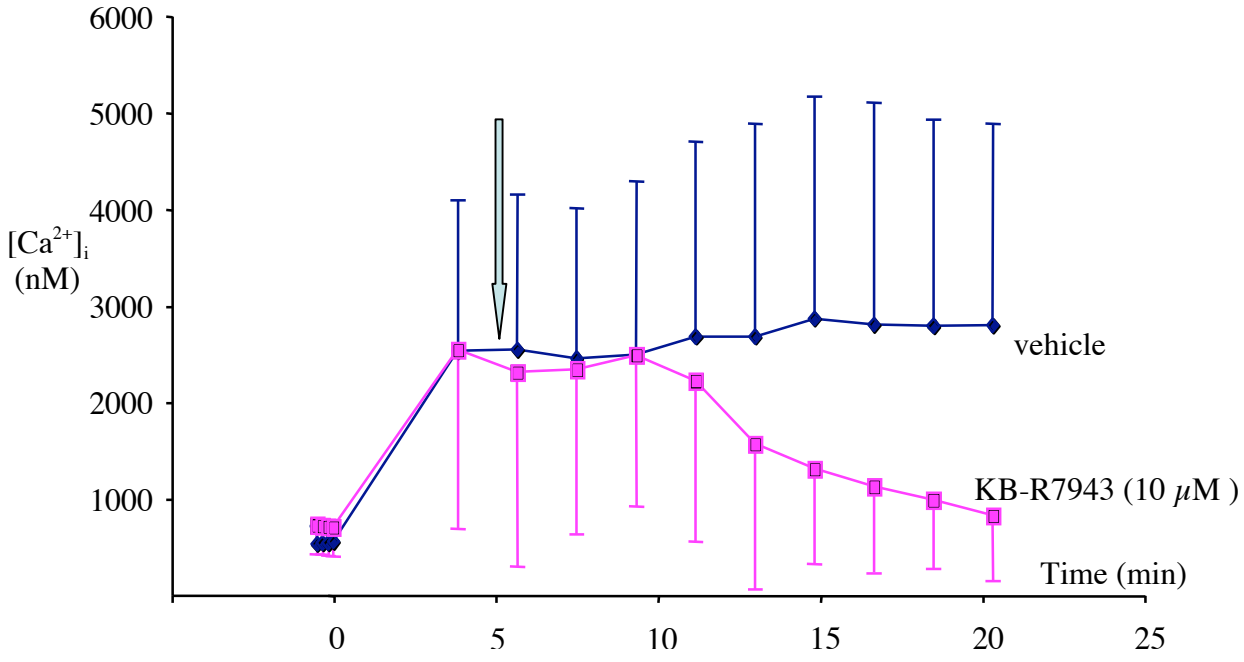

Figure 33. Mean±SD $[Ca2+]_i$ accumulation during VF in hearts treated with 10 μM KB-R7943 after VF induction compared to the control group. Sampling interval was 10 s before VF induction and 2 min after VF has been induced. Arrow indicates beginning of KB-R7943 infusion.

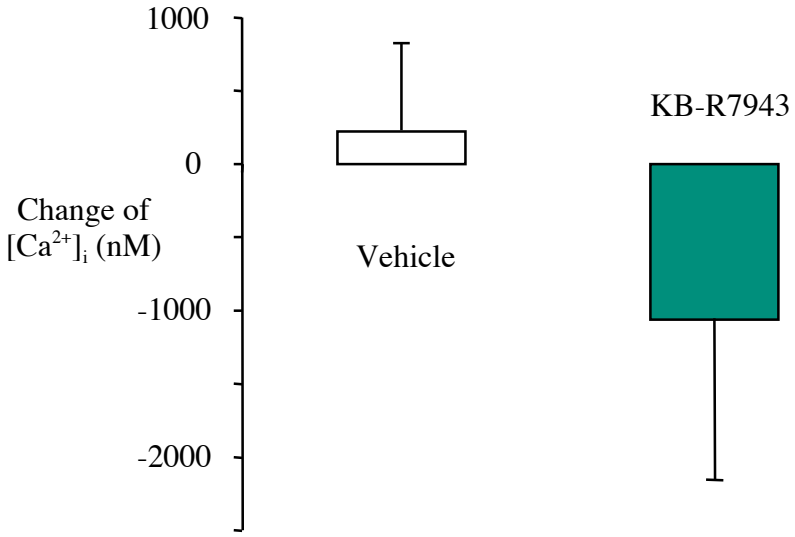

Figure 34. The reduction of $[Ca^{2+}]_i$ produced by perfusion of 10 μM KB-R7943 after induction of VF. ** $p < 0.01$, unpaired t-test.

5. DISCUSSION

Our study in isolated rat hearts shows that $[Ca^{2+}]_i$ rises biphasically during VF. During the first two minutes of VF $[Ca^{2+}]_i$ increases rapidly to double of systolic $[Ca^{2+}]_i$, that is ≈2 – 2.5 μM. Thereafter $[Ca^{2+}]_i$ increases more slowly, approaching ≈3 μM after 5 min of VF. Such increase of $[Ca^{2+}]_i$ over physiological levels is sufficient to activate calpains, which are known to be activated by 1-20 μM $[Ca^{2+}]_i$ in vitro[105] and by ischemia/reperfusion.[106] The substrates for calpains include important cardiac myofibrillar proteins troponin I and troponin T.[47] Therefore, postfibrillatory myocardial dysfunction is a consequence of reduced myofilament Ca^{2+} responsiveness following myocyte Ca^{2+} overload caused by VF.

Our study also shows that both L-type Ca^{2+} channels and Na^+/Ca^{2+}-exchange are important ways of Ca^{2+} entry into cardiac myocytes during initial stage of VF in rat hearts. Additionally, Na^+/Ca^{2+}-exchange is an important Ca^{2+} -source in persisting VF. Specifically, both nifedipine, the blocker of L-type Ca^{2+} channels, and KB-R7943, the specific blocker of the reverse mode of Na^+/Ca^{2+}-exchange, significantly reduced Ca^{2+} overload both after 10 and after 60 s (Fig. 30 A and B) of VF induction by rapid pacing; KB-R7943 at 5 μM also significantly reduced Ca^{2+} overload after 1 min sustained VF (Fig 30 C). Furthermore, hearts treated with 10 μM KB-R7943 before VF frequently defibrillated after the end of rapid pacing while untreated control hearts did not (Table 4, $p<0.05$). Nifedipine, both at 0.05 and at 0.2 μM, slowed Ca^{2+} accumulation rate (increased time constant □, $p<0.05$, Fig. 31). Additionally, 10 μM KB-R7943 infused 5 min after VF had been induced also significantly reduced Ca^{2+} overload (Fig. 34).

The role of Na^+/Ca^{2+}-exchange in VF

To the best of our knowledge, there has been no study on the role of Na^+/Ca^{2+}-exchange on Ca^{2+} overload during VF so far. This is partly due to the lack of a proper pharmacological tool. However, KB-R7943, the inhibitor of the reverse mode of Na^+/Ca^{2+}-exchange, has been available since 1996.[88] Therefore, to a large extend this is due to the difficulties of the technique of measuring $[Ca^{2+}]_i$ by surface fluorescence of

indo-1 in isolated perfused heart (this problem was extensively discussed in section 3.4.3). Based on some studies, however, the role of Na^+/Ca^{2+}-exchange in VF can be suggested. For example, there is evidence obtained in isolated rat ventricular myocytes that Na^+/Ca^{2+}-exchange is involved in the generation of Ca^{2+} overload and of spontaneous Ca^{2+} oscillations induced by inhibition of Na^+/K^+ ATP-ase after strophanthidin administration.[89] Such Na^+/K^+ ATP-ase inhibition leads to an increase of $[Na^+]_i$, which changes the electrochemical potential for Na^+/Ca^{2+}-exchange promoting its operation in the reverse mode that results in excessive Ca^{2+} entry into the cytosol. The rapid activation rate in VF is also the cause of increased $[Na^+]_i$, which via change of the reversal potential of Na^+/Ca^{2+}-exchange can promote Ca^{2+} entry resuting in Ca^{2+} overload.

Our results directly show the involvement of Na^+/Ca^{2+}-exchange in myocardial Ca^{2+} overload during VF. Already at the early stage of VF, after 10 s of rapid pacing, KB-R7943 significantly reduced Ca^{2+} overload, on average by 51% and by 59% in hearts treated with 5 and 10 μM KB-R7943, respectively (Fig. 30 A). This reduction did not decline afterwards and was 40 and 70% for the corresponding groups at the end of rapid pacing (Fig. 30 B). After 1 min sustained VF Ca^{2+} overload was reduced by 43% in hearts treated with 5 μM KB-R7943 (Fig. 30 C). Furthermore, in hearts treated with 10 μM KB-R7943, the incidence of spontaneous defibrillations was significantly higher than in control (Table 5). Moreover, KB-R7943 infusion after 5 min of persisting VF also significantly reduced Ca^{2+} overload (Fig. 33, 34) and led to spontaneous defibrillations (Table 5). These findings indicate for the first time that Na^+/Ca^{2+}-exchange plays an important role in the generation of myocardial Ca^{2+} overload at all stages of VF and thus in maintaining VF.

.[56] This is also confirmed in our experiments, which show, that blocking reverse mode of Na^+/Ca^{2+}-exchange by KB-R7943 was sufficient to lower diastolic and, especially, systolic $[Ca^{2+}]_i$, reducing the $[Ca^{2+}]_i$ transient amplitude (Fig. 23). Consequently, Na^+/Ca^{2+}-exchange contributes to loading of cardiomyocyte with Ca^{2+} from the very beginning of VF. This contribution can be expected to increase as VF continues because 1) the balance of Ca^{2+} flux mediated by Na^+/Ca^{2+}-exchange is shifted further into the reverse mode favoring Ca^{2+} entry with the rapid increase of $[Na^+]_i$ and 2) as VF persists,

the contribution of L-type Ca^{2+} channels is known to decrease[5] while $[Ca^{2+}]_i$ continues to increase.[38-41] Since blocking Na^+/Ca^{2+}-exchange with KB-R7943 infused after VF induction reduced Ca^{2+} overload and led to spontaneous defibrillation, it can be concluded that Na^+/Ca^{2+}-exchange is the only source of Ca^{2+} maintaining VF. This conclusion is in line with the concept of vicious circle, that is: VF supports Ca^{2+} overload and Ca^{2+} overload supports VF.[4] Our results add to this concept that the structure supporting the vicious circle is Na^+/Ca^{2+}-exchange.

The role of L-type Ca^{2+} channels in VF

The involvement of L-type Ca^{2+} channels in Ca^{2+} overload during VF has been shown in previous studies.[6,107] In particular, the L-type Ca^{2+} channel blocker diltiazem at 1 μM prevented VF-induced Ca^{2+} overload in isolated rat hearts.[6] This role of L-type Ca^{2+} channels was prominent at the initial stages of VF but decreased as VF persisted because diltiazem perfusion after 5 min of VF could not prevent Ca^{2+} overload from increasing further in perfused rat hearts.[5] These results support the idea that the contribution of L-type Ca^{2+} channels in VF-induced Ca^{2+} overload is time-dependent. The first novel evidence of the prominent role of L-type Ca^{2+} channels at the initial stage of VF is that nifedipine both at 0.05 and at 0.2 μM significantly reduced Ca^{2+} accumulation rate in our experiments (Fig. 31). In contrast, the corresponding effect of KB-R7943 at both concentrations did not reach statistical significance (Fig. 31) The second novel evidence is that after 10 s of rapid pacing nifedipine significantly reduced the extend of Ca^{2+} accumulation (Fig. 30 A). At the end of rapid pacing this reduction was smaller but still significant (Fig. 30 B). However, in the group treated with 0.2 μM nifedipine the reduction of Ca^{2+} accumulation at the end of rapid pacing was significantly smaller than after 10 s of rapid pacing ($p<0.02$). This difference was not significant in the group treated with 0.05 μM nifedipine, probably due to insufficient blocking of L-type Ca^{2+} channels, and, therefore, insufficient reduction of Ca^{2+} overload after 10 s of rapid pacing. Also in the groups treated with both concentrations of KB-R7943 there was no significant difference of Ca^{2+} accumulation measured at corresponding time points (Fig. 30).

Limitations

Estimation of Ca^{2+} overload during VF using indo-1 fluorescence is intrinsically hampered by reduced sensitivity of this fluorescent dye at high $[Ca^{2+}]_i$. The sensitivity of indo-1 is already reduced when cytosolic Ca^{2+} is as high as 1 μM[65,70] (Fig. 13). The sensitivity of indo-1 is reduced even further with higher $[Ca^{2+}]_i$ observed in our experiments during VF. This can explain the high variability of $[Ca^{2+}]_i$ of our data (Fig. 25, 27, 29, 32). Additionally, due to the reduced sensitivity of indo-1, $[Ca^{2+}]_i$ during VF could be underestimated. The underestimation of $[Ca^{2+}]_i$ during VF, however, can not undermine our results, and, most important, our conclusions. That is, during VF $[Ca^{2+}]_i$ increases to levels double of systolic and higher. This level of $[Ca^{2+}]_i$ is sufficient to activate calpains, the proteases degrading contractile proteins and causing in such way postfibrillatory myocardial dysfunction.

Our protocol with sequential induction of VF in the same heart, the first time with vehicle and the second time with the drug being perfused, may invoke the following criticism. First, there is data suggesting that Ca^{2+} is one of triggers of ischemic preconditioning of myocardium.[108] Therefore, transitory $[Ca^{2+}]_i$ overload experienced by hearts during first VF could have preconditioning effect on the hears, similar to the effect of ischemic preconditioning. The ischemic preconditioning itself, however, results in better tolerance to Ca^{2+} overload and reduced elevation of $[Ca^{2+}]_i$ during the following episode of ischemia.[109] Therefore, the same mechanism could lead to reduced Ca^{2+} accumulation during the second episode of VF. Second, due to photobleaching of indo-1 the increase of fluorescence ratio during the second VF may be reduced. Furthermore, fluorescence ratio could also be reduced due to the gradual deterioration of the isolated heart preparation. To rule out these two concerns, we confirmed the validity of our results in the control group (Fig. 28, 29, 30). Repetitive induction of VF in this group, both times with vehicle, showed no significant difference of $[Ca^{2+}]_i$ neither after 10 nor after 60 s of rapid pacing nor after 1 min sustained VF. Additionally, there was no difference of Ca^{2+} accumulation rate between the first and the second VF (Fig. 31). Accordingly, in the control group, spontaneous defibrillations did not occur during second VF (Table 5). On average, there was virtually no difference in $[Ca^{2+}]_i$ between the first and the second VF in the control

group at baseline and throughout the period of rapid pacing (Fig. 24, 29, 30). Only after 1 min sustained VF Ca^{2+} accumulation was reduced by 20% during the second VF (Fig. 29, 30); this reduction, however, was not significant (p=0.20). The similar levels of $[Ca^{2+}]_i$ at baseline and during rapid pacing during the first and the second VF in the control group allow to rule out the effects of photobleaching or of deterioration in our experiments.

Another potential limitation is the specificity of KB-R7943 in concentrations, used in our experiments. As has been mentioned in section 3.5.1, the majority of studies demonstrates specificity of KB-R7943 in the micromolar range.[86,87,89-91] However, there is another study suggesting the opposite.[88] Specifically, using ramp pulse protocol, it has been shown that KB-R7943 inhibits Na^+ currents, L-type Ca^{2+} currents and inward rectifier K^+ currents with IC_{50} 14, 8 and 7 μM, respectively.[88] The inhibition of Na^+ and L-type Ca^{2+} currents could be the cause of reduced Ca^{2+} accumulation in hearts treated with KB-R7943 in our experiments. The ramp pulse protocol, however, is considered to be too severe and has little relevance to physiological conditions.[53] Other studies showed that in rat ventricular myocytes KB-R7943 at 5 μM did not alter steady-state twitches, Ca^{2+} transients, Ca^{2+} load in the SR, or rest potentiation.[89] In guinea pig papillary muscle, however, KB-R7943 at up to 10 μM did not significantly affect the resting membrane potential or various action potential parameters.[87,90] Similarly, 10 or 30 μM KB-R7943 did not alter spontaneous beating rate and developed tension in isolated guinea pig atria.[91] Based on foregoing, we consider KB-R7943 to be specific enough at concentrations used in our experiments.

Species considerations

Our study showing the role of Na^+/Ca^{2+}-exchange in VF was performed in isolated rat hearts. It is important to note that the central role of Ca^{2+} in excitation-contraction coupling involving Ca^{2+}-induced Ca^{2+} release in cardiac muscle[26] suggests that VF leads to myocyte Ca^{2+} overload in most species including adult human beings. However, important inter-species and developmental differences exist regarding Ca^{2+}-induced Ca^{2+} release from the sarcoplasmic reticulum and regarding Ca^{2+} removal processes[26]. Consequently, activator Ca^{2+} in cardiac muscle of various species depends on different

contributions from the sarcoplasmic reticulum, from L-type Ca^{2+} channels, and from Na^{+}/Ca^{2+}-exchange [26]. The kinetics and the degree of VF-induced myocyte Ca^{2+} overload may therefore vary among species and be part of the reason why some species are better protected against sustained VF than others (similar to myocardial mass). Based on the foregoing, VF in adult human beings most likely induces cardiomyocyte Ca^{2+} overload and the Ca^{2+} sources of this overload may be to some extend but not fundamentally different from adult rat ventricles.[4] The relative contribution of Na^{+}/Ca^{2+}-exchange to Ca^{2+} extrusion from cardiomyocytes in rat and in human differs in the following way: Na^{+}/Ca^{2+}-exchange extrudes ≈30% of Ca^{2+} required to activate the myofilaments in human ventricles but a much smaller portion (≈7%) in rat ventricles.[25] This suggests possibility of a similar interspecies difference in contribution of Na^{+}/Ca^{2+}-exchange to Ca^{2+} entry during cardiac cycle. If this is the case, the role of Na^{+}/Ca^{2+}-exchange in Ca^{2+} overload during VF and in the vulnerability to VF in human beings can be more prominent than in rat. In heart failure patients, Na^{+}/Ca^{2+}-exchange has been found to be overexpressed potentially compensating for reduced SERCA function.[57] Consequently, enhanced electrogenic Na^{+}/Ca^{2+}-exchange-activity may not only lead to delayed afterdepolarizations but also maintain VF providing further Ca^{2+} entry during prolonged VF. Thus, blocking enhanced Na^{+}/Ca^{2+}-exchange in failing hearts might be beneficial in both reducing the incidence of VF and undermining the self-maintaining nature of VF.

In summary, we have shown that during the first two minutes of VF $[Ca^{2+}]_i$ increases to ≈2 – 2.5 μM. Thereafter it increases slowly, approaching ≈3 μM. We have also shown that both L-type Ca^{2+} channels and Na^{+}/Ca^{2+}-exchange are important ways of Ca^{2+} entry into cardiac myocytes during initial stage of VF in rat hearts. Additionally, Na^{+}/Ca^{2+}-exchange is an important Ca^{2+} -source in persisting VF. An important clinical implication of our results is that blocking Na^{+}/Ca^{2+}-exchange might help in both reducing incidence and interrupting the vicious circle of VF.

6. CONCLUSIONS

1. During the first two minutes of VF $[Ca^{2+}]_i$ increases to 2 – 2.5 μM. Thereafter it is increasing slowly, approaching 3 μM .

2. Both L-type Ca^{2+} channels and Na^+/Ca^{2+}-exchange are important ways of Ca^{2+} entry into cardiac myocytes during VF in normal rat hearts. The role of L-type Ca^{2+} channels is more important at the initial stage of VF.

3. Na^+/Ca^{2+}-exchange is an important Ca^{2+} -source maintaining VF.

7. REFERENCES

1. Burkhardt J, Müller, H.K., Tschanz, R. *Das Gesundheitswesen in der Schweiz.* Basel; 2003.
2. Weiss JN, Chen PS, Wu TJ, Siegerman C, Garfinkel A. Ventricular fibrillation: new insights into mechanisms. *Ann N Y Acad Sci*. 2004;1015:122-32.
3. Moss AJ, Zareba W, Hall WJ, Klein H, Wilber DJ, Cannom DS, Daubert JP, Higgins SL, Brown MW, Andrews ML. Prophylactic implantation of a defibrillator in patients with myocardial infarction and reduced ejection fraction. *N Engl J Med*. 2002;346:877-83.
4. Zaugg CE. Current concepts on ventricular fibrillation: A Visious Circle of Cardiomyocyte Calcium Overload in the Initiation, Maintenance and Termination of Ventricular Fibrillation. *Indian Pacing and Electrophysiology Journal*. 2004;4:85-92.
5. Zaugg CE, Wu ST, Barbosa V, Buser PT, Wikman-Coffelt J, Parmley WW, Lee RJ. Ventricular fibrillation-induced intracellular Ca2+ overload causes failed electrical defibrillation and post-shock reinitiation of fibrillation. *J Mol Cell Cardiol*. 1998;30:2183-92.
6. Zaugg CE, Ziegler A, Lee RJ, Barbosa V, Buser PT. Postresuscitation stunning: postfibrillatory myocardial dysfunction caused by reduced myofilament Ca2+ responsiveness after ventricular fibrillation-induced myocyte Ca2+ overload. *J Cardiovasc Electrophysiol*. 2002;13:1017-24.
7. Callans DJ. Out-of-hospital cardiac arrest--the solution is shocking. *N Engl J Med*. 2004;351:632-4.
8. Katz AM. *Physioloty of the heart*. 3rd ed. Philadelphia.: Lippincott Williams & Williams.; 2001.
9. De Groot JR, Coronel R. Acute ischemia-induced gap junctional uncoupling and arrhythmogenesis. *Cardiovasc Res*. 2004;62:323-34.
10. Aronson RS, Ming, Z. Cellular mechanisms of arrhythmias in hypertrophied and failing myocardium. *Circulation*. 1993;87:VII-76 - VII-83.
11. Akar FG, Rosenbaum DS. Transmural electrophysiological heterogeneities underlying arrhythmogenesis in heart failure. *Circ Res*. 2003;93:638-45.
12. Pak PH, Nuss HB, Tunin RS, Kaab S, Tomaselli GF, Marban E, Kass DA. Repolarization abnormalities, arrhythmia and sudden death in canine tachycardia-induced cardiomyopathy. *J Am Coll Cardiol*. 1997;30:576-84.
13. Gilmour RF, Jr., Heger JJ, Prystowsky EN, Zipes DP. Cellular electrophysiologic abnormalities of diseased human ventricular myocardium. *Am J Cardiol*. 1983;51:137-44.
14. Pogwizd SM, Schlotthauer K, Li L, Yuan W, Bers DM. Arrhythmogenesis and contractile dysfunction in heart failure: Roles of sodium-calcium exchange, inward rectifier potassium current, and residual beta-adrenergic responsiveness. *Circ Res*. 2001;88:1159-67.
15. Vermeulen JT, McGuire MA, Opthof T, Coronel R, de Bakker JM, Klopping C, Janse MJ. Triggered activity and automaticity in ventricular

trabeculae of failing human and rabbit hearts. *Cardiovasc Res*. 1994;28:1547-54.
16. Kihara Y, Morgan JP. Intracellular calcium and ventricular fibrillation. Studies in the aequorin-loaded isovolumic ferret heart. *Circ Res*. 1991;68:1378-89.
17. Zaugg CE, Wu ST, Lee RJ, Parmley WW, Buser PT, Wikman-Coffelt J. Importance of calcium for the vulnerability to ventricular fibrillation detected by premature ventricular stimulation: single pulse versus sequential pulse methods. *J Mol Cell Cardiol*. 1996;28:1059-72.
18. Lakatta EG, Guarnieri T. Spontaneous myocardial calcium oscillations: are they linked to ventricular fibrillation? *J Cardiovasc Electrophysiol*. 1993;4:473-89.
19. Kleber G. The potential role of Ca2+ for electrical cell-to-cell uncoupling and conduction block in myocardial tissue. *Basic Res Cardiol*. 1992;87 Suppl 2:131-43.
20. Fabiato A. Calcium-induced release of calcium from the cardiac sarcoplasmic reticulum. *Am J Physiol*. 1983;245:C1-14.
21. Fabiato F, Fabiato A. [Excitation-contraction coupling and regulation of contractility studied on isolated adult myocardial cells]. *Acta Cardiol*. 1972;27:243-8.
22. Fabiato A, Fabiato F. Contractions induced by a calcium-triggered release of calcium from the sarcoplasmic reticulum of single skinned cardiac cells. *J Physiol*. 1975;249:469-95.
23. Sipido KR, Maes M, Van de Werf F. Low efficiency of Ca2+ entry through the Na(+)-Ca2+ exchanger as trigger for Ca2+ release from the sarcoplasmic reticulum. A comparison between L-type Ca2+ current and reverse-mode Na(+)-Ca2+ exchange. *Circ Res*. 1997;81:1034-44.
24. Bers DM. Calcium fluxes involved in control of cardiac myocyte contraction. *Circ Res*. 2000;87:275-81.
25. Bers DM. Cardiac excitation-contraction coupling. *Nature*. 2002;415:198-205.
26. Bers DM. *Excitation-contraction coupling and cardiac contractile force.* 2nd ed. Dordrecht: Kluwers Academic Press; 2002.
27. Puglisi JL, Yuan W, Bassani JW, Bers DM. Ca(2+) influx through Ca(2+) channels in rabbit ventricular myocytes during action potential clamp: influence of temperature. *Circ Res*. 1999;85:e7-e16.
28. Shannon TR, Ginsburg KS, Bers DM. Potentiation of fractional sarcoplasmic reticulum calcium release by total and free intra-sarcoplasmic reticulum calcium concentration. *Biophys J*. 2000;78:334-43.
29. Stern MD, Song LS, Cheng H, Sham JS, Yang HT, Boheler KR, Rios E. Local control models of cardiac excitation-contraction coupling. A possible role for allosteric interactions between ryanodine receptors. *J Gen Physiol*. 1999;113:469-89.
30. Zahradnikova A, Dura M, Gyorke S. Modal gating transitions in cardiac ryanodine receptors during increases of Ca2+ concentration produced by photolysis of caged Ca2+. *Pflugers Arch*. 1999;438:283-8.
31. Katz AM, Repke DI, Dunnett J, Hasselbach W. Dependence of calcium permeability of sarcoplasmic reticulum vesicles on external and internal calcium ion concentrations. *J Biol Chem*. 1977;252:1950-6.

32. Davidenko JM, Pertsov AV, Salomonsz R, Baxter W, Jalife J. Stationary and drifting spiral waves of excitation in isolated cardiac muscle. *Nature*. 1992;355:349-51.
33. Fast VG, Kleber AG. Role of wavefront curvature in propagation of cardiac impulse. *Cardiovasc Res*. 1997;33:258-71.
34. Thandroyen FT, Morris AC, Hagler HK, Ziman B, Pai L, Willerson JT, Buja LM. Intracellular calcium transients and arrhythmia in isolated heart cells. *Circ Res*. 1991;69:810-9.
35. Viatchenko-Karpinski S, Terentyev D, Gyorke I, Terentyeva R, Volpe P, Priori SG, Napolitano C, Nori A, Williams SC, Gyorke S. Abnormal calcium signaling and sudden cardiac death associated with mutation of calsequestrin. *Circ Res*. 2004;94:471-7.
36. Terentyev D, Viatchenko-Karpinski S, Gyorke I, Volpe P, Williams SC, Gyorke S. Calsequestrin determines the functional size and stability of cardiac intracellular calcium stores: Mechanism for hereditary arrhythmia. *Proc Natl Acad Sci U S A*. 2003;100:11759-64.
37. Wehrens XH, Lehnart SE, Huang F, Vest JA, Reiken SR, Mohler PJ, Sun J, Guatimosim S, Song LS, Rosemblit N, D'Armiento JM, Napolitano C, Memmi M, Priori SG, Lederer WJ, Marks AR. FKBP12.6 deficiency and defective calcium release channel (ryanodine receptor) function linked to exercise-induced sudden cardiac death. *Cell*. 2003;113:829-40.
38. Koretsune Y, Marban E. Cell calcium in the pathophysiology of ventricular fibrillation and in the pathogenesis of postarrhythmic contractile dysfunction. *Circulation*. 1989;80:369-79.
39. Kojima S, Wikman-Coffelt J, Wu ST, Parmley WW. Nature of [Ca2+]i transients during ventricular fibrillation and quinidine treatment in perfused rat hearts. *Am J Physiol*. 1994;266:H1473-84.
40. Zaugg CE, Wu ST, Kojima S, Wikman-Coffelt J, Parmley WW, Buser PT. Role of intracellular calcium in the antiarrhythmic effect of procainamide during ventricular fibrillation in rat hearts. *Am Heart J*. 1995;130:351-8.
41. Kojima S, Wu ST, Wikman-Coffelt J, Parmley WW. Acute amiodarone terminates ventricular fibrillation by modifying cellular Ca++ homeostasis in isolated perfused rat hearts. *J Pharmacol Exp Ther*. 1995;275:254-62.
42. Zaugg CE, Kojima S, Wu ST, Wikman-Coffelt J, Parmley WW, Buser PT. Intracellular calcium transients underlying interval-force relationship in whole rat hearts: effects of calcium antagonists. *Cardiovasc Res*. 1995;30:212-21.
43. Jones DL, Kim YH, Natale A, Klein GJ, Varin F. Bretylium decreases and verapamil increases defibrillation threshold in pigs. *Pacing Clin Electrophysiol*. 1994;17:1380-90.
44. Jones DL, Klein GJ, Guiraudon GM, Yee R, Brown JE, Sharma AD. Effects of lidocaine and verapamil on defibrillation in humans. *J Electrocardiol*. 1991;24:299-305.
45. Zaugg CE, Wu ST, Lee RJ, Wikman-Coffelt J, Parmley WW. Intracellular Ca2+ handling and vulnerability to ventricular fibrillation in spontaneously hypertensive rats. *Hypertension*. 1997;30:461-7.
46. Chen PS, Shibata N, Dixon EG, Martin RO, Ideker RE. Comparison of the defibrillation threshold and the upper limit of ventricular vulnerability. *Circulation*. 1986;73:1022-8.

47. Bolli R, Marban E. Molecular and cellular mechanisms of myocardial stunning. *Physiol Rev*. 1999;79:609-34.
48. Crespo LM, Grantham CJ, Cannell MB. Kinetics, stoichiometry and role of the Na-Ca exchange mechanism in isolated cardiac myocytes. *Nature*. 1990;345:618-21.
49. Blaustein MP, Lederer WJ. Sodium/calcium exchange: its physiological implications. *Physiol Rev*. 1999;79:763-854.
50. Reeves JP, Hale CC. The stoichiometry of the cardiac sodium-calcium exchange system. *J Biol Chem*. 1984;259:7733-9.
51. Mattiello JA, Margulies KB, Jeevanandam V, Houser SR. Contribution of reverse-mode sodium-calcium exchange to contractions in failing human left ventricular myocytes. *Cardiovasc Res*. 1998;37:424-31.
52. Bridge JH, Smolley JR, Spitzer KW. The relationship between charge movements associated with ICa and INa-Ca in cardiac myocytes. *Science*. 1990;248:376-8.
53. Shigekawa M, Iwamoto T. Cardiac Na(+)-Ca(2+) exchange: molecular and pharmacological aspects. *Circ Res*. 2001;88:864-76.
54. Mullins LJ. The generation of electric currents in cardiac fibers by Na/Ca exchange. *Am J Physiol*. 1979;236:C103-10.
55. Sham JS, Cleemann L, Morad M. Functional coupling of Ca2+ channels and ryanodine receptors in cardiac myocytes. *Proc Natl Acad Sci U S A*. 1995;92:121-5.
56. Litwin SE, Li J, Bridge JH. Na-Ca exchange and the trigger for sarcoplasmic reticulum Ca release: studies in adult rabbit ventricular myocytes. *Biophys J*. 1998;75:359-71.
57. Hasenfuss G. Alterations of calcium-regulatory proteins in heart failure. *Cardiovasc Res*. 1998;37:279-89.
58. Tani M. Mechanisms of Ca2+ overload in reperfused ischemic myocardium. *Annu Rev Physiol*. 1990;52:543-59.
59. Smith TW. Digitalis. Mechanisms of action and clinical use. *N Engl J Med*. 1988;318:358-65.
60. Zink R, Heiny, O., Steiert, H., Döhring, H., Linton., P. *Bedienungsanleitung zur Apparatur isoliertes Herz, Typ 830*. March-Hugstetten, Germany; 1988.
61. Döhring HJ, H., D. *The isolated perfused warm-blooded heart according to Langendorff.* March: Biomesstechnik-Verlag March GmbH; 1988.
62. Treves S. Satellite Workshop. In. Basel: Research Department Kantonsspital Basel; 2003.
63. Grynkiewicz G, Poenie M, Tsien RY. A new generation of Ca2+ indicators with greatly improved fluorescence properties. *J Biol Chem*. 1985;260:3440-50.
64. Probes M. Molecular Probes Handbook. Fluorescent Ca2+ Indicators Excited with UV Light; Fura-2, Indo-1 and Derivatives. In: Molecular Probes; 2002.
65. Baker AJ, Brandes R, Schreur JH, Camacho SA, Weiner MW. Protein and acidosis alter calcium-binding and fluorescence spectra of the calcium indicator indo-1. *Biophys J*. 1994;67:1646-54.
66. Poenie M. Alteration of intracellular Fura-2 fluorescence by viscosity: a simple correction. *Cell Calcium*. 1990;11:85-91.

67. Ikenouchi H, Peeters GA, Barry WH. Evidence that binding of Indo-1 to cardiac myocyte protein does not markedly change Kd for Ca2+. *Cell Calcium*. 1991;12:415-22.
68. Bassani JW, Bassani RA, Bers DM. Calibration of indo-1 and resting intracellular [Ca]i in intact rabbit cardiac myocytes. *Biophys J*. 1995;68:1453-60.
69. Brandes R, Figueredo VM, Camacho SA, Baker AJ, Weiner MW. Investigation of factors affecting fluorometric quantitation of cytosolic [Ca2+] in perfused hearts. *Biophys J*. 1993;65:1983-93.
70. Brandes R, Figueredo VM, Camacho SA, Baker AJ, Weiner MW. Quantitation of cytosolic [Ca2+] in whole perfused rat hearts using Indo-1 fluorometry. *Biophys J*. 1993;65:1973-82.
71. Miyamae M, Camacho SA, Rooney WD, Modin G, Zhou HZ, Weiner MW, Figueredo VM. Inorganic phosphate and coronary perfusion pressure mediate contractile dysfunction during mild ischemia. *Am J Physiol*. 1997;273:H566-72.
72. Maier LS, Brandes R, Pieske B, Bers DM. Effects of left ventricular hypertrophy on force and Ca2+ handling in isolated rat myocardium. *Am J Physiol*. 1998;274:H1361-70.
73. Brandes R, Maier LS, Bers DM. Regulation of mitochondrial [NADH] by cytosolic [Ca2+] and work in trabeculae from hypertrophic and normal rat hearts. *Circ Res*. 1998;82:1189-98.
74. Brandes R, Bers DM. Simultaneous measurements of mitochondrial NADH and Ca(2+) during increased work in intact rat heart trabeculae. *Biophys J*. 2002;83:587-604.
75. Probes M. Loading and Calibration of Intracellular Ion Indicators. In. Molecular Probes Handbook ed: Molecuar Probes; 2004.
76. Brandes R, Figueredo VM, Camacho SA, Weiner MW. Compensation for changes in tissue light absorption in fluorometry of hypoxic perfused rat hearts. *Am J Physiol*. 1994;266:H2554-67.
77. Kojima S, Wu ST, Watters TA, Parmley WW, Wikman-Coffelt J. Effects of perfusion pressure on intracellular calcium, energetics, and function in perfused rat hearts. *Am J Physiol*. 1993;264:H183-9.
78. Wikman-Coffelt J, Stefenelli T, Wu ST, Parmley WW, Jasmin G. [Ca2+]i transients in the cardiomyopathic hamster heart. *Circ Res*. 1991;68:45-51.
79. Halpern MH. The dual blood supply of the rat heart. *Am J Anat*. 1957;101:1-16.
80. Kojima S, Wu ST, Wikman-Coffelt J, Parmley WW. Contractile and intracellular Ca2+ decay in potentiated contractions following multiple extrasystolic beats. *Cell Calcium*. 1995;18:155-64.
81. Miyata H, Silverman HS, Sollott SJ, Lakatta EG, Stern MD, Hansford RG. Measurement of mitochondrial free Ca2+ concentration in living single rat cardiac myocytes. *Am J Physiol*. 1991;261:H1123-34.
82. Williford DJ, Sharma VK, Korth M, Sheu SS. Spatial heterogeneity of intracellular Ca2+ concentration in nonbeating guinea pig ventricular myocytes. *Circ Res*. 1990;66:241-8.
83. Wahl M, Lucherini MJ, Gruenstein E. Intracellular Ca2+ measurement with Indo-1 in substrate-attached cells: advantages and special considerations. *Cell Calcium*. 1990;11:487-500.

84. Fralix TA, Heineman FW, Balaban RS. Effects of tissue absorbance on NAD(P)H and Indo-1 fluorescence from perfused rabbit hearts. *FEBS Lett*. 1990;262:287-92.
85. Wikman-Coffelt J, Wu ST, Parmley WW. Intracellular endocardial calcium and myocardial function in rat hearts. *Cell Calcium*. 1991;12:39-50.
86. Iwamoto T, Kita S, Uehara A, Inoue Y, Taniguchi Y, Imanaga I, Shigekawa M. Structural domains influencing sensitivity to isothiourea derivative inhibitor KB-R7943 in cardiac Nna(+)/Ca(2+) exchanger. *Mol Pharmacol*. 2001;59:524-31.
87. Iwamoto T, Watano T, Shigekawa M. A novel isothiourea derivative selectively inhibits the reverse mode of Na+/Ca2+ exchange in cells expressing NCX1. *J Biol Chem*. 1996;271:22391-7.
88. Watano T, Kimura J, Morita T, Nakanishi H. A novel antagonist, No. 7943, of the Na+/Ca2+ exchange current in guinea-pig cardiac ventricular cells. *Br J Pharmacol*. 1996;119:555-63.
89. Satoh H, Ginsburg KS, Qing K, Terada H, Hayashi H, Bers DM. KB-R7943 block of Ca(2+) influx via Na(+)/Ca(2+) exchange does not alter twitches or glycoside inotropy but prevents Ca(2+) overload in rat ventricular myocytes. *Circulation*. 2000;101:1441-6.
90. Mukai M, Terada H, Sugiyama S, Satoh H, Hayashi H. Effects of a selective inhibitor of Na+/Ca2+ exchange, KB-R7943, on reoxygenation-induced injuries in guinea pig papillary muscles. *J Cardiovasc Pharmacol*. 2000;35:121-8.
91. Watano T, Harada Y, Harada K, Nishimura N. Effect of Na+/Ca2+ exchange inhibitor, KB-R7943 on ouabain-induced arrhythmias in guinea-pigs. *Br J Pharmacol*. 1999;127:1846-50.
92. Ladilov Y, Haffner S, Balser-Schafer C, Maxeiner H, Piper HM. Cardioprotective effects of KB-R7943: a novel inhibitor of the reverse mode of Na+/Ca2+ exchanger. *Am J Physiol*. 1999;276:H1868-76.
93. Yamamoto M, Gotoh Y, Imaizumi Y, Watanabe M. Mechanisms of long-lasting effects of benidipine on Ca current in guinea-pig ventricular cells. *Br J Pharmacol*. 1990;100:669-76.
94. Lee KS, Tsien RW. Mechanism of calcium channel blockade by verapamil, D600, diltiazem and nitrendipine in single dialysed heart cells. *Nature*. 1983;302:790-4.
95. Carmeliet E, Mubagwa K. Antiarrhythmic drugs and cardiac ion channels: mechanisms of action. *Prog Biophys Mol Biol*. 1998;70:1-72.
96. Akiyama T. Intracellular recording of in situ ventricular cells during ventricular fibrillation. *Am J Physiol*. 1981;240:H465-71.
97. Stefenelli T, Wikman-Coffelt J, Wu ST, Parmley WW. Intracellular calcium during pacing-induced ventricular fibrillation. Effects of lidocaine. *J Electrocardiol*. 1992;25:221-8.
98. Stowe DF, Varadarajan SG, An J, Smart SC. Reduced cytosolic Ca(2+) loading and improved cardiac function after cardioplegic cold storage of guinea pig isolated hearts. *Circulation*. 2000;102:1172-7.
99. Stowe DF, Fujita S, An J, Paulsen RA, Varadarajan SG, Smart SC. Modulation of myocardial function and [Ca2+] sensitivity by moderate hypothermia in guinea pig isolated hearts. *Am J Physiol*. 1999;277:H2321-32.

100. An J, Camara AK, Chen Q, Stowe DF. Effect of low [CaCl2] and high [MgCl2] cardioplegia and moderate hypothermic ischemia on myoplasmic [Ca2+] and cardiac function in intact hearts. *Eur J Cardiothorac Surg*. 2003;24:974-85.
101. Di Lisa F, Gambassi G, Spurgeon H, Hansford RG. Intramitochondrial free calcium in cardiac myocytes in relation to dehydrogenase activation. *Cardiovasc Res*. 1993;27:1840-4.
102. Griffiths EJ, Stern MD, Silverman HS. Measurement of mitochondrial calcium in single living cardiomyocytes by selective removal of cytosolic indo 1. *Am J Physiol*. 1997;273:C37-44.
103. Isenberg G, Han S, Schiefer A, Wendt-Gallitelli MF. Changes in mitochondrial calcium concentration during the cardiac contraction cycle. *Cardiovasc Res*. 1993;27:1800-9.
104. Robert V, Gurlini P, Tosello V, Nagai T, Miyawaki A, Di Lisa F, Pozzan T. Beat-to-beat oscillations of mitochondrial [Ca2+] in cardiac cells. *Embo J*. 2001;20:4998-5007.
105. Suzuki K. *Intracellular Calcium-Dependent Proteolysis*: Boca Raton, FL, CRC, Inc.; 1990.
106. Yoshida K, Sorimachi Y, Fujiwara M, Hironaka K. Calpain is implicated in rat myocardial injury after ischemia or reperfusion. *Jpn Circ J*. 1995;59:40-8.
107. Merillat JC, Lakatta EG, Hano O, Guarnieri T. Role of calcium and the calcium channel in the initiation and maintenance of ventricular fibrillation. *Circ Res*. 1990;67:1115-23.
108. Cain BS, Meldrum DR, Cleveland JC, Jr., Meng X, Banerjee A, Harken AH. Clinical L-type Ca(2+) channel blockade prevents ischemic preconditioning of human myocardium. *J Mol Cell Cardiol*. 1999;31:2191-7.
109. Smith GB, Stefenelli T, Wu ST, Wikman-Coffelt J, Parmley WW, Zaugg CE. Rapid adaptation of myocardial calcium homeostasis to short episodes of ischemia in isolated rat hearts. *Am Heart J*. 1996;131:1106-12.

8. PUBLICATIONS AND PRESENTATIONS

8.1 Original publications

Driamov S, Bellace M , Ziegler A, Barbosa V, Traub D, Butz S, Buser PT, Zaugg CE. Antiarrhythmic effect of ischemic preconditioning during low-flow ischemia. The role of bradykinin and sarcolemmal versus mitochondrial ATP-sensitive K^+ channels. *Basic Research in Cardiology (2004) 99 (4): 299-308*

Butz S, **Driamov S**, Remondino A, Bellahcene μM , Beier K, Ziegler A, Buser PT, Zaugg CE. Losartan but not enalaprilat acutely reduced reperfusion ventricular tachyarrhythmias in hypertrophied rat hearts after low-flow ischemia. Journal of Pharmacy and Pharmacology (2004) 56 (4): 521-528

Zaugg CE, Butz S, Barbosa V, John D, **Driamov S.** Molekulare Selbstverteidigung für Herzen - Endogene Protektion des insuffizienten Herzens gegen Rhythmusstörungen. *Swiss Medical Forum (2003)48:1172-1174*

8.2 Abstracts, oral and poster presentations

Abstracts

Driamov S, Butz S, Buser PT, Zaugg CE. Selective closing of ATP-sensitive potassium channel subtypes is not pro-arrhythmic during low-flow ischaemia in isolated rat hearts. *Kardiovaskuläre Medizin (2004)7:29S*

Driamov S, Bellahcene M, Butz S, Traub D, Buser PT, Zaugg CE. Bradykinin is a mediator but not a trigger of anti-arrhythmic effects of ischaemic preconditioning. *Kardiovaskuläre Medizin(2003)6:44S*

Driamov S, Bellahcene M, Butz S, Traub D, Buser PT, Zaugg CE. Bradykinin is a mediator but not a trigger of anti-arrhythmic effects of ischaemic preconditioning. *European Journal of Heart Failure Supplement (2003)2/1:9*

Butz S, Remondino A, **Driamov S,** Bellahcene M,Traub D, Buser PT, Zaugg CE. No acute antiarrhythmic effects of losartan and enalapril in hypertrophied rat hearts. *European Journal of Heart Failure Supplement (2003)2/1:12*

Butz S, Remondino A, **Driamov S,** Bellahcene M,Traub D, Buser PT, Zaugg CE. No acute antiarrhythmic effects of losartan and enalapril in hypertrophied rat hearts. *Kardiovaskuläre Medizin(2003)6:55S*

Oral Presentations

Driamov S, Bellahcene M, Butz S, Traub D, Buser PT, Zaugg CE. Bradykinin is a mediator but not a trigger of anti-arrhythmic effects of ischaemic preconditioning. *Gemeinsame Jahrestagung Schweizerische Gesellschaft für Kardiologie, Schweizerische Gesellschaft für Thorax-, Herz- und Gefässchirurgie, Schweizerische Gesellschaft für Intensivmedizin. Lausanne (Switzerland) May 8 - 10, 2003*

Posters

Driamov S, Butz S, Buser PT, Zaugg CE. Selective closing of ATP-sensitive potassium channel subtypes is not pro-arrhythmic during low-flow ischaemia in isolated rat hearts. *Gemeinsame Jahrestagung Schweizerische Gesellschaft für Kardiologie, Schweizerische Gesellschaft für Thorax-, Herz- und Gefässchirurgie, Schweizerische Gesellschaft für Intensivmedizin. Basel (Switzerland) June 2 - 4, 2004*

Driamov S, Bellahcene M, Butz S, Traub D, Buser PT, Zaugg CE. Bradykinin is a mediator but not a trigger of anti-arrhythmic effects of ischaemic preconditioning. *8th Cardiovascular Biology and Clinical Implications Meeting. Villars (Switzerland) October 24 - 26, 2002*

Driamov S, Bellahcene M, Butz S, Traub D, Buser PT, Zaugg CE. Bradykinin is a mediator but not a trigger of anti-arrhythmic effects of ischaemic preconditioning. *Heart Failure 2003 (European Society of Cardiology). Strasbourg (France) June 21 - 24, 2003*

Butz S, Remondino A, **Driamov S,** Bellahcene M,Traub D, Buser PT, Zaugg CE. Losartan acutely reduces reperfusion arrhythmias in hypertrophied rat hearts. *9th Cardiovascular Biology and Clinical Implications Meeting. Interlaken (Switzerland) October 23 - 25, 2003*

Butz S, Remondino A, **Driamov S,** Bellahcene M,Traub D, Buser PT, Zaugg CE. No acute antiarrhythmic effects of losartan and enalapril in hypertrophied rat hearts. *Heart Failure 2003 (European Society of Cardiology). Strasbourg (France) June 21 - 24, 2003*

Butz S, Remondino A, **Driamov S,** Bellahcene M,Traub D, Buser PT, Zaugg CE. No acute antiarrhythmic effects of losartan and enalapril in hypertrophied rat hearts.

Gemeinsame Jahrestagung Schweizerische Gesellschaft für Kardiologie, Schweizerische Gesellschaft für Thorax-, Herz- und Gefässchirurgie, Schweizerische Gesellschaft für Intensivmedizin. Lausanne (Switzerland) May 8 - 10, 2003

Butz S, Remondino A, **Driamov S,** Bellahcene M,Traub D, Buser PT, Zaugg CE. Losartan and enalaprilat have no acute antiarrhythmic effects on hypertrophied rat ventricle. *8th Cardiovascular Biology and Clinical Implications Meeting. Villars (Switzerland) October 24 - 26, 2002*